Validation of a Device to Accurately Monitor Knee Kinematics during Dynamic Movements

by

Ruchika Tadakala

A thesis submitted in partial fulfillment
of the requirements for the degree of
Master of Science in Engineering
(Mechanical Engineering)
in the University of Michigan-Dearborn
2018

Master's Thesis Committee:

Assistant Professor Amanda Esquivel, Chair
Professor Alan Argento
Assistant Professor Samir Rawashdeh

Acknowledgements

Foremost, I would like to express my sincere and deepest gratitude to my advisor Dr. Amanda Esquivel, Ph.D., Assistant professor, Department of Mechanical Engineering at the University of Michigan-Dearborn who ploughed through several fundamental versions of my content, making critical suggestions and posing challenging questions. Her expertise, invaluable guidance, continuous encouragement, affectionate attitude, comprehension, persistence and healthy criticism added considerably to my experience. The door to Dr.Esquivel's office was always open whenever I ran into trouble spot or had a question about my research and writing. She consistently allowed this paper to be my own work, but steered me in the right direction whenever she thought I needed it. Without her ceaseless motivation, it would have not been possible to complete this study.

Besides my advisor, I would like to thank the rest of my thesis committee: Dr. Alan Argento, Ph.D., Professor, Department of Mechanical Engineering, Director of Bioengineering Program and Dr. Samir Rawashdeh, Ph.D., Assistant Professor, Department of Electrical and Computer Engineering for their guidance, encouragement, insightful comments and valuable suggestions that have been very helpful for this study.

I gratefully acknowledge the financial assistance in the form of Graduate Student Research Assistantship, under the Master's program, University of Michigan Dearborn, USA. I extend my thanks to the librarians of the Mardigian Library, University of Michigan Dearborn, especially Ms. Elaine Meyer for her assistance and consultation for literature work and also the graduate advisor for the Department of Mechanical Engineering, Ms. Rebekah Awood for her constant guidance throughout.

Nobody has been more important to me in the pursuit of this research than the members of my family. I would like to thank my father Mr. T. Kumara Swamy and my mother T. Archana and my sister Ms. T. Unnathi, whose love and guidance are always with me in whatever I pursue. It is their

blessing and belief that provide me constant encouragement, divine presence and spiritual support throughout. I would also like to thank my Grandparents and all my relatives for always bestowing their blessings upon me.

I sincerely admire the contributions of all my lab mates (former and present) Jessica Buice, Mirel Ajdaroski, Shadi Saati and Sara Khalil for the stimulating discussions, for the times we worked together before deadlines and for all the fun we had in the lab. I would also like to thank my friend Paul Sujeeth Marumudi along with my lab mates for extending their unstinted support, timely motivation, sympathetic attitude and unfailing help during the course of the entire study.

Last but not the least I would like to thank all the people who were involved in the research project as my subjects. Without their participation and contribution, the research study could not have been successfully conducted.

Table of Contents

List of Tables

List of Figures

Abstract

The incidence of anterior cruciate ligament (ACL) injury in athletes who play multidirectional sports has increased over recent times. Female athletes are at a higher risk of sustaining the ACL injury when compared to their male counterparts involved in the same sport. Various intrinsic (anatomical and hormonal) and extrinsic (biomechanical) factors have been identified that contribute to the increased risk of injury. Sex differences in the kinematics and kinetics of the lower extremity between males and females have been identified while performing various physical tasks has been a topic of discussion since a long time. While it's difficult to control the anatomical and hormonal factors, identifying and modifying the biomechanical factors that contribute to the ACL injury is possible. Wearable sensors involving inertial measurement units (IMUs) have been developed to monitor lower extremity motion and help in assistance with rehabilitation.

The purpose of this study was to validate a set of wearable IMUs against a 3D motion analysis system to monitor the lower extremity motion during jumps and runs in a laboratory and to determine whether IMUs could be used to estimate ground reaction force at landing. An average difference of 5°-10° for flexion, 4°-6° abduction and internal rotation was reported during jump and run. The results of this study showed that correlation between ground reaction force and tibial acceleration is poor when data from all the subjects were included together. However, the correlation was improved when subjects were examined individually. A strong correlation was observed between the resultant ground reaction force and the resultant tibial acceleration during jumping and running between both the legs for the eight subjects when examined individually.

CHAPTER 1: INTRODUCTION

In the United States approximately 20-30 million adolescents every year are injured playing sports [29] [42] [92]. In multidirectional sports like soccer, basketball, wrestling and lacrosse injuries to lower extremity are prevalent. Both men and women sustain sport related injuries at about same rate but due to differences between the sexes, the mechanism of injury differs. Body composition, physiology and kinematics differ throughout the growth cycle. The majority of sport related injuries (80%) involve the musculoskeletal system [29] [2] [26] [4]. Musculoskeletal injuries are injuries that affect the human body's movement or the musculoskeletal system (i.e. muscles, tendons, ligaments, nerves, discs, blood vessels). One of the most common injuries is a sprain or tear of a ligament. Injuries related to the knee have become the most common cause of disability in secondary athletes, representing up to 91% of season-ending injuries and 94% requiring surgery [57]. Anterior cruciate ligament tear is the most common knee injury or ligament tear observed in female athletes. In the United States, every year 20,000-80,000 high school female athletes injure their ACL, with most resulting from soccer and basketball [57]. ACL injuries can occur directly, due to contact or from a non-contact mechanism. Recent studies show that adolescent female athletes are more likely to suffer a non-contact ACL injury than male counterparts [13]. The incidence of anterior cruciate ligament (ACL) injury in female high school and collegiate athletes is 2-8 times [109] [57] higher than in male athletes when comparing athletes in the same sport, and the rate of ACL injury has also been reported to be increasing in recent years [36] [48] [9] [71]. It has been estimated that every year at least one ACL tear is reported in every 50-70 female athletes [11]. The Centers for Disease Control and prevention has stated that in the year 2006 more than 46,000 female athletes age 19 and younger have suffered due to ACL. The cost of ACL injury is estimated to be in the area of $27,000-$35,000 for reconstruction [12]. In addition, studies have shown that even after ACL reconstruction, patients are at an increased risk of early onset osteoarthritis of the knee and female patients are more likely to injure the contralateral knee [58] [14] [101].

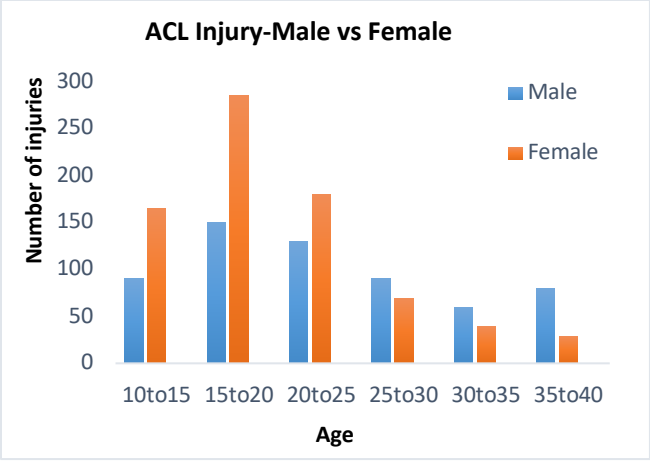

Figure 1: ACL injury rate Male vs Female

Female patients were reported with worse outcomes than male patients before and at 1 and 2 years after the reconstructive surgery. Multiple anatomic, hormonal [49] and biomechanical differences in the female athlete have been identified as reasons for the gender disparity in ACL injuries. In two studies it was found that there was a significant difference in kinematics of the lower extremities between male and female athletes [105] [83]. While anatomical and hormonal factors cannot be controlled, identifying and modifying biomechanical factors that contribute to ACL injury or reducing exposure to severe loading cycles is possible.

The primary goal of this thesis was to validate a device which can accurately monitor knee kinematics and kinetics during dynamic movements including an estimation of ground reaction force, knee flexion and abduction angles using commercially available wearable device system involving inertial measuring units (IMU). Data from the wearable IMUs were compared to an optical motion capture tracking system and force plate.

CHAPTER 2: BACKGROUND

2.1 Anatomy and Physiology of the Lower Limb

The lower limb supports the body's weight and helps in locomotion to maintain equilibrium. It is divided into three regions-the thigh, leg (shank) and foot as shown (Fig 2). The portion of the lower limb located between the hip joint and knee joint is the thigh containing the femur. The region between the knee joint and the ankle joint is the leg containing the tibia (shin bones) and fibula. The foot is distal to the ankle containing the tarsus (connects ankle and foot), metatarsus and phalanges (toe bones) [96].

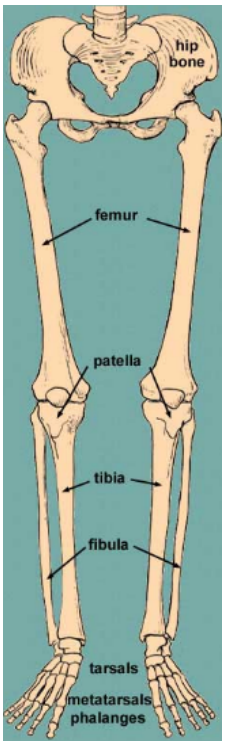

Figure 2: Bones of the Lower Limb [82]

The femur, also known as the thigh bone, is the longest, heaviest and strongest bone of the body. It transmits the body weight from the hip bone to the tibia while a person is standing. It consists of a shaft (body) and proximal and distal ends. The proximal end consists of the head, neck and

two trochanters. The femoral head is attached to the shaft by the neck of the femur at an angle of 115°-140°, averaging 126°. This angle varies with age and gender. The angle is more acute in females due to increased width of lesser pelvis. The distal end of the femur consists of medial and lateral bony expansions or femoral condyles [96].

The patella, also known as the knee cap, is the largest sesamoid bone of the body (Figure 2). A sesamoid bone is a bone that is incorporated into the tendon of a muscle where that tendon crosses a joint. This triangular-shaped bone articulates with the underlying bones preventing the damage to the muscle tendon due to rubbing against the bones during movements of the joint [91].

The tibia, also known as the shin bone, is the medial bone of the lower leg and is larger than the fibula, with which it is paired. It is the weight bearing bone of the lower leg and second longest bone of the body (Figure 1). The tibia articulates with the femoral condyles superiorly, the talus inferiorly, and laterally with the fibula at its proximal and distal ends. On the posterior side of the tibia is located the soleal line, it forms the large bony bump found on the medial side of the ankle region. The smooth surface on the inside of the medial malleolus and the smooth area at the distal end of the tibia articulate with the talus bone of the foot as a part of the ankle joint [96].

The fibula is the slender bone located on the lateral side of the lower leg. It does not bear any weight. It serves primarily for the muscle attachments and thus is largely surrounded by muscles. At its distal ends, the fibula enlarges to form the lateral malleolus, which forms the easily palpated bony bump on the lateral side of the ankle (Figure 2).

The foot comprises the ankle, heel, the tarsus, metatarsus, and phalanges. The ankle refers to the region of the ankle joint. The skeleton of the foot consists of 7 tarsal, 5 metatarsal and 14 phalanges [24]. The foot and its bones are divided into three parts: Hind foot: talus and calcaneus. Midfoot: navicular, cuboid and cuneiform. Forefoot: metatarsals and phalanges. The calcaneus (heel bone) is the largest and strongest bone in the foot. Most of the body's weight is transmitted by the calcaneus from the talus to the ground [27]. Metatarsus of the foot is formed by the five metatarsal bones, which are located between the tarsal bones of the posterior foot and the phalanges of the toes. These elongated bones are numbered 1-5 from the medial side of the foot. The toes contain a total of 14 phalanx bone, they are numbered 1-5 starting from the big toe (hallux).

2.2 Joints of the lower limb

The joints of the lower limb are the hip joint, knee joint, tibiofibular joints, ankle joints and the foot joint [53].

2.2.1 Hip Joint

The hip joint forms the connection between the lower limb and pelvic girdle. It is designed for stability and also for a wide range of movement. The ligaments of hip joint are iliofemoral ligament which prevents hyperextension of the hip joint during standing, the pubofemoral ligament tighten during extension and abduction of hip joint. It also prevents over abduction of the hip joint. Ischiofemoral ligament prevents hyper extension of the hip joint like the iliofemoral ligament. The hip is considered a ball and socket joint that allows flexion-hyper extension, abduction-adduction, medial-lateral rotation and circumduction.

2.2.2 Knee joint

The knee is a modified hinge type of synovial joint allowing flexion and extension and a small degree of abduction/adduction and medial and lateral rotation [41]. The knee joint consists of two articulations, lateral and medial articulations.

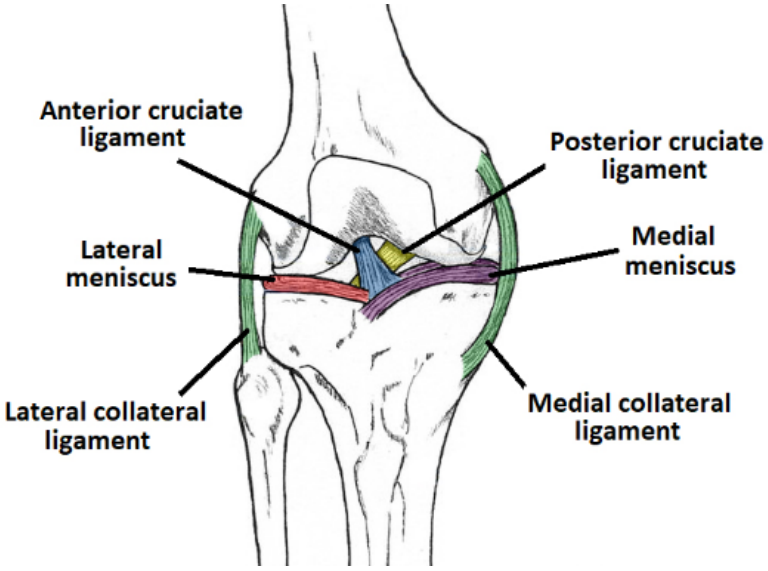

Figure 3: Knee Joint [55]

The stability of the knee joint depends on the strength and actions of surrounding muscles and their tendons, and the ligaments connecting the femur and tibia [55]. The large quadriceps muscle is the

most important muscle in stabilizing the knee joint. The fibrous capsule of the knee joint is strengthened by five extracapsular ligaments, patellar ligament, fibular collateral ligaments, tibial collateral ligament, oblique popliteal ligament, arcuate popliteal ligament. The patellar ligament, the distal part of the quadriceps tendon, is a strong, thick fibrous band passing from the apex and adjoining margins of the patella to the tibial tuberosity.

There are four ligaments that provide stabilization to the knee. The collateral ligaments are two strap like ligaments. They stabilize the hinge motion of the knee preventing excessive medial or lateral movements. The medial collateral ligament is a strong flat band that extends from the medial epicondyle of the femur to the medial condyle and superior part of the medial surface of the tibia [82]. At its midpoint, the deep fibers of the medial collateral ligament are firmly attached to the medial meniscus. The lateral collateral ligament is thinner and rounder than the medial collateral which attaches proximally to the lateral epicondyle of the femur, distally it attaches to a depression on the lateral surface of the fibular head [55]. The cruciate ligaments join the femur and tibia, crisscrossing within the articular capsule of the joint but outside of the synovial joint cavity. The X like shape provides stability to the joint.

The anterior cruciate ligament (ACL) attaches at the anterior intercondylar region of the tibia, just posterior to the attachment of the medial meniscus [41]. The ACL is weaker among the two cruciate ligaments. It extends superiorly, posteriorly and laterally to attach the posterior part of the medial side of the lateral condyle of the femur. The ACL has very poor blood supply. When the knee is flexed, it is slack. When the knee is extended it is taunt, preventing posterior displacement of the femur on the tibia and hyperextension of the knee joint. The tibia cannot be pulled anteriorly when the joint is flexed at right angle because it is held by the ACL [32]. The posterior cruciate ligament (PCL) is the stronger of the two cruciate ligaments, it arises from the posterior intercondylar area of the tibia. The anterior displacement of the femur on the tibia or posterior displacement of the tibia on the femur is prevented as the PCL tightens during flexion of the knee joint [32]. The hyperflexion of the knee joint is also prevented by PCL. PCL is the main stabilizing factor for the femur in the weight-bearing flexed knee. The menisci of knee joint act as shock absorbers. At their external margins, the menisci are thicker and taper to thin, unattached edges in the interior of the joint [32].

2.2.3 Tibiofibular joints

The tibia and fibula are connected by two joints: the proximal tibiofibular joint and the distal tibiofibular joint. Without movement at the distal one, the movement at the proximal joint is impossible [68]. The anterior and posterior ligaments of fibular head strengthen the fibrous capsule. The fibrous capsule is lined by the synovial membrane. Slight gliding movements of the proximal tibiofibular joint can occur during dorsiflexion and plantarflexion of the foot [87].

2.2.4 Ankle/Foot Joint

The ankle joint (talocrural) articulation is a hinge type of synovial joint. The ankle joint is located between the distal ends of the tibia and fibula and the superior part of the talus.

2.3 Knee Kinematics

The main knee movements are the flexion and extension; some rotation occurs when the knee is flexed with some abduction/adduction. The knee "locks" because of medial rotation of the femur on the tibia when the leg is fully extended with the foot on the ground. This makes the lower limb a solid column and more adapted for weight-bearing position. The main movements of the knee joint are [55]:

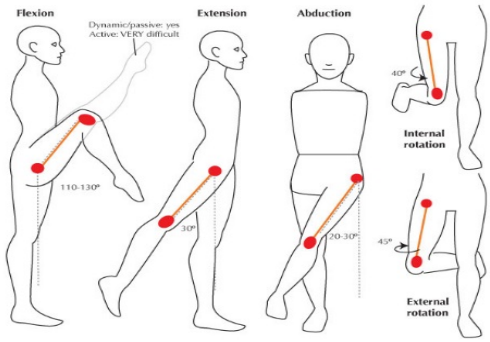

Figure 4: Knee Movements [99]

- Flexion-principally by the hamstrings but also by the gastrocnemius-movement is limited by contact between the calf and thigh.
- Rotation-increasingly possible as the knee is flexed.
- Medial rotation-popliteus, semitendinosus, and slightly by semimembranosus-movement is constrained by the cruciate ligaments.

- Lateral rotation-biceps femoris-as the collateral ligaments become taunt, its movement is constrained.
- Extension-principally by quadriceps-movement is limited as the cruciate and collateral ligaments become taunt.

2.4 Injuries related to the knee

For the knee to work each part of its anatomy should function properly. Acute injury as well as chronic overuse may cause inflammation and damage the knee. The knee is more susceptible to twisting or stretching injuries (hyper flexed /hyperextended). If the stress occurs from a specific direction, then the ligament that is trying to hold it in place against the force will stretch and tear. Such injuries are called sprains. Sprains are graded as first, second and third degree based on the damage caused [117]. The first-grade sprains stretch the ligament but don't tear the fibers, grade two sprains partially tear the fibers but not the ligaments and the third-grade tears completely disrupt the ligament. Twisting injuries to the knee put weight on the ligament or meniscus and can squeeze them between the tibial surface and the edges of the femoral condyle, conceivably causing tears.

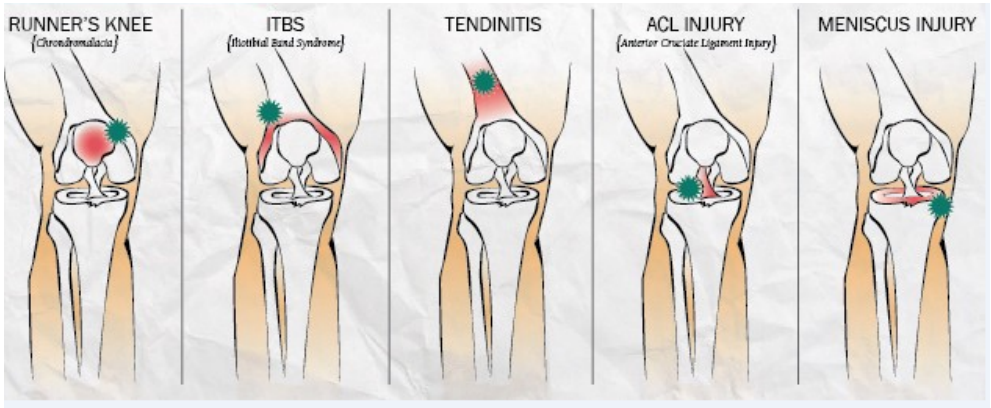

Figure 5: Common Knee Injuries [14]

The medial collateral ligament and the lateral collateral ligament can be stretched or torn when the foot is planted sideways, and a force is directed to the knee. Injuries to these ligaments may also damage the meniscus or cruciate ligaments. If the foot is planted and force is applied from front or back of the knee, the cruciate ligaments can be damaged. Meniscal tears often happen during sports. Tears in the meniscus can occur when twisting, cutting, pivoting, or being tackled. Meniscal tears may also occur as a result of arthritis or aging.

2.4.1 Anterior Cruciate Ligament injury (ACL)

In the United States alone as many as 100,000 to 250,000 people suffer from an ACL injury [91]. An anterior cruciate ligament injury is the over-stretching or tearing of the anterior cruciate ligament in the knee (Figure 6). The tear may be partial or complete. The mechanism of injury to the ACL can be contact or noncontact. An injury which occurs as a result of direct contact with the knee or any body part by player or an object is termed as a contact type of ACL injury. An injury where the athlete tears the ACL during any sudden movement that does not involve direct contact with another athlete is termed as a noncontact ACL injury. Of all reported ACL injuries only 30% [39] include contact from an outside force i.e. from an opposing player, goalpost or any other object on the field. Furthermore, many studies of video observational analysis reported that most of the ACL injuries were caused by noncontact mechanism [54].

On an average 70%-84% ACL injuries [20] [3] [21] [31] [88] are resulted from noncontact mechanisms like cutting movements, sudden changes in directions, hyperextension resulting from landing while jumps, unanticipated change in the direction of the play (lapse of concentration), one step/stop deceleration and rapidly stopping. Each year approximately 50,000 reconstructions of ACL are performed [34] at a cost of $17,000 per surgery.

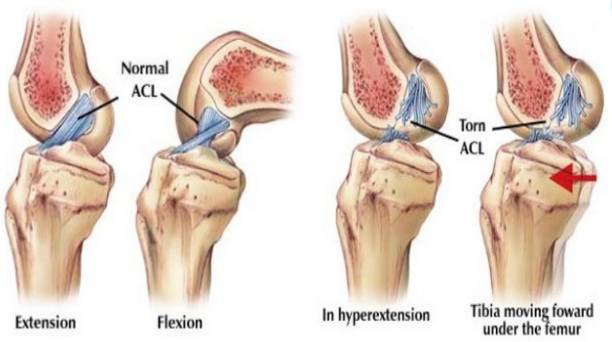

Figure 6: ACL Injury [106]

The non-contact type of injuries usually occur when players were in close vicinity (within 1m of the player injured) [22]. Additionally, the non-contact ACL injuries also occurred due to pressing (76%) at the time of defense [47] [22] in female soccer players [95]. The risk factors that have been recognized as related with noncontact ACL injury can be named under categories as ecological (equipment and shoe-surface contact) [57], anatomic (knee angle, hip angle, laxity and notch size), biomechanical, hormonal [61] (strength of muscle, movements of body and neuromuscular control) [39] and genetically [106]. Some studies have shown the involvement of

ecological factors in Non-Contact ACL [38] but none of the factors were related to gender in particular. Climate conditions, surface of the ground, footwear and its resistance on the surfaces are all the phenomena contributing towards environmental factors. Most of the non-contact injuries were observed to occur when the playing surfaces were dry and hard [33] [38], due to weather conditions as a result of which the players were exposed to high friction and torsional resistance between the sole of the shoe and the surface of the ground. From one study there was no difference observed in the occurrence of ACL injuries on ground surfaces (damp and dry) for male athletes but has shown that the ACL injury was frequently observed in female athletes who played on artificial turf compared with natural grass [74]. In the United States a few of the knee injuries were associated with the footwear design i.e. type of spikes on the sole of the training shoes of soccer players was a cause of the ACL injury [94].

The anatomical differences between males and females in the lower extremity alignment (hip varus, Q-angle and knee valgus, foot pronation and hip rotation) [52], length of the bone, joint laxity [78] and muscle development also considered to be a risk factor for non-contact ACL. As the length of the tibial and femoral bone increases in adolescents the knee torque also increases which results in the instability of the knee [47]. While this instability can be partly stabilized through muscle strength and stiffness in males, in females due to smaller muscle mass cannot be achieved, increasing their probability even more to the ACL injuries [47] [87] [64]. The Q-angle in the knee is also one of the factor responsible for the ACL injury. The angle formed by the line connecting the center of anterior superior iliac spine and the intersection of patella with the line connecting the center of patella and tibial tuberosity is known as the Q angle. The larger the Q angle the greater is the lateral pulling force exerted by the quadriceps femoris muscle of the patella on the medial knee. The size of the anterior cruciate ligament and its mechanical property also have an effect on the cause of the injury. The size of ACL is smaller in females than males [5] may contribute to the increase in ACL injuries [66] [99]. Likewise, small ACL inclines to a small intercondylar notch, where movements such as landing, jumping and cutting that require extension of the knee may lead to more prominent collision between the ligaments [89] [68]. The mechanical property of the ACL plays a key role in situations where there is application of high forces. Studies conducted on cadavers have demonstrated that ACLs of females have lower mechanical property compared to male ACLs [23]. The role of hormones has as of late been of interest. In 1996, estrogen and progesterone receptor locales were found in human ACL cells [61] indicating that

female sex hormones may play a role in ACL structure. Several studies have confirmed that female sex hormones can impact the composition and mechanical properties of the ACL [61] [90]. A survey conducted during 1998-1999 for 103 basketball female players injured by the ACL reported that the injuries occurred just before or after the onset of menses, irrespective of their usage of oral contraceptives (E. A. Arendt, MD, unpublished data, 1999). But up until now, the impact of oral contraception, which reduces estrogen levels, on the function of knee and damage of ACL in females remains obscure [52] [45], in spite of the fact that it has been demonstrated that athletes who take oral contraception are associated with less injury [8] [69], additionally use of oral contraception by college athletes did not increase non-contact ACL injuries [7].

Differences in gender have been found in the patterns of motion, positions and forces generated from the hip and trunk to the knee. These disparities are important since the position of the hip and motion influence the position, loads and stiffness of the knee [37] [38] [76]. Women have shown to have less hamstring and gluteus medius activity than men (W. B. Kibler, MD, unpublished data, 1999; L.J. Huston, MS, unpublished data, 1999) resulting at greater risk for non-contact ACL compared to their counterparts. It was also observed if the knee flexion angle was between 0º-30º, this increases the ACL strain [15]-[43]. In general women perform landing and cutting movements in a more erect stance than men, with less hip and knee flexion which makes them more susceptible to the ACL injury while performing such activities (R. A. Malinzak, MD, unpublished data, 1999; L. J. Huston, MS, unpublished data, 1999). In addition, the increase in knee valgus and more prominent quadriceps activation may further increase the risk of injury [50].

Kinetic, gravitational and muscle forces influence the risk of noncontact ACL. Most of the injuries occur while changing directions or landing from a jump where there is an action of deceleration and involve generation of forces by quadriceps (i.e., the muscle is lengthening under tension) and flexion of the knee angles. Furthermore, the knee valgus movements stress the ACL even more, while a posterior protection is provided to the ligament by the hamstring activation [63] [28]. Studies [73] [21] [102] which used videotapes to examine the non-contact ACL injuries revealed that most of the players slightly bumped or performed an awkward movement and quickly recovered by making a new movement before an injury occurred. For example a soccer player begins to make a goal towards the goalpost, but suddenly another player causes her to change the direction quickly and alter her already initiated movement. With the lack of time to get data, the

central nervous system attempts to recuperate, and regularly the movement turns out to be more quadriceps prevailing as the player attempts to regain balance. This happens when the ACL is most susceptible to the shear forces of the quadriceps.

Preventative strategies have been proposed to most of the injuries occurred during playing the actual game or during practices. One current strategy suggested to help decrease the number of ACL injuries is functional screening combined with neuromuscular training. Athletes can undergo screening of the knee where a fitness professional examines parameters such as the two-legged squat, drop-jump and running and cutting maneuvers to determine whether an athlete is at risk of knee injury [83] [100] [47]. These programs tend to offer a combination of proprioception training to improve balance and coordination, plyometric exercises that involved jumping and landing, strengthening exercises and dynamic joint stability. Several studies that incorporate these techniques into their warm-up and practice have been shown to be effective at reducing ACL injury [49] [58] [60] [85]. However, there are barriers to effective neuromuscular training including equipment, personnel and time constraints. Teams that have a limited amount of practice time or do not have access to an athletic trainer or physical therapist may not be able to include this training [66]. In addition, it has been reported that there is some discrepancy between observed functional screening and measured 3D motion analysis indicating that just observing these motions may not be accurate [83]. Many protocols have been provided by the International Olympic Committee for biomechanical and neuromuscular training, agility, balance, stability of the core and plyometrics [18] [77]. It was found out that women required on an average of 6 months or longer period to recover from the ACL surgeries than men [12] and a Swedish report demonstrated that post ACL reconstruction in females in a year or two after surgery showed some low scores, however a huge difference was not observed after two years [2]. Also extrinsic factors like ground surface, footwear and interaction between the ground surfaces can be controlled to a large extent as a prevention parameter.

2.5 Wearable Sensor Technology

Wearable sensor technology is a category of electronics which consists of a device that can be worn on body or attached to clothing. Information related to health and fitness can be tracked using such kind of technology. The wearable sensors continuously monitor physiology of a person as well as motion sensing [103] [104]. There are numerous applications of wearable technology like

the fitness devices which can track the fitness activities of a person like running, jumping, jogging etc. and the healthcare devices used to enable home diagnosis, make virtual health and remote monitoring possible. Some examples of the devices are bluetooths, body cameras, heart rate monitors, motion trackers, personal GPS devices, smart watches and implantables. One such type of wearable sensor system is composed of the inertial measurement unit (IMU).

2.5.1 Inertial Measurement Unit (IMU)

IMUs are electronic devices which measure and give a report on the body's linear acceleration, angular rate and magnetic field surrounding the body [113] [114]. They are a combination of gyroscopes, accelerometers and magnetometers (Figure 6). The accelerometer measures the linear acceleration along the X, Y, Z axes of the IMU. The gyroscope measures angular velocity. Similarly the magnetometer measures the earth's magnetic field. IMUs detect the change in pitch, roll and yaw. IMUs are used in various industries like the navigational industry as an integral part of the inertial navigation system in aircrafts, missiles, and satellites. Besides these navigational uses, they are also used in smartphones and tablets as orientation sensors. They are used in fitness trackers and wearables to measure motion while performing any gait activities in day to day lives. Gaming systems also use IMUs to measure motion in their remote controls.

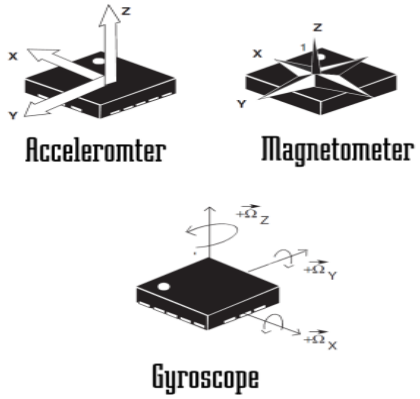

Figure 7: Accelerometer, Magnetometer and Gyroscope

2.5.2 Accelerometers

Accelerometer is a device that measures acceleration i.e. the rate of change of velocity [113]. Acceleration is measured in meters per second squared (m/s^2) or in gravitational forces (g). The gravitational force on earth's equivalent to 9.8 m/s^2 but it varies slightly with elevation and is different for different planets due to the gravitational pull.

2.5.3 Gyroscopes

Gyroscopes are the devices that can measure the rotation about an axis. They measure the angular velocity in degrees/sec. A single axis gyroscope can measure the rotation of a single axis while a three axis gyroscope can measure in three different axes. They are very accurate in controlled conditions [30] [113] [114]. Gyroscopes with accelerometers together measure rotational velocities. Gyroscopes are used in M.E.M.S scale and many devices [79] [67] [93]. Over time due to drift the accuracy of a gyroscope gets affected. A drift occurs when the data starts to skew in the positive or negative direction, due to temperature changes in the device. Voltage fluctuations can also generate drift. Filtering the results helps remove drift [80, 79]. The gyroscope can be used as a precise device for measuring angular velocity about an axis just by controlling the drift.

2.5.4 Magnetometers

A magnetometer is an instrument that measures magnetic fields, the direction of the field and its strength. It measures earth's magnetic field in Gauss or 'uT'. Its applications extend into various industries like military to detect submarines, geographical surveys, metal detectors, directional drilling and space explorations etc. There are two different types of magnetometers bases on their applications.

Wearable sensors have been developed to monitor lower extremity motion using a variety of methods for several applications, including gait analysis and assistance with rehabilitation [66-70]. The wearable sensors involve the inertial measurement units (IMUs), consisting of accelerometers, gyroscopes and magnetic field sensors which provide information about the acceleration, velocity and position of one body segment with respect to another and have been used to estimate various limb angles [113] [114] and ground reaction force [75]. Wearable IMU sensors provide the opportunity for non-obtrusive activity monitoring in a real world setting. Wearable sensors using IMUs have successfully measured a variety of kinematic data.

2.6 APDM Opal System

APDM (Ambulatory Parkinson's Disease Monitoring), the products developed by the APDM Inc. specialize in monitoring gait patterns for a person. The mobility lab is the host program that configures and runs trials based on plug-ins. The Opal sensor by APDM (APDM Inc., Portland OR) is an inertial measurement unit (IMU) that consists of a tri-axial accelerometer, tri-axial

gyroscope and tri-axial magnetometer. Each Opal sensor is about the size of a wristwatch and weighs less than 22 grams. One major benefit of the Opal sensor is it can collect data for an entire day (up to 16 hours) on one charge and store up to 28 days' worth of data.

Figure 8: APDM Opal sensor

Therefore, the Opal sensor is small and compact, has a long battery life and large storage capacity, and thus can be used outside of a motion analysis laboratory setting and during a person's activities of daily living. Since the Opal sensors meet both the user's preferences, it was selected as the wearable sensor for the WMAS (wearable motion analysis system).

The characteristics of the sensor used are given in the tables below:

Table 1: Characteristics of the Opal Sensors [6]

	Accelerometer (2)	**Gyroscope**	**Magnetometer**
Axes	**3 axes**	**3 axes**	**3 axes**
Range	**± 16g, ± 200g**	**± 2000 deg/s**	**± 8 Gauss**
Noise	**120 µg/√Hz, 5 mg/√Hz**	**0.025 deg/s/√Hz**	**2m Gauss/√Hz**
Sample Rate	**20 to 128 Hz**	**20 to 128 Hz**	**20 to 128 Hz**
Bandwidth	**50 Hz**	**50 Hz**	**32.5 Hz**
Resolution	**14 bits, 17.5 bits**	**16 bits**	**12 bits**

Table 2: Hardware characteristics of Opal sensor [6]

Dimensions	**43.7 x 39.7 x 13.7 mm (LxWxH)**
Weight	**< 25 grams (with battery)**
Material	**PC-ABS Plastic, Glass**
Internal Storage	**8 Gb (~720h Storage)**

Battery Life	**SynchronousLogging:12h,Asynchronous Logging: 16h**

Table 3: Wireless characteristics of Opal sensor [6]

Wireless Radio	**Nordic Semiconductor nRFL01 + radio, ultra-low power**
Frequency Band	**2.40-2.48GHz ISM band, adjustable**
Data Rate	**2Mbps on-air data rate**
Latency*	**300ms (typical) with data buffer, 30ms (typical) without data buffer**
Transmission Range	**30m line of sight, 10m indoors**
Data Buffer	**8Gb (~720 hours)**
Synchronization	**≤1ms difference, up to 24 Opals**
Bluetooth^2	**No**
Wifi^2	**No**

* Latency is defined as the time when sample is recorded on the Opal, to the time it is emitted from the host libraries.

Table 4: Orientation Estimates of Opal sensor [6]

Static Accuracy (Roll/Pitch)	**1.15 deg**
Static Accuracy (Heading)	**1.50 deg**
Dynamic Accuracy	**2.80 deg**

The APDM system along with the opal sensors came with a pair of docking station for charging and configuring the opal sensors, two access control points used for wireless communication between the monitor and the opal sensors, a wireless remote control to make data collection easy, a footplate which standardizes the stance width if used, a USB drive with the Mobility software and seven straps for each of the opal sensors and USB cables (Figure 9).

Figure 9: (a) Access Control Points, (b) Docking station with USB connector

2.7 Optical Tracking System

Optical tracking systems utilize camera-based technology to measure precise and accurate movements of a subject. Because of their accuracy, they are considered to be a gold standard. The entire system requires the use of a large room to set up the cameras, cables, computer workstations and calibration equipment. Cameras are placed strategically around an area to provide a field of view that the subject will be working in. Cameras track the markers placed on the subject's body and locations of the markers are dependent on the type of study being conducted. Passive markers are retro-reflective spherical balls with adhesive backings to them. The markers are wrapped in reflective tape that is highly reflective to infrared illuminators that surround the optical cameras. The markers represent body segments that cameras can track [30].

2.7.1 Optitrack Motive System

Optitrack motive is an optical tracking system for motion analysis. The system uses multiple optical cameras to track human movements. The system calibrates all the cameras to a common reference plane. This type of study drives the configuration for the cameras. This reference plane calibrates to a global coordinate frame, which is referenced in Visual 3D. The calibration of this plane sets the distance between markers for any other future calculations in the analysis program. The software platform allows the user to calibrate and configure 3D data and also provides interfaces for capturing and processing the 3D data. It compiles 2D images of markers to obtain 3D coordinates. By using these 3D coordinates from tracked markers, motive obtains six degrees

of freedom (3D position and orientation) data for rigid bodies and skeletons. Motive enables the tracking of complex movements in 3D spaces.

Figure 10: Prime 13 Camera [72]

We used 12 Prime 13 (Optitrack, Corvallis, OR) motion capture cameras (Figure 10). These particular cameras were used because of their potable size and high resolution and many technical specifications [72]. The resolution provided by these cameras is 1280*1024 at an adjustable frame rate of 30-240 FPS, the latency being 4.2ms [72]. The cameras came with twelve tripod stands and the required cables to connect. These particular type of cameras were chosen due to their excellent range and coverage.

2.8 Force plate

A force plate is a device which measures force, pressure and movement generated by a body standing on or moving across them (Figure 11). They are composed of strain gauge load transducers and a digital amplifier for signal conditioning. They are portable, lightweight, and can be moved from one place to another easily. They have adjustable foot for levelling on surfaces for accurate measurements.

Figure 11: Bertec Force plate [51]

The force plates used in this study were manufactured by the Bertec Acquire Columbus, Ohio. Two of the FP4060-05-PT type of force plates were used. The force plates have six component load transducers. They measure the orthogonal components of the resultant forces on the plate and three components of resultant moment in the same direction of the coordinate system. A 16-bit

digital gain amplifier and signal conditioner inside each plate makes the signal acquisition and conditioning obsolete. Each plate has a calibration matrix digitally stored on it. With the help of external amplifiers three outputs of the signal are achieved; digital, analog, and dual (digital/analog). The output was directly plugged into the computer sing a USB port without any use of additional PC card for signal conversion. The specifications of the force plates are in the Table 5.

Table 5: Force plate Specifications [51]

Model Designation	**FP4060-05-PT**
Width, mm(in)	**400 (15.75)**
Length, mm(in)	**600 (23.62)**
Height, mm(in)	**50 (1.97)**
Mass, kg(lb.)	**8 (18)**
Max. Load Fz, N (lb.)	**5,000 (1,100)**
Max Load Fx, Fy, N (lb.)	**2,500 (550)**
Max. Load My, N·m (in·lb)	**1,000 (8,900)**
Max. Load Mz, N·m (in·lb)	**750 (6,600)**
Natural Frequency Fz (Hz)	**250**
Natural Frequency Fx, Fy (Hz)	**150**
Static Resolution* Fz, N (lb.)	**±0.5 (0.11)**
Resolution Fz, N/LSB (lb./LSB)**	**0.09 (0.02)**
Linearity, %FSO†	**0.2**

* Static Resolution is the peak-to-peak noise amplitude of the static signal.

** Resolution is given in terms of the sensitivity of the internal digitization and indicates the amount of signal produced (in N or lb.) per LSB (least significant bit) of digitized signal.

† FSO: Full Scale Output

2.9 Visual 3D

Visual 3D is a motion analysis software by C-motion, Kingston, ON, Canada which mathematically analyzes the kinematic and kinetic (inverse dynamics) data for biomechanical 3D motion captured data. The files from the motion capture systems are taken as input in visual 3D in the .c3d format to analyze. The .c3d files contain movement point data, force plate data and analog signals (EMG, accelerometer, foot pads, etc.). The saved .cmo output file contains c3d data, static data, processed signal, kinematic and kinetic data. The models in visual 3D are called six-degree-of-freedom link models, which comprise of 6 DOF segments (thigh, shank and foot in leg), which corresponds to the major bone structure of the body. Each segment is a rigid body which has mass and fixed dimensions and doesn't undergo any deformations with respect to any external force. Each segment is defined by two points in space, proximal and distal end, corresponding to endpoints of major bones and a third point that defines the orientation of the vector between the endpoints. A pipeline helps in creation of many models for number of subjects at the same time which saves time. The joint angle data is obtained from visual 3D.

2.10. MATLAB

Matlab is a programming software which uses a matrix based language to analyze data, develop algorithms and create models and applications. By developing a script any data can be obtained using matlab. The use of MATLAB in this study was to get the acceleration, time, joint angle data and develop graphs from the APDM Opal sensors using the .h5 files as input, through which all the required parameters were calculated like ground reaction force, min acceleration, body weight etc.

CHAPTER 3: METHODOLOGY

3.1 Institutional Review Board Approval

This research study "Validation of a device to accurately monitor knee kinematics during dynamic movements" was approved by the University of Michigan-Dearborn Institutional Review Board (IRB). The principal investigator of the study was Dr. Amanda Esquivel, and the research staff included Ruchika Tadakala and Jessica Buice. Before participating in the study, each participant was briefed about the consent form: the purpose of the study, procedures, benefits, risks, disclosures, privacy, how the information will be used, and their rights and ability to withdraw from the study at any time. After the briefing and participant's questions, the subjects signed the consent form to perform two activities (vertical jump and run) in the biomechanical laboratory.

3.2 Participant Data

Eight subjects, four females (1-4) and four males (5-8), aged 20-39 participated in the study. The subjects were all healthy and did not have any history of knee injuries before or any type of gait abnormalities. The subjects were asked preferably to wear sport shorts above knees and a tight tank top or tee-shirts which would not interrupt the placement of markers or sensors. Each subject was given an identification number to protect their data and their height and weight were also recorded. Any data relating to the subject or which would be published was secured on a password protected computer and was confidential and only members of the research team had access to the files and data. Subjects were asked to perform two activities (running and jumping) which were recorded using both motion capture and a set of wearable IMU sensors. Detailed information about the experimental setup and activities follows.

Table 6: Participant Data

Subject id	Age	Height(m)	Weight(kg)
1	22	1.67	53.5
2	39	1.58	67.13
3	25	1.57	44
4	23	1.52	80
5	23	1.90	108.86
6	20	1.72	63.5
7	20	1.90	81.64
8	22	1.79	84.82

3.3 Instrumentation and Experimental Setup

The study took place at the University of Michigan-Dearborn, in the IAVS (Biomechanical) laboratory. Subjects used an 8-foot walkway as a path to perform the activities on which the force plates were installed and was located in the middle of twelve optical tracking cameras which were mounted on adjustable tripods as shown in the Figure 12. The field of view of the Optitrack system was not able to monitor the full space of study instead the cameras focused on the wooden walkway with force plates where each of the trails took place which made data collection optimal. The field of view was limited and allowed a limited space to collect data.

Figure 12: Camera Setup

All the cameras were located high above the ground and would not interrupt the study space (Figure 12). The cameras were connected to a main computer which powered and received the data. Both the Optitrack system and APDM system were calibrated and configured before the study to ensure accurate collection of data for each subject. Both the Optitrack and APDM systems were set up to record data and activities performed by the subjects simultaneously.

3.3.1 Optitrack Motive Calibration

After starting the motive software and warming up the cameras for five minutes, all the grayscale image of cameras was checked (Figure 13). It was made sure that there was no reflective material in the focused space or the subject was wearing anything reflective, if so it was covered with gaffer tape.

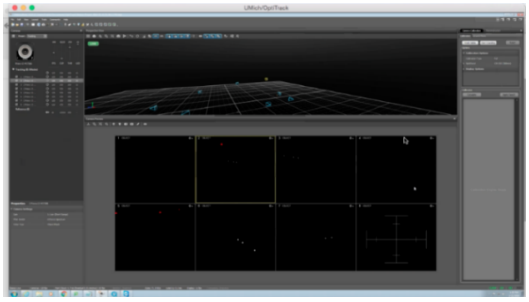

Figure 13: Masking the cameras free of any reflective material

After completing the above procedure, the camera calibration was done using the wanding option using the calibration wand. The wanding was done until all the cameras were covered as shown in Figure 14 and the results were calculated and applied to the particular subject's take.

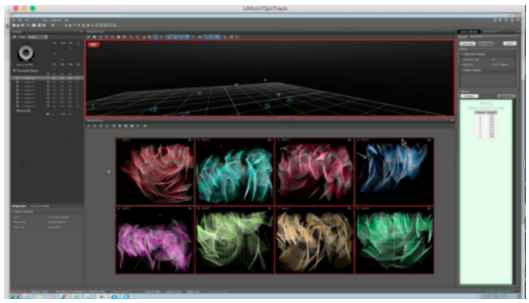

Figure 14: Calibration using the wand to cover whole space

After this, the next step was to set the ground plane using the L-frame. In the lab, the force plate was considered to be the ground since the activities would take place on it (Figure 15).

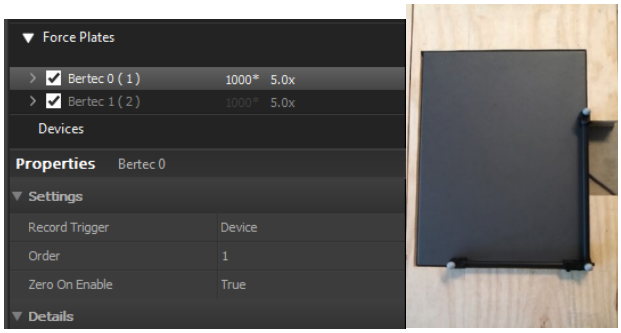

Figure 15: Setting up of force plate

The force plates were positioned in two different ways on the walkway as shown in the Figure 16 (a) and (b) for a jump and a run activity respectively.

Figure 16: Force plate position on walkway for (a) Jump trial (b) Run trial

Reflective markers were secured onto each subject using the “Lower body Rizzoli” protocol. The lower body Rizzoli skeleton has thirty-two markers specified. An extra sixteen markers were placed on the body for better tracking of the segments while creating a rigid body. The markers were placed on key bony locations, such as the joints by manually palpating the subject and the extra sixteen markers were placed in the form of a square cluster on the lateral side of both the thighs above the opal sensors and four on the gastrocnemius (lower back part of shank) just below knee for both the legs. Table 7 below lists all the marker labels that are required to be placed in the lower section of body.

Table 7: Marker Labels

Waist	Right leg	Left leg	Right foot	Left foot
▪ RASIS	▪ RTH	▪ LTH	▪ RLM	▪ LLM
▪ LASIS	▪ RLE	▪ LLE	▪ RMM	▪ LMM
▪ LGT	▪ RHF	▪ LHF	▪ RCA	▪ LCA
▪ RGT	▪ RME	▪ LME	▪ RFM	▪ LFM
	▪ RTT	▪ LTT	▪ RDP	▪ LDP
	▪ RSK	▪ LSK	▪ RVM	▪ LVM
			▪ RSM	▪ LSM

Figure 17 shows all the key bony points of the lower limb for where the reflective markers have to be placed.

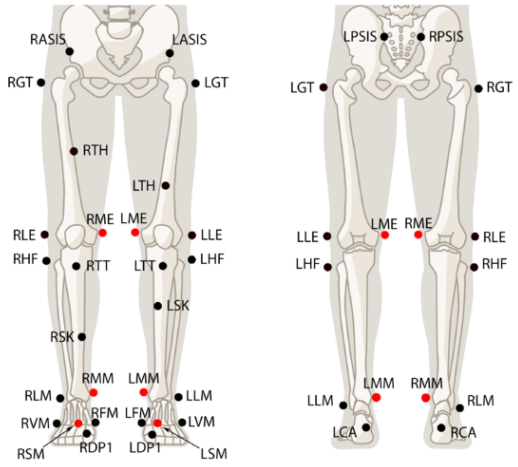

Figure 17: Biomechanics Gait Marker Set for Lower Limb [30]

The description of all the thirty two Rizzoli lower body protocol to be placed on the body at various locations has been explained briefly in the Table 8.

Table 8: Marker Descriptions

Body Segment	Marker Label	Anatomical Location	Description of Location
Waist	RASIS	Right Anterior superior iliac spine	On the top of the anterior iliac spine.
	LASIS	Left Anterior superior iliac spine	
	RPSIS	Right Posterior superior iliac spine	On top of the bony locations where the spine joins the pelvis.
	LPSIS	Left Posterior iliac spine	

Right Upper Leg	RGT	Right great trochanter	Right most lateral prominence of the greater trochanter external surface.
	RTH	Right thigh	Lower 1/3 of the lateral surface of right thigh.
	RLE	Right lateral epicondyle	Most lateral prominence of the lateral femoral epicondyle.
	RME	Right medial epicondyle	Right medial prominence of the medial femoral epicondyle.
Left Upper Leg	LGT	Left great trochanter	Left most lateral prominence of the greater trochanter external surface.
	LTH	Left thigh	Lower 1/3 of the lateral surface of left thigh.
	LLE	Left lateral epicondyle	Most lateral prominence of the lateral femoral epicondyle.
	LME	Left medial epicondyle	Left medial prominence of the medial femoral epicondyle.
Right Lower Leg	RHF	Right proximal tip of the head of the fibula	
	RTT	Right most anterior border of the tibial tuberosity	
	RSK	Right shin of the knee	Near the midline of the shin below the right knee.
	RMM	Right medial malleolus	On the distal apex of the medial malleolus of right knee.
Left Lower Leg	LHF	Left proximal tip of the head of the fibula	
	LTT	Left most anterior border of the tibial tuberosity	
	LSK	Left shin of the knee	Near the midline of the shin below the left knee.
	LMM	Left medial malleolus	On the distal apex of the medial malleolus of left knee,
Right Foot	RCA	Right calcaneus	Upper ridge of the calcaneus posterior surface.
	RVM	Right fifth metatarsal head	On the fifth toe of the right foot
	RFM	Right first metatarsal head	Dorsal of the first foot head
	RDP1	Right distal phalanx	Near the end of big toe, distal end of right phalanges
	RSM	Right second metatarsal head	Dorsal of the second foot head.

Left foot	LCA	Left calcaneous	Upper ridge of the calcaneus posterior surface.
	LVM	Left fifth metatarsal head	On the fifth toe of the left foot
	LFM	Left first metatarsal head	Dorsal of the first foot head
	LDP1	Left distal phalanx	Near the end of big toe, distal end of right phalanges
	LSM	Left second metatarsal head	Dorsal of the second foot head.

3.3.2 APDM Moveo Calibration

Figure 18: APDM setup

The APDM system was also configured before recording any data of the subjects. The hardware setup was done using the Moveo Explorer software on the computer. If any error occurred, the sensors would not be configured which was indicated by the software. After completing the configuration of the sensors, a test subject was added on the Mobility system software by filling in the required fields. The type of test form used for this study was “free form” as the activities (jump and run) which we performed were not listed in the software. The opal sensors were placed at particular locations specified by the software for the lower limb protocol (Figure 19).

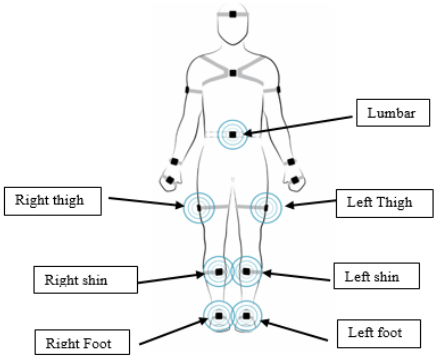

Figure 19: Sensor placement [6]

Table 9 below gives a detailed description about how the APDM opal sensors were to be placed on the subject's body. In this study we only used the lower leg and upper leg sensors avoiding the foot and lumbar one. Upper and lower leg sensors were fixed to the subjects using co-flex bands at the required positions specified in the table.

Table 9: Sensor Location Description [6]

Body part	Anatomical Description	Common Description	Orientation
Lower Leg	Just medial to the anterior surface of the tibia, high enough for the strap to wrap just above the widest part of the gastrocnemius	Just inside the front of the shin, on the flat surface of the bone, high enough for the strap to wrap just above the widest part of the calf muscle.	Connector pointed straight down towards the floor
Upper leg	Lateral side of thigh, on top of the iliotibial band,~4inches above the knee	Side of thigh, midline, between muscular tissue, one hand's width above the knee	Connector pointed straight down towards the floor

3.4 Research Trials

APDM opal sensors and reflective markers were placed on the subject prior to recording the trial as described in the previous sections (Figure 20). The opal sensors were placed at key locations specified by the APDM given in the Table 9.

Figure 20: Markers and sensors placed on subject's body

A skeleton was created for each subject with their unique identification number after all the markers and sensors were secured before starting the recording (Figure 21). Subjects were asked

to stand in a T-shaped pose by putting their hands and legs apart and stand still for 2-3 seconds. A static trial was recorded first before starting any activity. While performing the trials, if a subject happened to lose any markers, a new static was recorded before the start of next trial to aid in accurate measurements. The skeleton and static are an important part as the average location of the markers are determined using all frames of the data and were later used to compute the kinematic model.

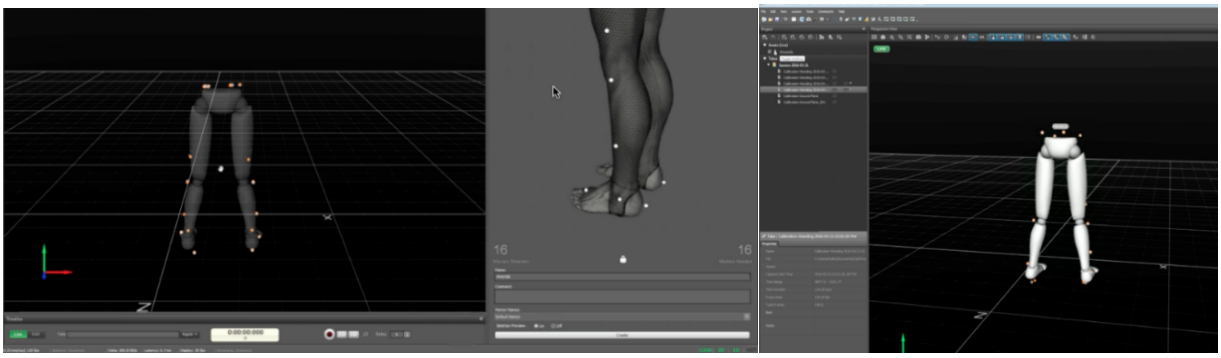

Figure 21: Skeleton creation and static take

All the subjects performed two types of activities (jump and run) four times. The trials started when the subjects were instructed by the research member to start. The subjects stood still for three seconds for the calibration of the APDM opal sensors and then would start the activity upon the instruction given by the researcher. This three seconds time was known as the buffer area and was used to help eliminate the drift from the gyroscopic data during calculations. Simultaneously, the trial would be recorded on the Optitrack motive window. The subjects were allowed to practice the activities on the walkway before starting to record the data to make them feel comfortable while actually performing and to avoid any occurrences of redoing the trials.

The subject would make a run on the walkway by stepping on both the force plates for a run trial (Figure 22), and for a jump trial would jump off a 30cm wooden box placed on the walkway to hit both the force plates once and then jump up again and land on the force plates for a second jump (Figure 23). Testing required two operators, one that operated the computer and recorded the data, and the other would observe the subject to make sure no marker falls off or the sensors and to make notes in the laboratory book regarding all the events taking place. Each trial ended when the subject relaxed after performing the activities and would not take any longer than 10 seconds to complete and the whole study was completed in approximately 60 minutes which included calibration of the systems and marker and sensor placement.

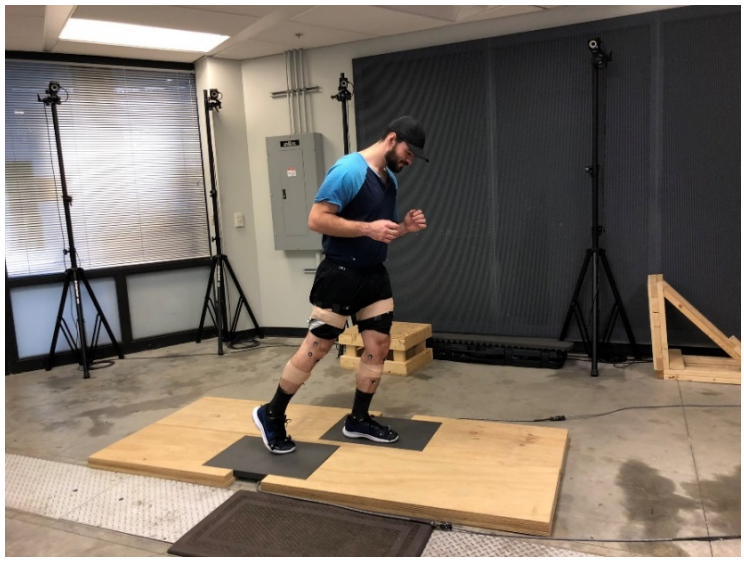

Figure 22: Subject performing a run

Figure 23: Subject performing a jump

3.5 Data Analysis

3.5.1 Motive and Visual 3D Data

The processing of the kinematic data after recording all the trials was done using the Optitrack software and the kinetic data related to the ground reaction forces was acquired from the two force plates. The sampling rate of the cameras and the force plates was set at 240Hz. All the markers were assigned to their respective locations and the extra sixteen markers were assigned to the

thighs and shank manually (four to each thigh and four to each shank of the legs). Each trial was viewed and the markers were tracked manually when the automatic tracking failed. This was done to ensure smooth tracking and better construction of the rigid body (Figure 24). Once the editing was completed for all the trials they were saved as .c3d files.

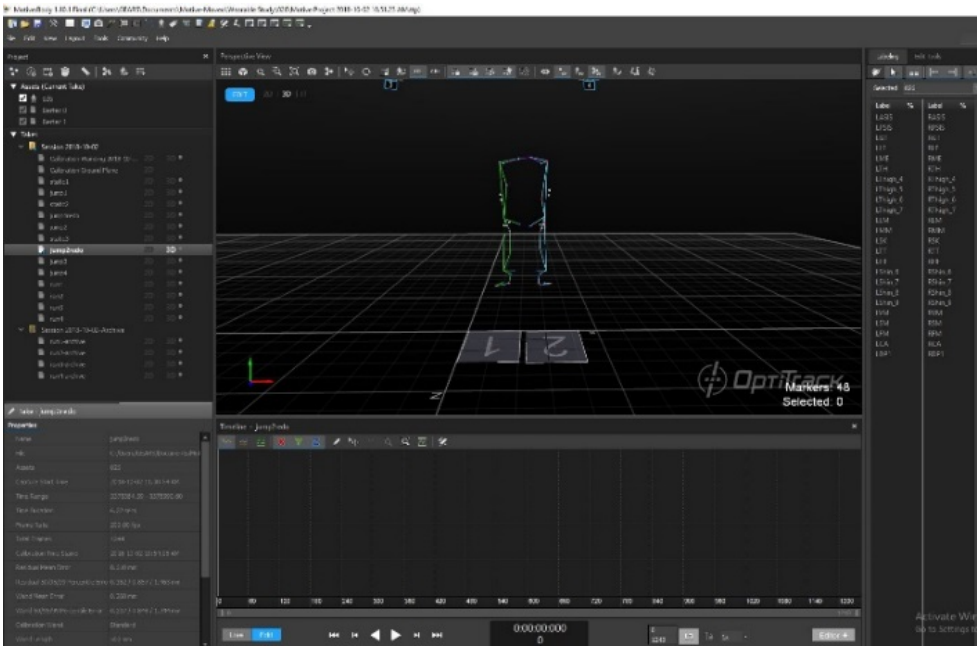

Figure 24: A completely edited trial in Motive

Data collected from the Motive system were analyzed using Visual 3D. Each trial was edited and exported as a .c3d file to run in visual 3D. All the files were then opened and processed using Visual 3D. The linked segments used to build the lower body were pelvis, thigh, shank and foot. Instead of building each segment separately which was time consuming for many subjects a pipeline was used to for all the files to create the body segments to build a rigid body model. A pipeline is a set of commands in Visual 3D which are processed in a sequence. The height and weight of the subject was entered into the program in order to create local coordinate system of the pelvis, thigh, lower leg, angle and foot. Before running the pipeline the corresponding static trial was assigned to each trial take by importing the static .c3d files. A static trial is a recording taken with the subject being stationary which can also be considered as a calibration trial which is used to define the link model which is a collection of landmarks, segments and muscles. From the static trial, a lower extremity kinematic model was created for each subject, which included the pelvis, thigh, shank and foot. This kinematic model was used to quantify the motion at hip, knee and ankle joints.

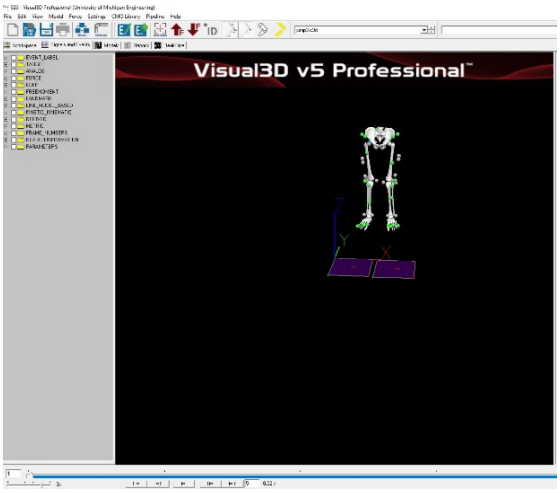

Figure 25: Rigid body in Visual 3D

After all the frames were constructed using the pipeline, another pipeline was run to calculate the kinetic data (vertical and posterior ground reaction forces) which gave the frame number at which these movements occurred. Additional kinematic data and mathematical analyses was completed using Visual 3D with plots for each trial.

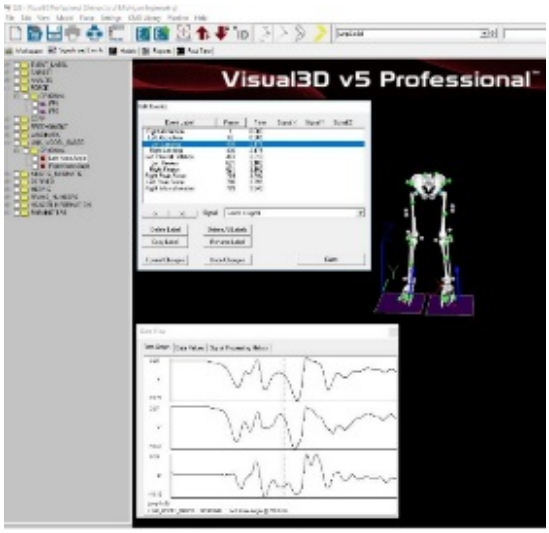

Figure 26: Parameters obtained from Visual 3D

The coordinate system directions for the medial and lateral of the left and right sides are different. The sign convention for angles is also different due to this i.e. the inward rotation of the right leg about the long axis towards medial is positive but the inward rotation of the left leg about the long axis towards medal is negative. In Visual 3D the direction of the angles are determined with respect to the segment coordinate system using the 'Right Hand Rule'. The flexion/extension have the

same sign for both left and right legs, but the inward/outward rotation and abduction/adduction have the opposite signs. Figure 26 represents the knee coordinate system used by Visual 3D.

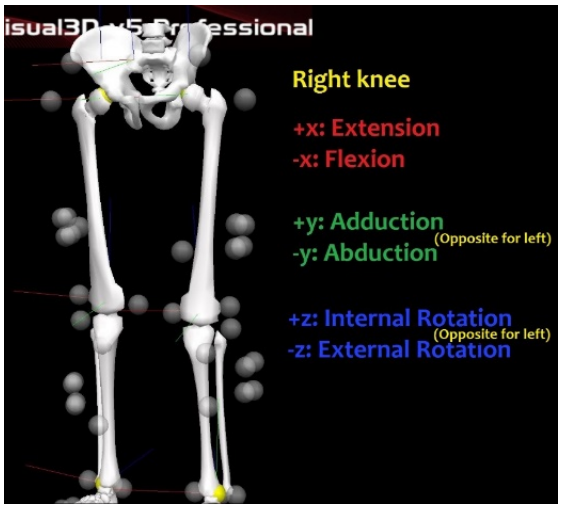

Figure 27: Knee coordinate system

3.5.1.1 Joint Angles at Peak Ground Reaction Force

A joint angle is known as the angle between two segments on the either side of a joint. It is measured in degrees and is relative to the segment angles i.e. it does not change with body's orientation. The knee joint angles at peak forces were obtained for left and right knees.

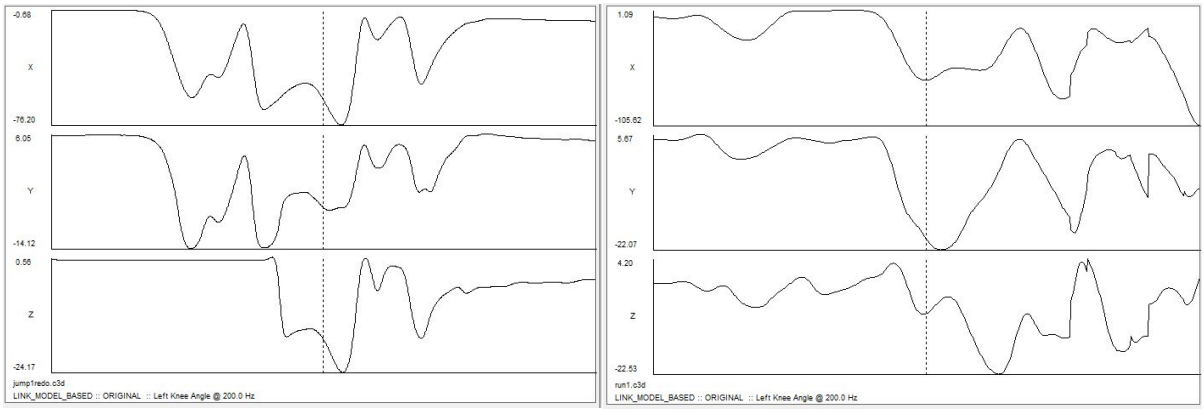

Figure 28: Waveforms for left knee angle (a) Jump (b) Run

Figure 28 shows the waveform of joint angles from visual 3D in all the three directions (X-Flexion, Y-Abduction, Z-internal rotation). The frame number where the peak force was maximum was obtained from Visual 3D for both left and right legs and the angles at the peak forces in all the three directions i.e. X, Y and Z were tabulated into excel.

3.5.1.1.1 Normalization

The standing posture is considered to be a reference posture from which all the joint angles are computed. All the joint angles during a standing pose are considered to be zero. Angle normalization is a method where a joint angle is referenced to a reference posture (standing posture or still posture). Normalization is used to clean up errors in determining the segment coordinate system caused by the misplacement of markers. Initially for normalization we assumed that the angle values obtained from a standing position in X (+ flexion/ -extension), Y (+valgus/- varus) and Z (+internal rotation/- external rotation) directions for a subject can be subtracted from the joint angles obtained at peak ground reaction force but the joint angles are not vector quantities, which means they cannot be added or subtracted. Therefore the normalized joint angles could not be obtained by simply subtracting the joint angles in the reference position from the joint angles at a given frame of data or at the peak ground reaction. A method proposed by the Visual 3D software was later used for normalization in this study to calculate the normalized joint angles. This method used a reference segment by creating a reference shank and the corresponding normalized joint angles were obtained in Visual 3D at peak ground reaction force and compared.

3.5.1.2 Ground Reaction Force

The vertical ground reaction force was measured using the force plates mounted on the ground for both jump and run activities. The maximum of the force in Z-direction was the maximum GRF from the force plate. The resultant force was calculated using the formula-

$$= \sqrt{(\text{force in x} - \text{direction})2 \ + (\text{force inY} - \text{direction})2 \ + (\text{force in Z} - \text{direction})2}$$

Figure 28 shows a typical waveform observed while jumping from a wooden box at a height of 30cm and landing with both feet at around same time on the force plates. The force is zero when the subject is standing still on the box and when the subject is in air, and it rises rapidly to a value significantly larger than ‘mg’ (‘m’ is the mass of the subject and ‘g’ is the acceleration due to gravity) when they land on the force plate and becomes zero again when the subject is in air for the second jump and is greater than ‘mg’ again while they land back on the force plate after the second jump and comes back to zero once they stand still. The two peaks in the Figure 29 represent the maximum vertical force exerted by the subject while performing the two jump activities in the Z-direction from the force plates.

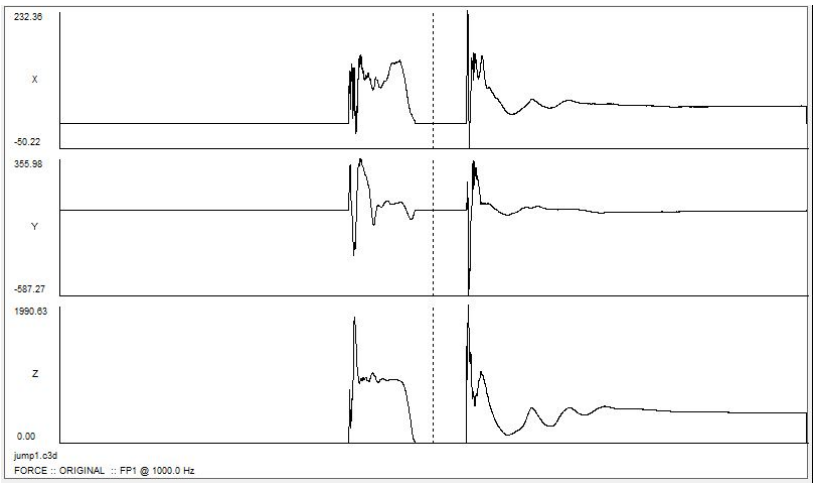

Figure 29: Wave form observed while jumping on the force plate for one leg

Since running differs from walking, in that there is a flight phase where both the feet are off the ground. Each foot is off the ground for 40% of the time during walking and 70%-80% off the ground while running [25] at different speeds. The vertical component of the ground force acting on one foot while running is shown in Figure 30 in the Z- direction from the force plate.

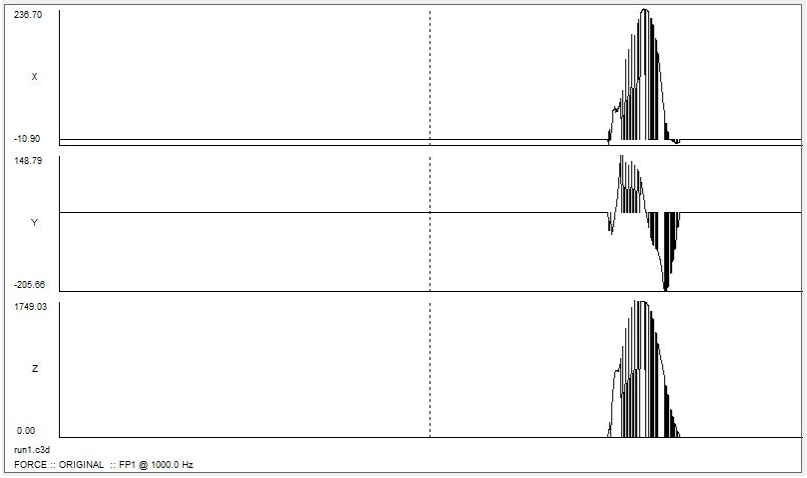

Figure 30: Waveform observed while running from the force plate for one leg

Generally, there is an initial spike when the foot lands on the force plate due to the heel strike, then there is an increase in the ground force, reaches maximum and then the ground force decreases rapidly as the subject crosses the force plate. Ground reaction force was reported as a percentage of body weight. This was calculated using each subject's mass and the maximum force in Z-direction from the force plates. The formula used for calculating percent body weight –

$$= \frac{maximum\ ground\ reaction\ force\ in\ Z{-}direction(N)}{mass(kg){*}9.81}$$

This GRF from force plates was correlated with the tibial acceleration from the sensor data.

3.5.2 APDM and MATLAB Data

The unprocessed joint angle data from the APDM wearable sensors after the recording of the trials is shown in the Figures 31 and 32.

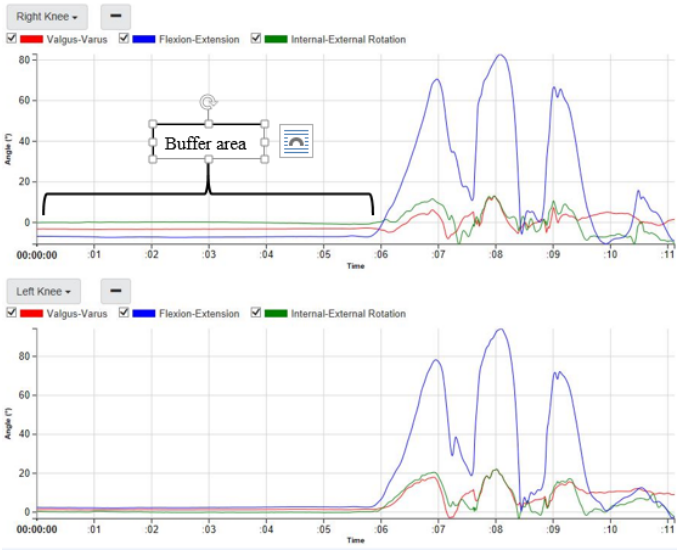

Figure 31: Unprocessed Jump APDM data using Moveo

The buffer time can be seen in Figure 31 and 32 at the start of each trial, where the subject was standing still.

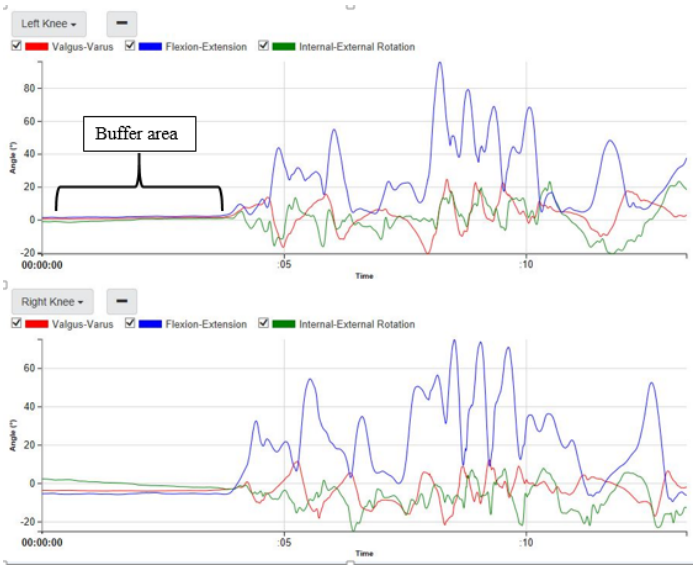

Figure 32: Unprocessed Run data using Moveo

The coordinate system for the joint angles for the APDM opal sensors is shown in Figure 33.

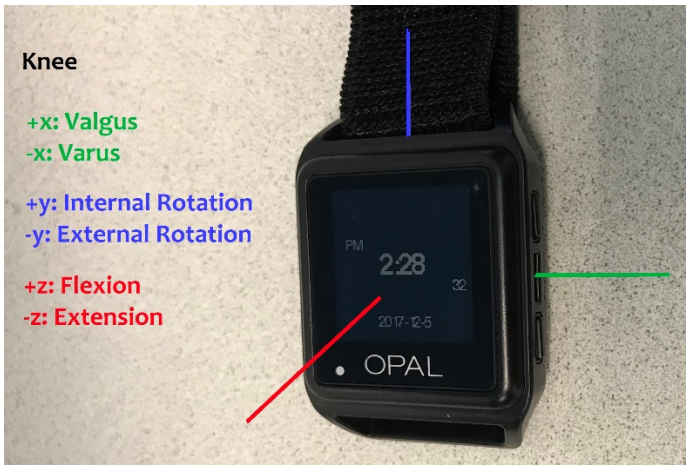

Figure 33: Knee coordinate system for APDM opal sensor

The unprocessed trials were exported from the Moveo software in the '.h5' format. The raw data were processed using a custom written script in Matlab which could read the '.h5' files and generate the required output with related graphs. The Matlab script gave acceleration data and the knee angles of the lower limb for both left and right legs. The acceleration and angle data was recorded into Excel separately for further mathematical analyses. The acceleration from the opal sensors for each activity was obtained from running the MATLAB script as seen in the Figures 34 and 35.

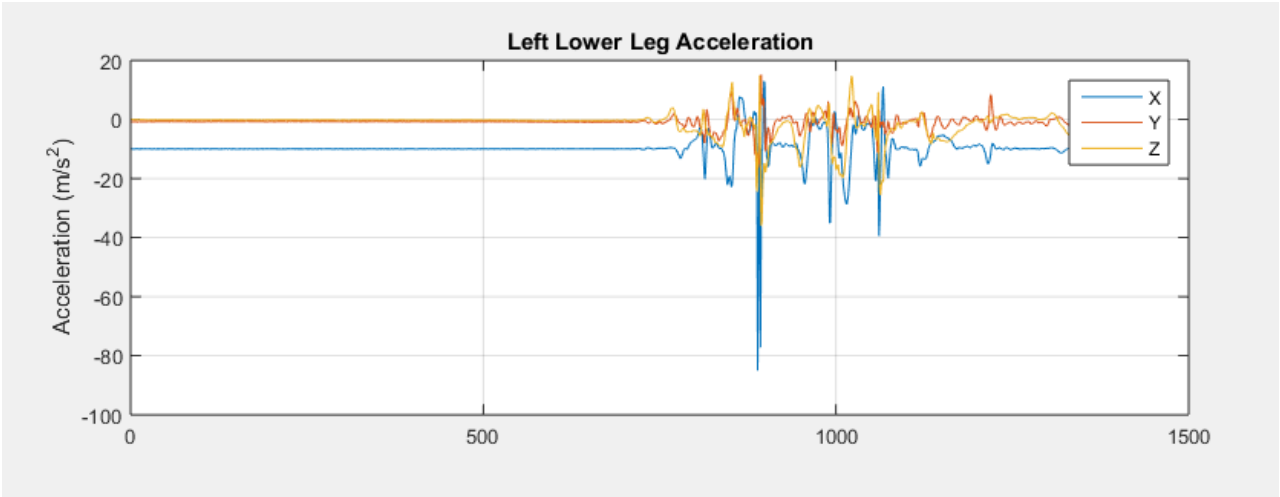

Figure 34: Acceleration plot for Jump trial

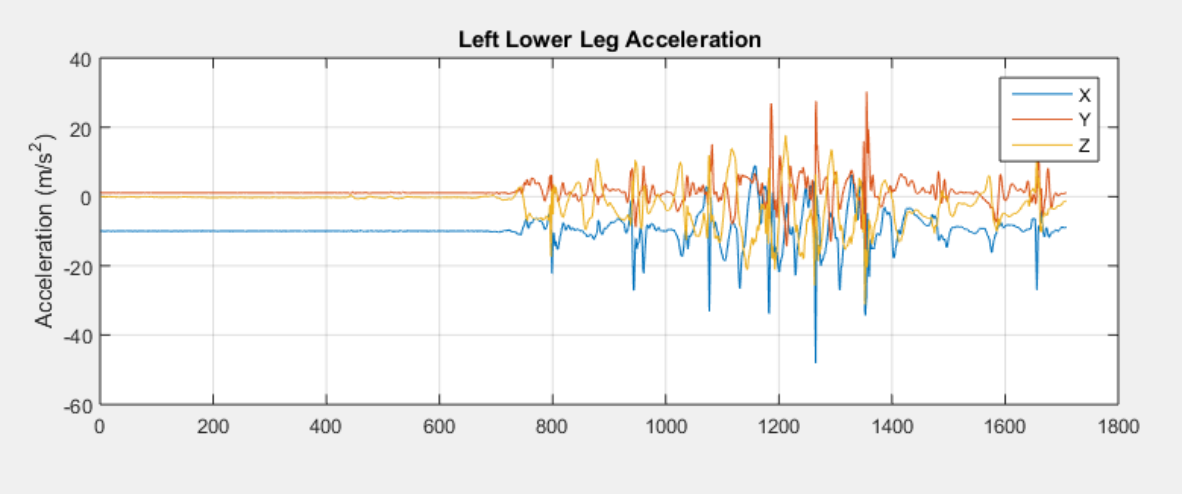

Figure 35: Acceleration plot for run trial

The graphs obtained from the MATLAB script were used for further analysis of the gait parameters. The MATLAB script was written to calculate at what particular point/frame the maximum peak occurred and the angles at those peaks. These frame numbers at maximum peaks were used to find out the minimum acceleration at that point. Using the data cursor in Matlab, these frame number and the angles were cross verified from the plots. The tibial acceleration was in the negative X-direction for both the jump and run trials.

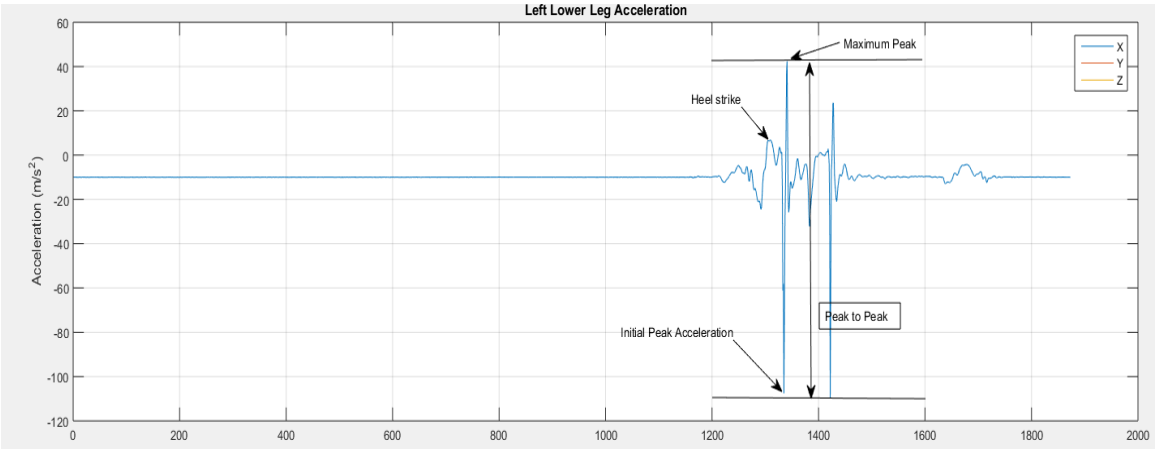

Figure 36: Typical acceleration graph in X-direction from sensors for jump trial

Analyzation of the run trials posed a difficult challenge from the graphs as there were many instances where the foot would come in contact with the ground giving rise to many peaks in the graphs. So it was difficult for the MATLAB script to generate the exact frame numbers for maximum peaks with respect to the force plates. This was overcome by cross verifying the frame

numbers obtained from MATLAB and watching the videos from the Optitrack Motive software, i.e. the point at which the foot hit the force plates and its peak obtained. The APDM opal sensors sampled accelerations at 128Hz.

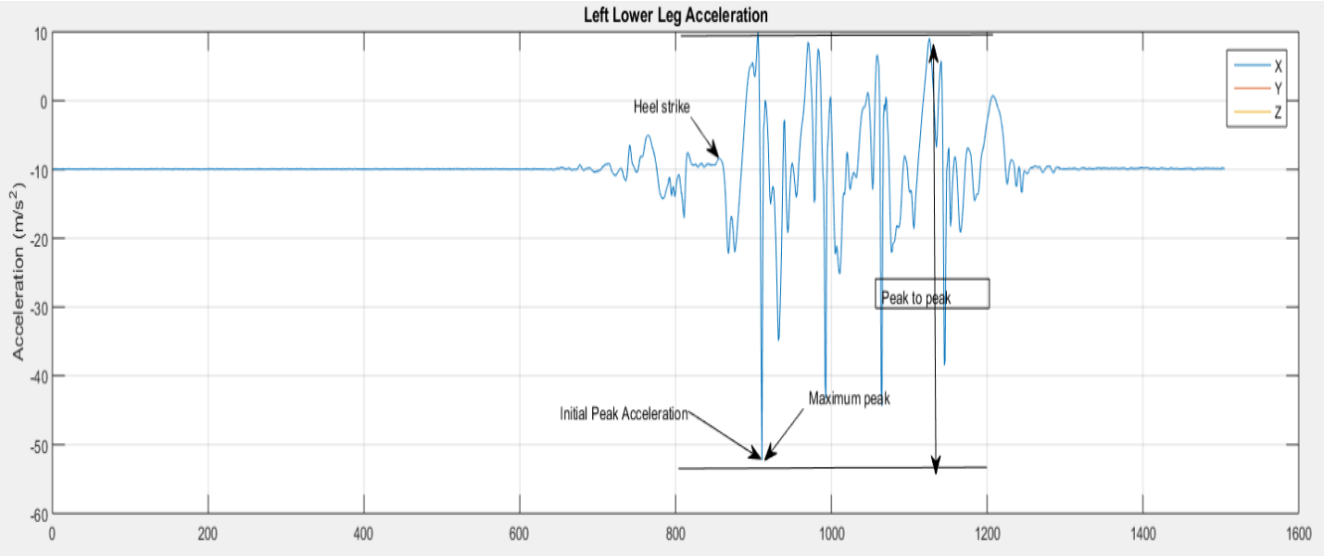

Figure 37: Typical acceleration graph in X-direction from sensors for run trial

3.5.2.1 Angles at Peak Ground Reaction Force

The APDM opal sensors use a kalman filter for orientation estimation with the complex fusion of accelerometer, gyroscope and magnetometer [6]. The orientation estimates are given using the quaternion format where the first component is the scalar part and the last three components are the x-y-z complex part. The quaternions are used to represent orientations for mathematical properties but for the interpretation, Euler angles are used. Euler angle representation describe 3 rotations in this order: flexion/extension, abduction/adduction, and internal/external rotation.

The data stored in the output files (csv and .h5 files) from the APDM opal sensors are all in the sensor's frame of reference. The x-axis gyroscope data refers to rotational velocities about the movement monitor's x-axis. The orientation data can be used to transform sensor frame data to earth's frame of reference using MATLAB scripts. The MATLAB script generated the angles at peak force directly, they were tabulated into Excel and compared to the angles obtained at peak force from the motion capture system.

3.5.2.2 Tibial Acceleration

A typical representation of the tibial acceleration is represented in the Figures 36 and 37 for a jump and run trial. There was an occurrence of four events namely, heel-strike, Initial peak acceleration (during first jump), maximum peak and peak-to-peak. This tibial acceleration was correlated with the vertical GRF obtained from the force plates shown in Figures 28 and 29 for jump and run activities in the Z-direction. The minimum acceleration in the X-direction from the sensors was calculated using the formula-

$$= \frac{(minimum\ acceleration\ in\ X{-}direction){+}(9.81)}{(-9.81)}$$

According to the coordinate system of the APDM opal sensors the up and down direction is equivalent to the x-direction. Acceleration is positive as the subject is falling, zero when the subject initially lands on the ground and is negative as the subject is decelerating which can be seen in Figures 36 and 37 for both jump and run trials. The maximum ground reaction force occurs when acceleration peaks in the negative direction (Figure 36 and 37). These time points were confirmed using the data from the force plate (Figure 29 and 30). Similarly the knee flexion angles were recorded at these two time points and compared with values found using the motion capture system.

CHAPTER 4: RESULTS AND DISCUSSION

The purpose of the study was to validate the APDM system against the Optitrack Motive system. The study examined the correlation between knee angles at peak forces and the vertical ground reaction force with tibial acceleration.

4.1. Knee Joint Angles at Peak Ground Reaction Force

The knee joint angle data at the peak ground reaction force from the Optitrack motion capture system were compare with the APDM sensor system. The data in the tables 10-14 represent all the trials performed by the subjects, the joint angle values in three directions(X, Y, and Z) obtained from the motion capture system and the sensors for left and right leg and the difference values. The coordinate system for knee angles is as follows-

X-direction (+ flexion/ -extension)

Y-direction (+valgus/- varus)

Z-direction (+internal rotation/- external rotation)

4.1.1 Jump Results

The knee joint angles at peak ground reaction force for each jump were calculated in all the three directions(X, Y and Z) for flexion/extension, abduction/adduction and internal/external rotation. The average difference for the knee flexion angle between the APDM opal wearable sensors and the motion capture system was 10.96° during the first jump for left leg and was 8.13° for the right leg (Table 14). The average difference for abduction was 5.78° for left leg for the same first jump and 6.94° for right leg (Table 14). The average difference for internal rotation was 5.76° for left leg and 5.60° for right leg (Table 14). The average difference between the APDM opal sensors and the motion capture system for flexion during the second jump was 11.65° for left leg and 9.91° for the right leg (Table 15). The average difference for abduction was 5.86° for left leg and 4.89° for right leg (Table 15). The average difference for internal rotation during second jump was 4.46° for

the left leg and 3.54° for the right leg (Table 15). The knee flexion angles was in a range of 20° to 55° for both the APDM opal wearable sensors and the motion capture system for both the legs. The range of the abduction angles was of 0.07° to 18° for both the systems and the range of internal rotation was in a range of 0.08° to 12° during jumping (Table 10, 11, 12 and 13). Table 12 shows the normalized joint angle values from the motion capture system and the sensors with their differences.

After the data were normalized using the joint angle normalization method the average difference improved slightly for most angles. The average difference for the knee flexion angle between both the systems was 9.65° and 8.73° for left and right legs respectively during first jump (Table 14). The average difference for abduction was 5.45° and 5.48° for left and right legs during the same jump. The average difference for the internal rotation was 4.10° and 3.60° for left and right legs (Table 14). The average difference during the second jump for the knee flexion angle was 10.75° and 9.62° for left and right legs (Table 15). The average difference for abduction in for left and right leg was 5.47° and 6.23° (Table 15). The average difference was 4.54° and 4.64° for left and right leg internal rotation (Table 15). The range of knee flexion after normalization was 16.12° to 50°, range for abduction was 0.13° to 18° and the range for internal rotation was 0.19° to 16° for both the systems (Table 10, 11, 12 and 13). The angles in all three directions i.e. X (flexion/extension), Y (abduction/adduction) and Z (internal/external rotation) were compared individually for all the eight subjects. Tables 10-13 show the results of joint angle data for flexion, abduction and internal rotation for a jump activity.

Table 10: Knee joint angles for first jump

Peak 1												
LEFT	X				Y				Z			
Subject	Trial	Motion Ca	Opal Sens	Diff		Motion Ca	Opal Sens	Diff		Motion Ca	Opal Sens	Diff
1	Trial 1	48.87	51.30	2.43		4.95	2.24	2.71		11.93	15.43	3.50
	Trial 2	53.00	41.96	11.04		18.12	16.16	1.96		5.00	6.50	1.50
	Trial 3	37.99	54.41	16.42		13.20	15.36	2.16		0.04	13.38	13.34
2	Trial 1	49.88	53.24	3.36		7.78	5.03	2.75		9.50	3.55	5.95
	Trial 2	48.61	35.89	12.72		7.88	10.18	2.29		9.70	1.74	7.96
	Trial 3	54.06	54.29	0.23		7.92	7.97	0.04		8.88	7.24	1.65
3	Trial 1	23.96	28.33	4.37		9.13	0.66	8.47		12.23	8.03	4.20
	Trial 2	25.25	27.56	2.31		8.93	2.06	6.87		12.95	2.74	10.21
	Trial 3	23.43	25.81	2.38		7.54	2.74	4.80		11.79	6.26	5.53
	Trial 4	22.16	27.07	4.91		9.15	6.30	2.85		12.64	7.98	4.66
4	Trial 1	45.98	23.02	22.96		7.35	3.69	3.66		3.02	2.92	0.10
	Trial 2	45.85	31.41	14.44		8.88	1.38	7.50		0.45	4.57	4.12
	Trial 3	48.13	34.92	13.21		10.21	5.68	4.53		1.05	9.94	8.89
5	Trial 1	35.10	26.43	8.67		14.07	15.86	1.79		6.13	6.94	0.81
	Trial 2	37.36	26.58	10.78		11.42	10.68	0.74		4.04	13.27	9.23
	Trial 3	46.16	30.96	15.19		13.38	12.04	1.33		2.86	11.89	9.03
	Trial 4	34.31	30.96	3.35		9.51	12.04	2.53		6.09	11.89	5.80
6	Trial 1	58.17	61.26	3.09		10.42	2.32	8.10		13.62	9.32	4.30
	Trial 2	55.09	57.31	2.22		11.58	3.07	8.51		12.61	6.25	6.36
	Trial 3	55.73	48.44	7.29		15.09	4.43	10.66		10.85	0.58	10.27
	Trial 4	59.22	63.23	4.01		17.06	2.07	14.99		10.23	4.30	5.93
7	Trial 1	43.49	33.19	10.31		8.39	14.72	6.32		6.04	17.46	11.42
	Trial 2	45.51	32.19	13.32		2.22	15.21	12.99		17.23	19.90	2.67
	Trial 3	41.25	34.60	6.65		1.17	14.14	12.96		16.87	18.54	1.67
	Trial 4	43.72	33.66	10.06		2.26	11.10	8.84		16.51	16.37	0.14
8	Trial 1	41.03	4.59	36.44		0.13	5.43	5.30		8.91	1.77	7.14
	Trial 2	37.68	6.63	31.05		6.45	11.62	5.17		0.00	4.58	4.58
	Trial 3	39.84	6.08	33.76		3.23	14.23	11.01		6.41	2.28	4.13
Average		42.89	35.19	10.96		8.84	8.16	5.78		8.49	8.41	5.54

Peak 1												
RIGHT	X				Y				Z			
Subject	Trial	Motion Ca	Opal Sens	Diff		Motion Ca	Opal Sens	Diff		Motion Ca	Opal Sens	Diff
1	Trial 1	46.27	35.20	11.07		4.54	10.09	5.55		11.59	11.77	0.18
	Trial 2	53.00	44.98	8.02		18.12	8.73	9.39		5.00	11.60	6.60
	Trial 3	37.99	32.65	5.34		13.20	8.18	5.02		0.04	2.77	2.73
2	Trial 1	49.63	47.37	2.26		2.00	4.98	2.98		9.21	3.16	6.05
	Trial 2	41.82	41.89	0.06		1.84	0.38	1.45		9.27	3.80	5.47
	Trial 3	48.56	47.76	0.80		3.49	5.23	1.73		10.59	3.21	7.38
3	Trial 1	53.96	37.83	16.13		9.13	15.21	6.08		12.23	1.16	11.07
	Trial 2	52.69	44.73	7.96		8.77	18.34	9.57		13.22	1.98	11.24
	Trial 3	53.44	34.25	19.19		7.54	16.27	8.73		11.79	0.80	10.99
	Trial 4	28.40	37.00	8.60		6.81	11.42	4.61		15.29	6.57	8.72
4	Trial 1	45.98	51.77	5.79		7.35	2.49	4.86		3.02	0.64	2.38
	Trial 2	45.85	49.35	3.50		8.88	4.48	4.40		0.45	3.86	3.41
	Trial 3	45.63	49.21	3.58		9.84	4.78	5.06		0.08	4.04	3.96
5	Trial 1	37.24	40.87	3.63		10.76	0.34	10.43		6.76	6.78	0.02
	Trial 2	39.66	42.14	2.48		9.89	0.41	9.48		5.27	7.37	2.11
	Trial 3	39.06	44.49	5.43		9.55	0.62	8.93		5.86	9.11	3.25
	Trial 4	36.36	48.14	11.78		8.20	4.04	4.16		7.34	1.04	6.30
6	Trial 1	48.60	32.39	16.21		10.96	2.66	8.30		14.55	3.56	10.99
	Trial 2	55.09	56.24	1.15		11.58	2.14	9.44		12.61	4.08	8.53
	Trial 3	63.83	52.79	11.04		17.07	2.86	14.21		14.47	0.34	14.13
	Trial 4	61.84	56.10	5.74		17.46	4.20	13.26		11.86	0.87	10.99
7	Trial 1	44.32	44.87	0.55		1.93	2.24	0.31		18.06	18.50	0.44
	Trial 2	48.28	44.10	4.18		3.07	0.12	2.96		18.05	16.17	1.88
	Trial 3	45.89	41.77	4.12		3.08	17.76	14.68		17.39	13.11	4.28
	Trial 4	47.17	40.17	7.00		0.74	16.14	15.40		19.80	12.43	7.37
8	Trial 1	44.23	27.29	16.94		2.26	6.12	3.86		4.34	2.72	1.62
	Trial 2	40.30	13.93	26.38		0.61	6.24	5.63		4.70	6.05	1.36
	Trial 3	42.76	23.99	18.76		1.66	5.55	3.89		10.70	7.28	3.43
Average		46.35	41.55	8.13		7.51	6.50	6.94		9.77	5.88	5.60

Table 11: Knee joint angles for second jump

Peak 2												
LEFT	X				Y				Z			
Subject	Trial	Motion Ca	Opal Sens	Diff		Motion Ca	Opal Sens	Diff		Motion Ca	Opal Sens	Diff
1	Trial 1	49.14	54.21	5.06		7.34	18.18	10.85		9.09	11.47	2.38
	Trial 2	44.83	40.53	4.30		12.27	19.46	7.19		12.01	17.12	5.10
	Trial 3	40.61	51.13	10.52		15.04	19.79	4.75		2.34	7.51	5.17
2	Trial 1	46.53	49.90	3.37		4.55	5.33	0.78		7.02	8.60	1.58
	Trial 2	48.25	49.88	1.63		2.83	7.60	4.77		5.15	11.71	6.56
	Trial 3	45.86	52.94	7.08		7.04	6.80	0.24		8.26	10.49	2.23
3	Trial 1	19.21	12.42	6.79		5.81	1.78	4.03		14.22	9.19	5.03
	Trial 2	27.30	18.42	8.88		2.52	7.11	4.59		11.03	4.51	6.52
	Trial 3	31.84	14.53	17.31		7.27	0.19	7.08		15.41	11.67	3.74
	Trial 4	26.98	13.84	13.14		6.40	1.54	4.86		15.39	9.06	6.33
4	Trial 1	45.41	28.64	16.76		5.20	0.94	4.26		9.89	1.54	8.35
	Trial 2	48.65	27.60	21.04		9.34	0.69	8.65		1.36	1.77	0.42
	Trial 3	43.92	30.83	13.09		9.01	3.13	5.88		2.12	5.28	3.16
5	Trial 1	29.41	22.14	7.27		7.72	6.04	1.68		3.64	7.64	4.00
	Trial 2	34.56	23.55	11.02		8.95	4.66	4.28		13.60	9.21	4.39
	Trial 3	32.56	23.37	9.19		9.47	5.63	3.84		6.42	10.01	3.59
	Trial 4	29.12	22.69	6.43		7.26	4.27	2.99		6.87	8.98	2.11
6	Trial 1	47.50	43.24	4.26		0.12	1.00	0.88		17.25	8.20	9.05
	Trial 2	45.64	46.80	1.15		11.00	1.18	9.82		8.46	6.35	2.11
	Trial 3	46.82	42.87	3.95		0.00	7.21	7.20		15.55	1.78	13.77
	Trial 4	57.21	61.33	4.12		14.37	1.04	13.33		12.85	6.06	6.79
7	Trial 1	34.63	26.45	8.18		6.08	9.49	3.41		16.85	16.37	0.48
	Trial 2	32.41	25.75	6.66		1.05	7.10	6.05		11.17	9.89	1.28
	Trial 3	34.91	23.32	11.59		0.47	6.25	5.78		10.93	14.90	3.97
	Trial 4	32.94	22.89	10.05		0.66	7.16	6.50		14.28	15.00	0.72
8	Trial 1	34.81	1.11	33.70		0.00	13.35	13.35		8.44	0.78	7.66
	Trial 2	42.21	0.60	41.61		10.18	11.41	1.23		0.63	6.94	6.31
	Trial 3	41.91	3.84	38.07		2.87	18.63	15.76		5.11	2.99	2.12
Average		39.11	29.82	11.65		6.24	7.03	5.86		9.48	8.39	4.46

Peak 2												
RIGHT	X				Y				Z			
Subject	Trial	Motion Ca	Opal Sens	Diff		Motion Ca	Opal Sens	Diff		Motion Ca	Opal Sens	Diff
1	Trial 1	42.19	26.46	15.73		0.91	0.52	0.39		2.44	3.98	1.54
	Trial 2	41.40	27.84	13.56		10.88	9.99	0.89		4.50	0.08	4.42
	Trial 3	39.11	26.15	12.96		8.60	6.12	2.47		6.39	4.68	1.71
2	Trial 1	48.83	45.29	3.54		2.84	3.08	0.24		11.00	4.30	6.70
	Trial 2	46.88	41.89	4.99		6.95	0.38	6.57		12.52	3.80	8.72
	Trial 3	46.34	42.81	3.53		4.20	0.23	3.97		11.40	5.22	6.18
3	Trial 1	20.71	17.93	2.78		3.80	6.76	2.96		9.41	10.39	0.98
	Trial 2	28.76	29.77	1.01		0.38	11.65	11.27		9.91	3.97	5.94
	Trial 3	38.39	26.94	11.45		0.82	10.04	9.22		6.39	10.24	3.85
	Trial 4	30.82	27.04	3.78		4.59	8.78	4.19		12.54	3.31	9.23
4	Trial 1	47.84	48.30	0.46		0.07	4.12	4.05		4.02	6.62	2.60
	Trial 2	50.28	49.49	0.79		0.43	0.38	0.05		5.25	4.93	0.32
	Trial 3	44.72	43.96	0.76		0.96	1.09	0.13		2.77	0.93	1.84
5	Trial 1	26.33	38.00	11.67		8.84	0.34	8.50		12.21	2.54	9.67
	Trial 2	33.59	38.53	4.94		12.19	0.13	12.07		10.98	6.76	4.23
	Trial 3	33.00	39.17	6.17		8.56	1.03	7.54		6.83	6.57	0.26
	Trial 4	31.86	42.08	10.22		8.88	2.79	6.09		6.49	3.36	3.13
6	Trial 1	52.84	36.69	16.16		6.08	1.00	5.08		1.97	2.25	0.28
	Trial 2	48.84	34.51	14.34		5.29	2.71	2.58		1.08	2.53	1.45
	Trial 3	49.25	33.51	15.73		2.95	2.01	0.94		2.00	3.36	1.36
	Trial 4	60.07	47.22	12.86		7.96	3.40	4.56		2.63	0.90	1.73
7	Trial 1	38.26	24.64	13.62		7.25	9.67	2.42		16.85	13.33	3.52
	Trial 2	32.41	21.83	10.58		1.05	7.28	6.23		11.17	10.42	0.75
	Trial 3	36.34	20.89	15.45		0.11	7.53	7.42		11.09	11.78	0.69
	Trial 4	34.55	22.23	12.32		1.14	8.70	7.56		14.64	12.99	1.65
8	Trial 1	34.81	19.36	15.45		0.00	8.09	8.09		8.44	5.74	2.70
	Trial 2	40.55	22.63	17.92		9.82	14.61	4.79		1.08	4.44	3.36
	Trial 3	40.18	15.39	24.79		2.77	9.43	6.66		4.87	2.56	2.31
Average		39.97	32.52	9.91		4.58	5.07	4.89		7.53	5.43	3.25

Table 12: Normalized knee joint angles for first jump

Peak 1												
LEFT	X				Y				Z			
Subject	Trial	Motion Ca	Opal Sens	Diff		Motion Ca	Opal Sens	Diff		Motion Ca	Opal Sens	Diff
1	Trial 1	49.34	51.30	1.96		17.10	2.24	14.86		6.16	15.43	9.27
	Trial 2	51.52	41.96	9.56		14.84	16.16	1.32		6.94	6.50	0.44
	Trial 3	41.27	54.41	13.14		13.71	15.36	1.66		14.57	13.38	1.19
2	Trial 1	49.81	53.24	3.43		6.03	5.03	1.00		2.31	3.55	1.23
	Trial 2	48.17	35.89	12.29		6.02	10.18	4.15		1.86	1.74	0.12
	Trial 3	53.71	54.29	0.58		6.25	7.97	1.72		2.54	7.24	4.70
3	Trial 1	28.11	28.33	0.23		7.63	0.66	6.97		7.83	8.03	0.20
	Trial 2	26.50	27.56	1.06		7.31	2.06	5.25		9.10	2.74	6.36
	Trial 3	28.19	25.81	2.38		6.40	2.74	3.66		7.87	6.26	1.61
	Trial 4	25.04	27.07	2.03		7.42	6.30	1.12		10.65	7.98	2.67
4	Trial 1	41.00	23.02	17.98		4.95	3.69	1.26		11.69	2.92	8.77
	Trial 2	46.58	31.41	15.17		6.32	1.38	4.94		12.90	4.57	8.33
	Trial 3	49.35	34.92	14.43		7.00	5.68	1.32		12.10	9.94	2.16
5	Trial 1	33.69	26.43	7.26		12.57	15.86	3.29		11.25	6.94	4.32
	Trial 2	34.63	26.58	8.05		10.20	10.68	0.48		8.22	13.27	5.05
	Trial 3	42.44	30.96	11.48		12.39	12.04	0.34		7.32	11.89	4.57
	Trial 4	31.17	30.96	0.21		8.83	12.04	3.21		8.22	11.89	3.67
6	Trial 1	54.65	61.26	6.61		3.40	2.32	1.08		5.00	9.32	4.32
	Trial 2	51.91	57.31	5.40		12.16	3.07	9.09		1.70	6.25	4.55
	Trial 3	52.29	48.44	3.85		13.47	4.43	9.04		0.19	0.58	0.39
	Trial 4	55.45	63.23	7.78		14.75	2.07	12.68		1.40	4.30	2.90
7	Trial 1	40.66	33.19	7.48		7.72	14.72	6.99		6.04	17.46	11.42
	Trial 2	42.64	32.19	10.45		2.13	15.21	13.08		11.32	19.90	8.58
	Trial 3	39.21	34.60	4.60		1.02	14.14	13.12		11.40	18.54	7.15
	Trial 4	45.18	33.66	11.53		1.08	11.10	10.02		13.17	16.37	3.20
8	Trial 1	36.79	4.59	32.20		1.22	5.43	4.21		3.01	1.77	1.24
	Trial 2	34.96	6.63	28.33		5.90	11.62	5.72		7.68	4.58	3.10
	Trial 3	36.83	6.08	30.76		3.30	14.23	10.94		5.53	2.28	3.25
Average		41.82	35.19	9.65		7.90	8.16	5.45		7.43	8.41	4.10

Peak 1												
RIGHT	X				Y				Z			
Subject	Trial	Motion Ca	Opal Sens	Diff		Motion Ca	Opal Sens	Diff		Motion Ca	Opal Sens	Diff
1	Trial 1	36.91	35.20	1.71		12.35	10.09	2.26		7.95	11.77	3.82
	Trial 2	49.29	44.98	4.31		14.25	8.73	5.52		7.09	11.60	4.51
	Trial 3	28.37	32.65	4.28		13.71	8.18	5.53		14.57	2.77	11.81
2	Trial 1	43.75	47.37	3.63		7.59	4.98	2.61		7.13	3.16	3.97
	Trial 2	43.54	41.89	1.65		5.22	0.38	4.84		5.61	3.80	1.82
	Trial 3	44.65	47.76	3.11		8.09	5.23	2.86		5.76	3.21	2.55
3	Trial 1	51.79	37.83	13.96		10.95	15.21	4.26		0.77	1.16	0.39
	Trial 2	50.94	44.73	6.21		7.82	18.34	10.52		0.65	1.98	1.33
	Trial 3	51.37	34.25	17.12		7.58	16.27	8.69		0.01	0.80	0.79
	Trial 4	47.57	37.00	10.57		8.75	11.42	2.67		3.53	6.57	3.04
4	Trial 1	42.67	51.77	9.10		3.37	2.49	0.89		4.71	0.64	4.07
	Trial 2	41.20	49.35	8.15		0.91	4.48	3.57		11.72	3.86	7.86
	Trial 3	40.60	49.21	8.61		4.51	4.78	0.27		1.83	4.04	2.21
5	Trial 1	35.49	40.87	5.38		10.14	0.34	9.81		12.97	6.78	6.19
	Trial 2	36.84	42.14	5.30		9.50	0.41	9.09		12.89	7.37	5.52
	Trial 3	36.03	44.49	8.46		9.32	0.62	8.70		11.99	9.11	2.88
	Trial 4	33.26	48.14	14.88		7.99	4.04	3.95		12.92	1.04	11.88
6	Trial 1	49.30	32.39	16.91		8.51	2.66	5.85		5.08	3.56	1.52
	Trial 2	40.89	56.24	15.35		6.22	2.14	4.08		4.40	4.08	0.32
	Trial 3	43.00	52.79	9.79		8.16	2.86	5.30		4.66	0.34	4.32
	Trial 4	44.43	56.10	11.67		7.81	4.20	3.61		2.33	0.87	1.46
7	Trial 1	41.95	44.87	2.92		1.26	2.24	0.98		13.98	18.50	4.52
	Trial 2	45.62	44.10	1.51		2.62	0.12	2.51		13.47	16.17	2.69
	Trial 3	42.90	41.77	1.13		2.07	17.76	15.69		13.77	13.11	0.66
	Trial 4	45.18	40.17	5.01		1.08	16.14	15.06		13.17	12.43	0.74
8	Trial 1	39.84	27.29	12.55		21.31	6.12	15.19		9.18	2.72	6.46
	Trial 2	38.72	13.93	24.79		1.14	6.24	5.11		8.43	6.05	2.38
	Trial 3	40.47	23.99	16.48		1.61	5.55	3.94		8.32	7.28	1.05
Average		42.38	41.55	8.73		7.28	6.50	5.83		7.82	5.88	3.60

Table 13: Normalized knee joint angles for second jump

Peak 2												
LEFT	X				Y				Z			
Subject	Trial	Motion Ca	Opal Sens	Diff		Motion Ca	Opal Sens	Diff		Motion Ca	Opal Sens	Diff
1	Trial 1	41.46	54.21	12.75		13.20	18.18	4.99		10.41	11.47	1.06
	Trial 2	38.42	40.53	2.11		13.88	19.46	5.58		9.08	17.12	8.04
	Trial 3	36.49	51.13	14.64		13.66	19.79	6.13		13.95	7.51	6.44
2	Trial 1	45.92	49.90	3.98		5.60	5.33	0.27		20.88	8.60	12.28
	Trial 2	47.14	49.88	2.74		6.24	7.60	1.36		22.59	11.71	10.88
	Trial 3	46.67	52.94	6.27		5.30	6.80	1.50		20.76	10.49	10.27
3	Trial 1	16.12	12.42	3.70		4.93	1.78	3.15		12.02	9.19	2.83
	Trial 2	27.23	18.42	8.81		2.62	7.11	4.49		3.04	4.51	1.47
	Trial 3	28.24	14.53	13.71		6.71	0.19	6.52		11.07	11.67	0.60
	Trial 4	23.30	13.84	9.46		5.69	1.54	4.15		12.27	9.06	3.21
4	Trial 1	23.86	28.64	4.79		7.28	0.94	6.34		9.66	1.54	8.12
	Trial 2	28.80	27.60	1.19		7.16	0.69	6.48		11.59	1.77	9.82
	Trial 3	48.23	30.83	17.40		6.97	3.13	3.84		12.95	5.28	7.67
5	Trial 1	28.00	22.14	5.86		7.01	6.04	0.97		8.27	7.64	0.63
	Trial 2	30.68	23.55	7.13		9.51	4.66	4.85		9.13	9.21	0.08
	Trial 3	29.32	23.37	5.95		8.65	5.63	3.02		10.18	10.01	0.17
	Trial 4	25.72	22.69	3.03		6.84	4.27	2.57		9.63	8.98	0.64
6	Trial 1	26.42	43.24	16.82		0.97	1.00	0.03		5.20	8.20	3.00
	Trial 2	42.27	46.80	4.53		9.80	1.18	8.62		1.10	6.35	5.25
	Trial 3	57.48	42.87	14.61		18.73	7.21	11.52		3.70	1.78	1.92
	Trial 4	53.34	61.33	7.99		13.37	1.04	12.33		0.49	6.06	5.57
7	Trial 1	31.08	26.45	4.63		1.38	9.49	8.11		8.62	16.37	7.75
	Trial 2	30.42	25.75	4.67		1.94	7.10	5.16		7.65	9.89	2.24
	Trial 3	33.04	23.32	9.72		1.96	6.25	4.29		8.42	14.90	6.48
	Trial 4	34.07	22.89	11.17		0.57	7.16	6.59		10.90	15.00	4.10
8	Trial 1	32.60	1.11	31.49		0.53	13.35	12.82		1.05	0.78	0.26
	Trial 2	38.28	0.60	37.68		9.59	11.41	1.82		11.20	6.94	4.26
	Trial 3	37.96	3.84	34.12		2.92	18.63	15.71		5.03	2.99	2.04
Average		35.09	29.82	10.75		6.89	7.03	5.47		9.67	8.39	4.54
Peak 2												
RIGHT	X				Y				Z			
Subject	Trial	Motion Ca	Opal Sens	Diff		Motion Ca	Opal Sens	Diff		Motion Ca	Opal Sens	Diff
1	Trial 1	21.38	26.46	5.08		11.66	0.52	11.13		13.25	3.98	9.27
	Trial 2	23.81	27.84	4.03		15.34	9.99	5.35		4.28	0.08	4.19
	Trial 3	22.84	26.15	3.31		0.00	6.12	6.12		0.00	4.68	4.68
2	Trial 1	26.24	45.29	19.05		7.00	3.08	3.92		7.44	4.30	3.14
	Trial 2	48.48	41.89	6.59		5.76	0.38	5.38		4.89	3.80	1.09
	Trial 3	47.32	42.81	4.51		6.02	0.23	5.79		5.49	5.22	0.27
3	Trial 1	18.63	17.93	0.70		3.27	6.76	3.49		3.25	10.39	7.14
	Trial 2	29.53	29.77	0.24		0.22	11.65	11.42		3.59	3.97	0.38
	Trial 3	34.83	26.94	7.89		0.75	10.04	9.29		2.33	10.24	7.91
	Trial 4	27.68	27.04	0.64		4.21	8.78	4.57		4.45	3.31	1.14
4	Trial 1	44.21	48.30	4.09		0.04	4.12	4.08		6.57	-6.62	13.19
	Trial 2	44.14	49.49	5.35		1.27	0.38	0.89		7.33	4.93	2.40
	Trial 3	42.15	43.96	1.80		0.90	1.09	0.19		4.34	0.93	3.41
5	Trial 1	25.15	38.00	12.85		8.57	0.34	8.23		16.01	2.54	13.47
	Trial 2	30.68	38.53	7.85		11.25	0.13	11.12		15.55	6.76	8.79
	Trial 3	30.42	39.17	8.75		8.21	1.03	7.18		12.10	6.57	5.53
	Trial 4	28.29	42.08	13.79		7.77	2.79	4.99		13.14	3.36	9.79
6	Trial 1	21.46	36.69	15.23		3.35	1.00	2.35		12.00	2.25	9.75
	Trial 2	46.41	34.51	11.91		4.87	2.71	2.16		6.80	2.53	4.28
	Trial 3	49.94	33.51	16.43		0.66	2.01	1.35		4.18	3.36	0.81
	Trial 4	60.74	47.22	13.53		7.95	3.40	4.55		4.99	0.90	4.09
7	Trial 1	34.59	24.64	9.95		0.37	9.67	9.31		12.30	13.33	1.03
	Trial 2	34.40	21.83	12.57		2.72	7.28	4.56		9.98	10.42	0.44
	Trial 3	35.69	20.89	14.80		1.04	7.53	6.49		12.33	11.78	0.55
	Trial 4	34.07	22.23	11.83		0.57	8.70	8.13		10.90	12.99	2.09
8	Trial 1	35.91	19.36	16.54		19.58	8.09	11.49		7.57	5.74	1.83
	Trial 2	39.42	22.63	16.79		1.47	14.61	13.14		7.91	4.44	3.47
	Trial 3	38.58	15.39	23.19		1.81	9.43	7.62		8.29	2.56	5.73
Average		34.89	32.52	9.62		4.88	5.07	6.23		7.90	4.95	4.64

Table 14: Average difference for first jump

Average Difference- Peak 1											
Left						Right					
Flexion/extension		Abduction/Adduction		Internal/external rotation		Flexion/extension		Abduction/Adduction		Internal/external rotation	
W/O	W/ norm	W/O	W/ norm	W/O	W/ norm	W/O	W/ norm	W/O	W/ norm	W/O	W/ norm
10.96°	9.65°	5.78°	5.45°	5.76°	4.10°	8.13°	8.73°	6.94°	5.48°	5.60°	3.60°

Table 15: Average difference for second jump

Average Difference- Peak 2											
Left						Right					
Flexion/extension		Abduction/Adduction		Internal/external rotation		Flexion/extension		Abduction/Adduction		Internal/external rotation	
W/O	W/ norm	W/O	W/ norm	W/O	W/ norm	W/O	W/ norm	W/O	W/ norm	W/O	W/ norm
11.65°	10.75°	5.86°	5.47°	4.46°	4.54°	9.91°	9.62°	4.89°	6.23°	3.54°	4.64°

4.1.2 Run Results

The average difference of knee flexion between both the systems during running was 14.60° for left leg and 17.60° for the right leg (Table 20). The average difference for abduction was 6.97° and 6.75° for left and right legs (Table 20). The average difference for internal rotation was 5.05°and 4.40° for left and right leg. After applying the normalization method the average differences were found to be 14.30° and 14.78° for knee flexion angles for left and right legs respectively (Table 20). Normalization greatly improved accuracy for the right leg. The average difference for abduction angle was 7.97° and 5.80° for left and right leg (Table 20). The average difference for internal rotation was 6.60° and 5.69° for the left and right leg between the wearable sensors and the motion capture system.

After using the normalizing method to compute the joint angles, the jump results (Table 12 and Table 13) did not show a great improvement but the run results (Table 16 and Table 17) showed a

good improvement for most of the subjects. For the left leg, the flexion angles for subjects 2, 5, 6 and 7 were similar between the two systems before normalization. Whereas, differences were larger for subjects 1, 3, 4 and 8. After normalization, data were improved for subject 4 but only slightly improved for the other subjects. For the right leg, flexion angles were similar between the two systems for subjects 1, 4, 5 and 7. Whereas, for subjects 2, 3, 6 and 8 there was a larger discrepancy.

Table 16: Knee joint angles for run (Left leg)

LEFT	X				Y				Z			
Subject	Trial	Motion Capture	Opal Sensors	Diff		Motion Capture	Opal Sensors	Diff		Motion Capture	Opal Sensors	Diff
1	Trial1	43.75	43.90	0.15		9.41	11.95	2.54		6.44	7.42	0.98
	Trial2	32.17	46.12	13.95		1.66	0.63	1.03		13.10	5.01	8.09
	Trial3	42.14	42.72	0.58		0.77	13.02	12.25		10.01	5.77	4.24
	Trial4	36.75	49.86	13.11		0.41	1.23	0.82		13.63	13.24	0.39
2	Trial1	47.04	42.23	4.81		9.33	15.89	6.56		6.88	13.14	6.26
	Trial2	43.64	43.63	0.01		0.95	18.62	17.67		5.30	12.51	7.21
	Trial3	51.09	38.82	12.27		8.54	3.18	5.36		7.14	18.41	11.27
	Trial4	43.00	45.39	2.39		3.03	17.14	14.11		4.67	14.26	9.59
3	Trial1	36.73	37.02	0.29		0.64	5.86	5.22		15.46	5.92	9.54
	Trial2	31.20	17.45	13.75		2.92	9.93	7.01		6.62	10.31	3.69
	Trial3	34.63	17.89	16.74		0.72	6.64	5.92		15.13	9.29	5.84
	Trial4	24.35	12.96	11.39		0.41	9.78	9.37		5.23	14.77	9.54
4	Trial1	43.19	7.03	36.16		9.12	8.74	0.38		1.97	0.32	1.65
	Trial2	50.13	5.55	44.58		12.84	8.13	4.71		0.04	1.41	1.37
	Trial3	46.49	12.57	33.92		14.91	7.80	7.11		0.75	2.05	1.30
5	Trial1	46.98	38.28	8.70		15.53	18.64	3.11		0.84	2.94	2.10
	Trial2	39.92	41.88	1.96		8.29	19.39	11.10		1.03	12.60	11.57
	Trial3	40.27	27.34	12.93		8.67	14.40	5.73		0.87	9.07	8.20
	Trial4	32.90	26.28	6.62		5.86	9.25	3.39		7.83	6.68	1.15
6	Trial1	36.05	26.44	9.61		9.21	0.59	8.62		7.72	4.52	3.20
	Trial2	36.32	27.60	8.72		10.36	9.96	0.40		1.22	12.17	10.95
	Trial3	40.24	27.31	12.93		9.03	4.10	4.93		9.80	9.41	0.39
7	Trial1	27.82	28.63	0.81		1.68	15.24	13.56		15.72	14.33	1.39
	Trial2	46.51	25.40	21.11		4.31	10.49	6.18		17.11	11.73	5.38
	Trial3	39.99	13.56	26.43		4.51	12.25	7.74		13.42	7.59	5.83
	Trial4	42.45	28.33	14.12		5.65	12.51	6.86		13.97	11.32	2.65
8	Trial1	27.98	5.10	22.88		1.49	10.81	9.32		5.14	1.94	3.20
	Trial2	35.31	1.33	33.98		3.33	10.85	7.52		6.22	2.80	3.42
	Trial3	31.98	4.26	27.72		1.50	7.60	6.10		8.61	3.30	5.31
	Trial4	29.79	4.52	25.27		2.08	16.64	14.56		5.95	0.13	5.82
	Average	38.69	26.31	14.60		5.57	10.38	6.97		7.59	8.15	5.05

Table 17: Knee joint angles for run (right leg)

RIGHT	X				Y			Z		
Subject	Trial	Motion Capture	Opal Sensors	Diff	Motion Capture	Opal Sensors	Diff	Motion Capture	Opal Sensors	Diff
1	Trial1	39.33	32.56	6.77	1.60	18.63	17.03	1.91	8.50	6.59
	Trial2	42.95	31.09	11.86	4.95	9.48	4.53	0.79	7.21	6.42
	Trial3	34.31	24.37	9.94	2.90	8.04	5.14	0.97	0.58	0.39
	Trial4	33.18	19.33	13.85	3.75	14.42	10.67	0.86	2.82	1.96
2	Trial1	45.39	28.02	17.37	9.46	10.91	1.45	1.95	4.38	2.43
	Trial2	44.37	18.04	26.33	3.21	11.13	7.92	0.18	0.51	0.33
	Trial3	46.66	16.77	29.89	1.17	9.50	8.33	2.84	3.89	1.05
	Trial4	42.87	17.35	25.52	0.73	7.80	7.07	2.02	7.15	5.13
3	Trial1	32.91	35.22	2.31	3.67	11.51	7.84	5.21	9.02	3.81
	Trial2	27.81	28.35	0.54	4.45	12.28	7.83	1.88	2.03	0.15
	Trial3	33.91	32.45	1.46	6.39	15.85	9.46	0.14	10.08	9.94
	Trial4	26.20	29.78	3.58	4.00	17.82	13.82	1.60	2.11	0.51
4	Trial1	37.34	24.24	13.10	0.08	11.21	11.13	4.90	4.23	0.67
	Trial2	47.39	20.12	27.27	5.11	7.91	2.80	10.95	0.96	9.99
	Trial3	44.75	18.29	26.46	0.14	9.53	9.39	7.04	12.95	5.91
5	Trial1	45.13	29.26	15.87	18.84	0.15	18.69	10.33	10.82	0.49
	Trial2	48.22	14.25	33.97	14.53	0.01	14.52	5.40	1.32	4.08
	Trial3	41.54	21.81	19.73	11.52	5.10	6.42	9.12	2.97	6.15
	Trial4	35.22	11.59	23.63	10.44	1.98	8.46	6.84	4.46	2.39
6	Trial1	42.85	22.32	20.53	3.41	1.64	1.77	13.06	9.85	3.21
	Trial2	41.44	17.71	23.73	2.02	2.49	0.47	6.65	11.36	4.71
	Trial3	42.61	28.69	13.92	0.81	6.66	5.85	7.50	12.65	5.15
7	Trial1	47.24	22.59	24.65	4.60	9.44	4.84	20.02	13.20	6.82
	Trial2	45.28	22.32	22.96	5.79	9.52	3.73	15.53	9.91	5.62
	Trial3	49.89	20.79	29.10	5.00	8.95	3.95	18.10	8.43	9.67
	Trial4	46.48	23.50	22.98	5.43	9.23	3.80	16.35	3.67	12.68
8	Trial1	28.93	11.73	17.20	0.16	1.10	0.94	8.86	3.65	5.21
	Trial2	34.61	16.36	18.25	2.48	4.62	2.14	7.88	3.56	4.32
	Trial3	30.71	19.63	11.08	0.24	2.67	2.43	6.30	2.02	4.28
	Trial4	30.09	15.48	14.61	0.18	0.01	0.17	4.46	2.59	1.87
	Average	39.65	22.47	17.62	4.57	7.99	6.75	6.65	5.90	4.40

Table 18: Normalized knee joint angles for run (left leg)

LEFT	X				Y			Z		
Subject	Trial	Motion Capture	Opal Sensors	Diff	Motion Capture	Opal Sensors	Diff	Motion Capture	Opal Sensors	Diff
1	Trial1	29.10	43.90	14.80	5.60	11.95	6.35	6.51	7.42	0.91
	Trial2	33.41	46.12	12.71	6.47	0.63	5.84	17.29	5.01	12.28
	Trial3	31.98	42.72	10.74	3.46	13.02	9.56	0.65	5.77	5.12
	Trial4	36.55	49.86	13.31	4.36	1.23	3.13	11.48	13.24	1.76
2	Trial1	47.04	42.23	4.81	9.34	15.89	6.55	6.89	13.14	6.25
	Trial2	43.65	43.63	0.02	0.95	18.62	17.67	5.31	12.51	7.20
	Trial3	51.10	38.82	12.28	8.54	3.18	5.36	7.15	18.41	11.26
	Trial4	43.00	45.39	2.39	3.03	17.14	14.11	4.68	14.26	9.58
3	Trial1	37.10	37.02	0.08	1.67	5.86	4.19	0.94	5.92	4.98
	Trial2	30.90	17.45	13.45	0.10	9.93	9.83	0.39	10.31	9.92
	Trial3	31.45	17.89	13.56	0.03	6.64	6.61	2.48	9.29	6.81
	Trial4	23.12	12.96	10.16	0.08	9.78	9.70	1.54	14.77	13.23
4	Trial1	44.61	7.03	37.58	6.06	8.74	2.68	14.17	0.32	13.85
	Trial2	45.52	5.55	39.97	6.43	8.13	1.70	14.45	1.41	13.04
	Trial3	48.77	12.57	36.20	12.31	7.80	4.51	19.80	2.05	17.75
5	Trial1	43.72	38.28	5.44	13.35	18.64	5.29	8.20	2.94	5.26
	Trial2	36.90	41.88	4.98	7.06	19.39	12.33	4.37	12.60	8.23
	Trial3	37.40	27.34	10.06	6.94	14.40	7.46	4.41	9.07	4.66
	Trial4	30.56	26.28	4.28	3.54	9.25	5.71	2.74	6.68	3.94
6	Trial1	33.37	26.44	6.93	6.33	0.59	5.74	1.99	4.52	2.53
	Trial2	32.75	27.60	5.15	4.20	9.96	5.76	0.05	12.17	12.12
	Trial3	37.77	27.31	10.46	9.71	4.10	5.61	3.68	9.41	5.73
7	Trial1	32.33	28.63	3.70	0.03	15.24	15.21	11.68	14.33	2.65
	Trial2	42.36	25.40	16.96	1.02	10.49	9.47	12.05	11.73	0.32
	Trial3	36.78	13.56	23.22	3.49	12.25	8.76	7.62	7.59	0.03
	Trial4	38.31	28.33	9.98	3.45	12.51	9.06	8.48	11.32	2.84
8	Trial1	26.17	5.10	21.07	0.64	10.81	10.17	5.01	1.94	3.07
	Trial2	33.11	1.33	31.78	1.95	10.85	8.90	5.26	2.80	2.46
	Trial3	31.20	4.26	26.94	0.95	7.60	6.65	7.52	3.30	4.22
	Trial4	30.52	4.52	26.00	1.60	16.64	15.04	5.99	0.13	5.86
	Average	36.68	26.31	14.30	4.42	10.38	7.97	6.76	8.15	6.60

Table 19: Normalized knee joint angles for run (right leg)

RIGHT	X				Y				Z			
Subject	Trial	Motion Capture	Opal Sensors	Diff	Motion Capture	Opal Sensors	Diff		Motion Capture	Opal Sensors	Diff	
1	Trial1	33.79	32.56	1.23	10.40	18.63	8.24		2.95	8.50	5.55	
	Trial2	36.86	31.09	5.77	12.69	9.48	3.21		6.57	7.21	0.64	
	Trial3	35.64	24.37	11.27	11.19	8.04	3.15		7.36	0.58	6.78	
	Trial4	31.09	19.33	11.76	9.85	14.42	4.57		5.48	2.82	2.65	
2	Trial1	38.12	28.02	10.11	9.46	10.91	1.45		6.51	4.38	2.13	
	Trial2	35.76	18.04	17.72	5.29	11.13	5.83		7.36	0.51	6.85	
	Trial3	34.42	16.77	17.65	9.51	9.50	0.01		9.45	3.89	5.56	
	Trial4	37.98	17.35	20.63	5.21	7.80	2.59		2.85	7.15	4.30	
3	Trial1	32.24	35.22	2.98	3.28	11.51	8.23		6.68	9.02	2.35	
	Trial2	29.61	28.35	1.26	3.70	12.28	8.58		6.91	2.03	4.88	
	Trial3	36.55	32.45	4.11	6.09	15.85	9.76		8.70	10.08	1.38	
	Trial4	24.84	29.78	4.94	3.20	17.82	14.62		7.33	2.11	5.22	
4	Trial1	34.56	24.24	10.32	1.19	11.21	10.02		7.12	4.23	2.89	
	Trial2	34.48	20.12	14.36	4.21	7.91	3.69		2.34	0.96	1.38	
	Trial3	42.48	18.29	24.20	0.67	9.53	8.85		5.82	12.95	7.14	
5	Trial1	39.73	29.26	10.47	16.97	0.15	16.82		20.62	10.82	9.80	
	Trial2	44.43	14.25	30.18	14.12	0.01	14.11		16.27	1.32	14.94	
	Trial3	40.45	21.81	18.64	10.97	5.10	5.87		16.74	2.97	13.77	
	Trial4	40.01	11.59	28.42	10.54	1.98	8.56		0.08	4.46	4.37	
6	Trial1	38.24	22.32	15.92	5.13	1.64	3.49		1.24	9.85	8.61	
	Trial2	41.26	17.71	23.55	2.09	2.49	0.40		2.23	11.36	9.13	
	Trial3	40.61	28.69	11.92	1.34	6.66	5.32		2.31	12.65	10.34	
7	Trial1	44.77	22.59	22.19	2.59	9.44	6.86		12.64	13.20	0.57	
	Trial2	43.16	22.32	20.84	5.29	9.52	4.24		8.76	9.91	1.15	
	Trial3	47.47	20.79	26.68	4.94	8.95	4.01		11.31	8.43	2.88	
	Trial4	44.17	23.50	20.67	5.00	9.23	4.23		9.16	3.67	5.49	
8	Trial1	28.65	11.73	16.92	0.52	1.10	0.58		13.06	3.65	9.41	
	Trial2	31.78	16.36	15.42	0.66	4.62	3.96		11.84	3.56	8.28	
	Trial3	29.93	19.63	10.30	0.75	2.67	1.92		8.40	2.02	6.38	
	Trial4	28.41	15.48	12.93	0.97	0.01	0.96		8.31	2.59	5.72	
	Average	36.72	22.47	14.78	5.93	7.99	5.80		7.88	5.90	5.69	

Table 20: Average difference for run

Average Difference- Run											
Left						Right					
Flexion/extension		Abduction/Adduction		Internal/external rotation		Flexion/extension		Abduction/Adduction		Internal/external rotation	
W/O	W/ norm	W/O	W/ norm	W/O	W/ norm	W/O	W/ norm	W/O	W/norm	W/O	W/norm
14.60°	14.30°	6.97°	7.97°	5.05°	6.60°	17.62°	14.78°	6.75°	5.80°	4.40°	5.69°

4.2 Vertical Ground reaction force vs Tibial Acceleration

4.2.1 Jump Results

Figures 38(a) and (b) show scatter plots of the linear function for acceleration and the corresponding vertical peak ground reaction force for all the eight subjects during jump trials for both left and right legs. The maximum peak ground reaction force upon landing resulting from

jump trials varied from subject to subject and ranged between 0.59 to 3.11 times body weight for left leg and 0.14 to 3.64 times the subject's body weight for right leg (Figure 38). The minimum peak tibial acceleration varied from subject to subject, ranging from 2.58g to 26.55g (Figure 38 (a)) for left leg jump activity, and 2.08g to 22.75g (Figure 38 (b)) for right leg jump activity. For the subjects 1, 2 and 4 out of the four trials only three jump trials were used as there was a technical error in editing.

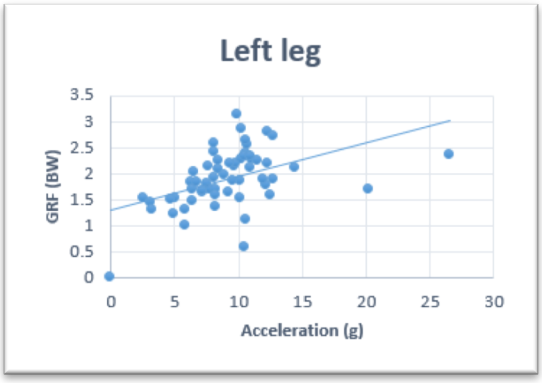

Figure 38: (a) Correlation between peak vertical GRF (BW) and Peak Vertical Acceleration Left Leg jump trial

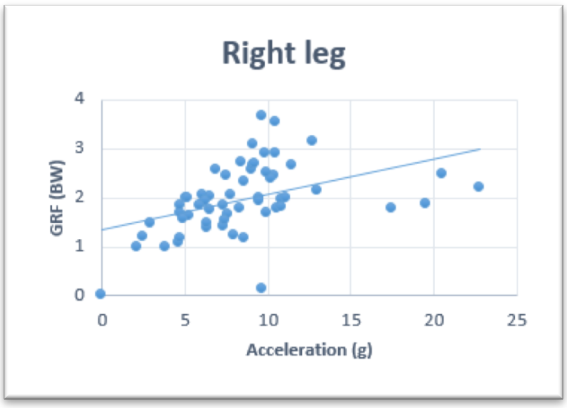

Figure 38: (b) Correlation between peak vertical GRF (BW) and Peak Vertical Acceleration Right Leg jump trial

Table 21: Correlation between GRF vs tibial acceleration for left and right leg for eight subjects jump

Left Leg (R^2)	Right Leg (R^2)
0.213	0.1852

We also looked at each subject's data individually, where the ground reaction force from the force plates was compared to the tibial acceleration (Figure 39 (a)-(h)). There was a weak correlation r^2 = 0.213 and r^2 = 0.1852 for left leg and right legs respectively between peak GRF (%BW) and peak tibial acceleration when the data for all eight subjects was combined during a jump activity (Figure 38 (a)and(b) and Table 21). The correlation between peak GRF (%BW) and peak tibial acceleration was observed for each subject individually and the correlation for subject 1, left and right leg was r^2 = 0.44 and r^2 = 0.88 (Table 22). Subject 2 showed a strong correlation for both left and right legs, r^2 = 0.89 and r^2 = 0.91 (Table 22). Subject 3 also showed a weak correlation between both the legs r^2 = 0.35 for left leg and r^2 = 0.27 for right leg. Subject 4 showed a strong relation between both the left and right leg r^2 = 0.80 and r^2 = 0.86 respectively. There was a weak correlation observed for subject 5 for both the left and right leg r^2 = 0.48 and r^2 = 0.60. While subject 6, 7 and 8 had a strong correlation for both left and right legs with correlation values r^2 = 0.87 for left leg and r^2 = 0.78 for right leg for subject 6, r^2 = 0.86 for left leg and r^2 = 0.72 for right leg for subject 7 and r^2 = 0.80 for left leg and r^2 = 0.90 for right leg for subject 8 (Table 22).

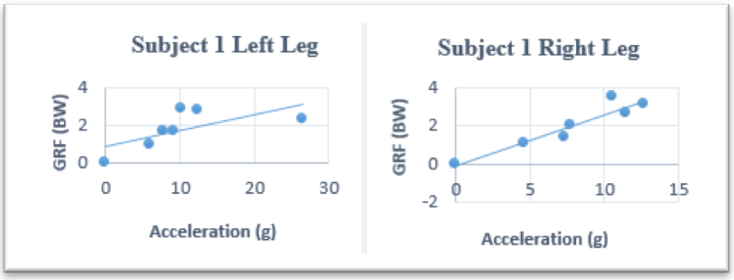

Figure 39: (a)

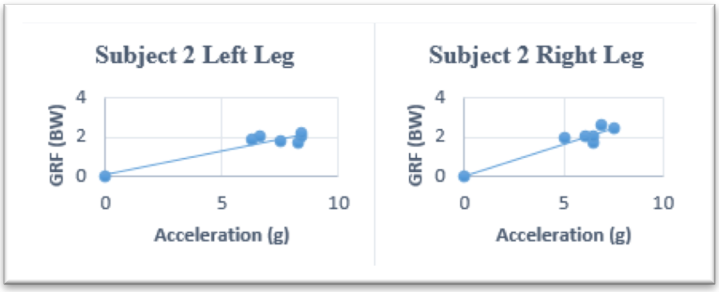

Figure 39: (b)

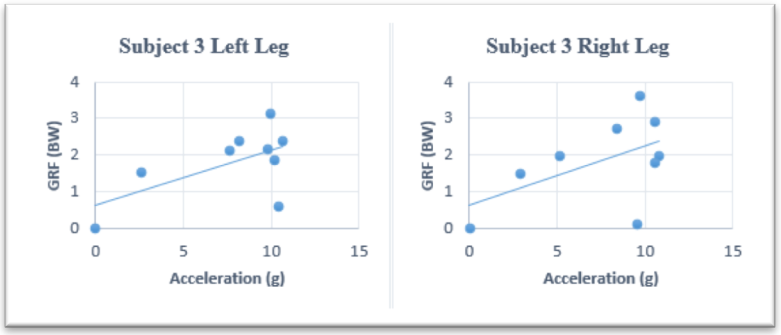

Figure 39: (c)

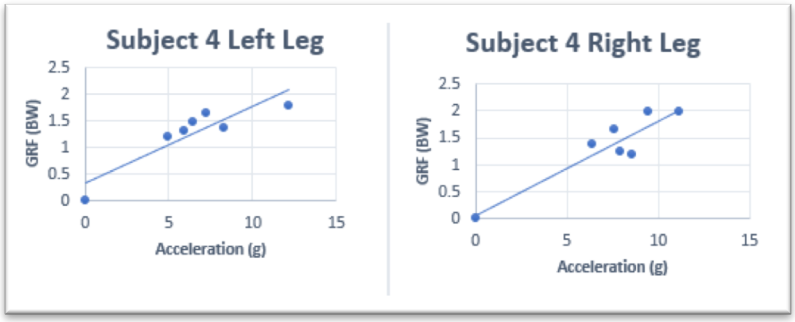

Figure 39: (d)

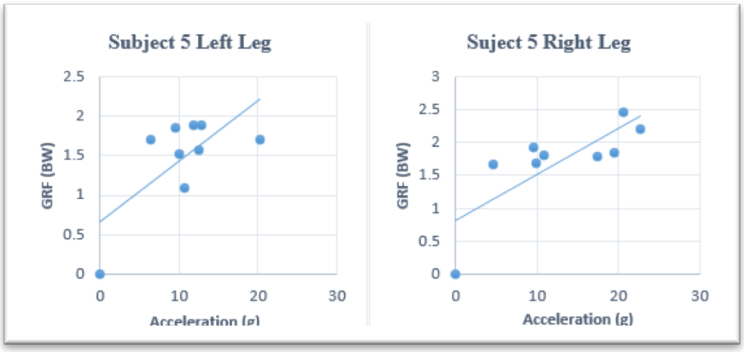

Figure 39: (e)

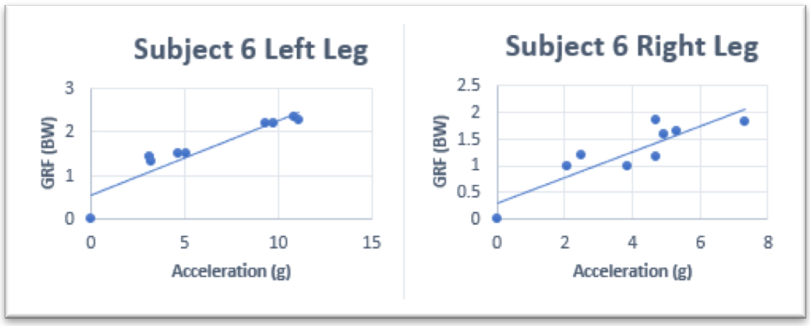

Figure 39: (f)

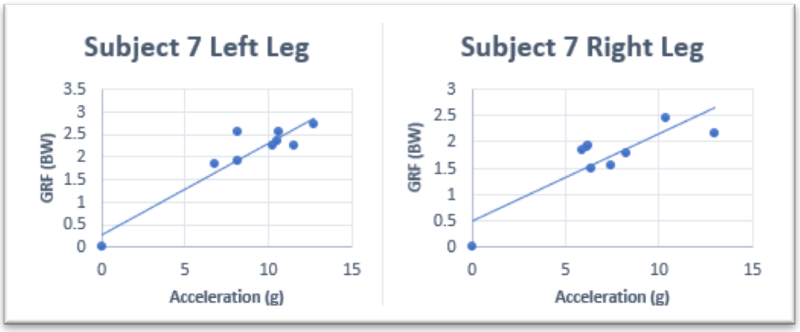

Figure 39: (g)

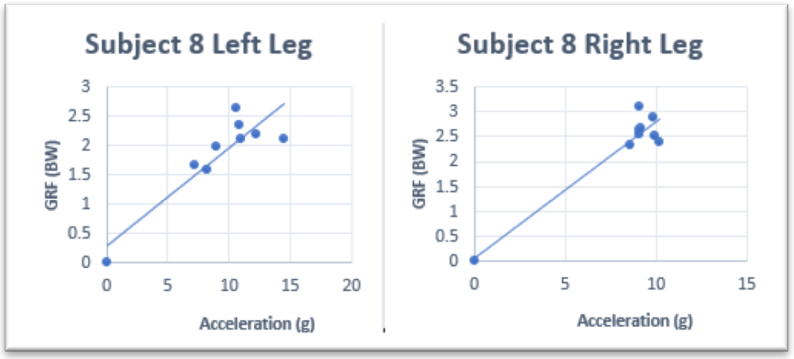

Figure 39: (h)

Figure 39: Correlation between peak vertical GRF (BW) and peak vertical acceleration for eight subjects (a) Subject 1; (b) Subject 2; (c) Subject 3; (d) Subject 4; (e) Subject 5; (f) Subject 6; (g) Subject 7; (h) Subject (8); jump trials

The calculated correlation value (R^2) for all the eight subjects for left and right legs has been given in the Table 22.

Table 22: Correlation Values for Jump Trials

Subject	Left Leg	Right Leg
1	0.44	0.88
2	0.89	0.91
3	0.35	0.27
4	0.80	0.86
5	0.48	0.60
6	0.87	0.78
7	0.86	0.72
8	0.80	0.90

4.2.2 Run Results

Figures 40 (a) and (b) show scatter plots of the linear function for acceleration and the corresponding vertical peak ground reaction force for all the eight subjects during a run trial for both left and right legs. The maximum peak ground reaction force upon landing resulting from run trials varied from subject to subject and ranged between 1.28 to 2.18 times body weight for left leg and 1.25 to 2.41 times the subject's body weight for right leg (Figure 40). The minimum peak tibial acceleration varied from subject to subject, ranging from 3.2g to 11.58g (Figure 40 (a)) for left leg run activity, and 3.20g to 13.6g (Figure 40 (b)) for right leg run activity. Out of the four trials for each subject, only three trials were used for subjects 1, 4 and 6 as the sensors failed to generate the acceleration output for these subjects, hence those trials were not used. There was a weak correlation $r^2 = 0.06$ and $r^2 = 0.03$ for left leg and right legs respectively between peak GRF (%BW) and peak tibial acceleration when data for all eight subjects was combined during a run activity (Figure 46 (a)and(b) and Table 23).

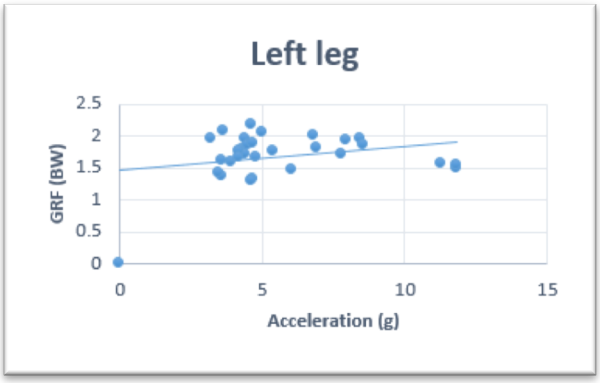

Figure 40: (a) Correlation between peak vertical GRF (BW) and peak vertical acceleration for eight subjects for a run trial, Left Leg

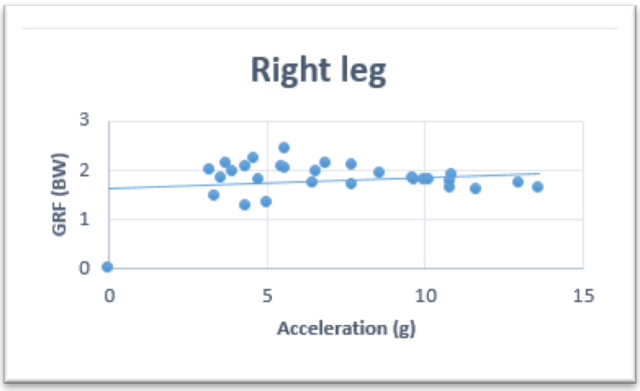

Figure 40: (b) Correlation between peak vertical GRF (BW) and peak vertical acceleration for eight subjects for a run trial, Right Leg

Table 23: Correlation between GRF vs tibial acceleration for left and right leg for eight subjects run trials

Left Leg (R^2)	Right Leg (R^2)
0.0673	0.0357

The correlation between peak GRF (%BW) and peak tibial acceleration for each subject individually was also observed (Figure 41 (a)-(h)). The correlation between peak GRF (%BW) and peak tibial acceleration for subject 1 left and right leg was $r^2 = 0.43$ (Table 24). While the correlation values for subject 1 left leg was strong, the correlation for right leg was weak for the same subject during a run activity. Subject 2 showed a strong correlation for left leg, $r^2 = 0.96$ and $r^2 = 0.62$ for right leg (Table 24). Subject 3 also showed a strong correlation for the left leg $r^2 = 0.98$ and $r^2 = 0.60$ for right leg. Subject 4 showed a strong relation $r^2 = 0.92$ and $r^2 = 0.84$ between both the left and right legs respectively. While subject 5, 6, 7 and 8 had a strong correlation for both left and right legs. The correlation values being $r^2 = 0.80$ for left leg and $r^2 = 0.84$ for right leg for subject 5, $r^2 = 0.95$ for left leg and $r^2 = 0.96$ for right leg for subject 6, $r^2 = 0.97$ for left leg and $r^2 = 0.91$ for right leg for subject 7 and $r^2 = 0.98$ for left leg and $r^2 = 0.95$ for right leg for subject 8 (Table 24).

The calculated correlation value (R^2) for all the eight subjects for left and right legs has been given in the Table 24 for a run trial.

Table 24: Correlation Values for Run trials

Subject	Left Leg	Right Leg
1	0.92	0.43
2	0.96	0.62
3	0.98	0.60
4	0.92	0.84
5	0.80	0.84
6	0.95	0.96
7	0.97	0.91
8	0.98	0.95

While the peak ground reaction force and the tibial acceleration was strongly correlated for three of the male subjects (Subjects 6, 7 and 8) for both left and right legs, and subject 5's correlation

was not so strong or weak, it was moderate. The correlation between the ground reaction force and the tibial acceleration was strong for both left and right legs for all the four male subjects during running. While the correlation varied among the female subjects. Subject 1 showed a strong correlation for left leg and a weak correlation for right leg. Subjects 2 and 3 showed a strong correlation for left leg and a moderate correlation for the right leg. While subjects 4-8 showed a strong correlation for both the legs. Among all the four female subjects only one subject (Subject 4) showed a strong correlation for both the legs.

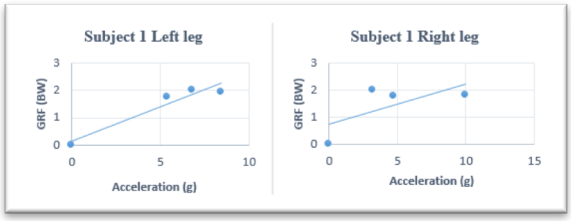

Figure 41: (a)

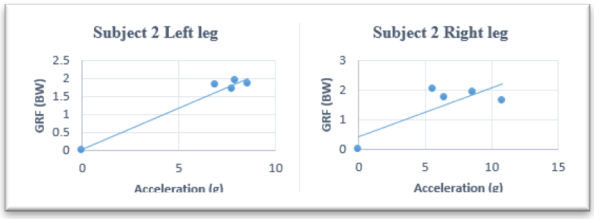

Figure 41: (b)

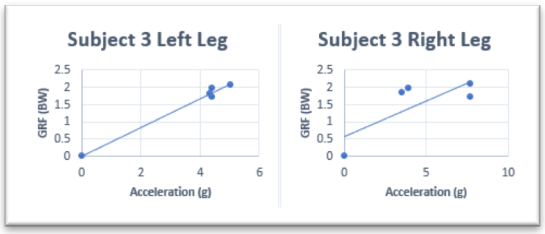

Figure 41: (c)

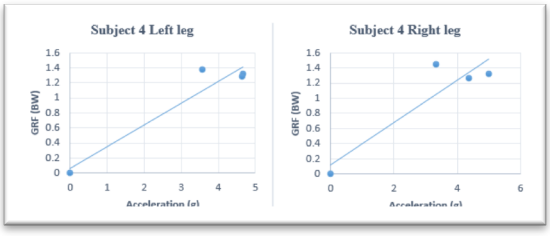

Figure 41: (d)

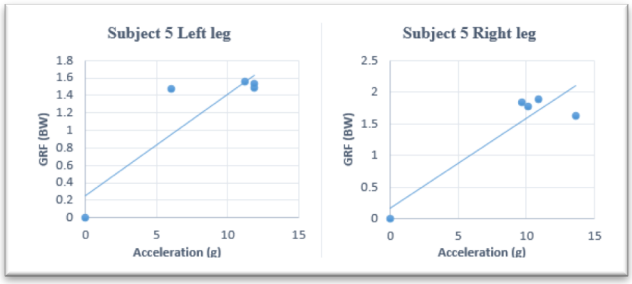

Figure 41: (e)

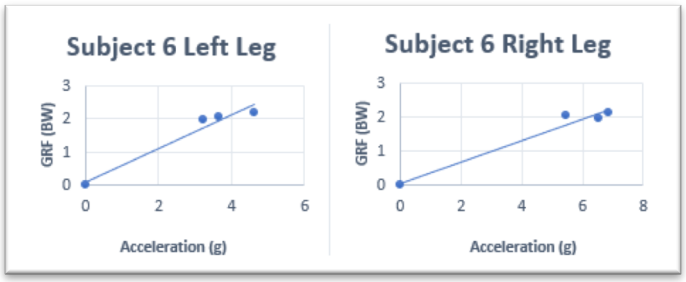

Figure 41: (f)

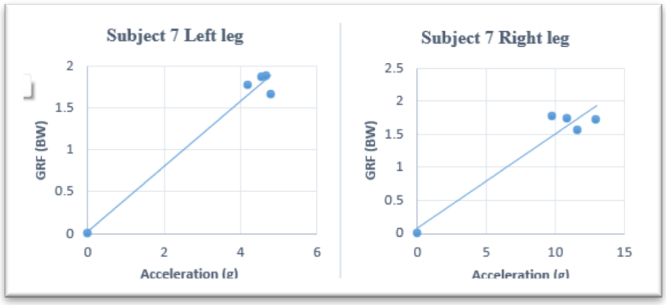

Figure 41: (g)

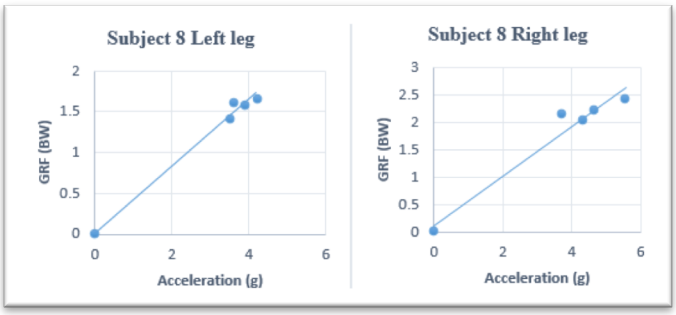

Figure 41: (h)

Figure 41: Correlation between peak vertical GRF (BW) and peak vertical acceleration for eight subjects (a) Subject 1; (b) Subject 2; (c) Subject 3; (d) Subject 4; (e) Subject 5; (f) Subject 6; (g) Subject 7; (h) Subject (8) run trial

4.2.3 Estimated Ground Reaction Force

The estimated ground reaction force has been calculated as a percentage of body weight from the equations obtained by plotting the tibial acceleration vs GRF (%BW).

The equation is in the form of: $y = mx + c$, where y = the estimated body weight, m = slope of the line, x = tibial acceleration and c = constant

The Tables 25-28 with estimated or calculated ground reaction force are given as follows:

Table 25: Estimated GRF for Left leg (Jump trials)

Left					
Subject	Trial	Acceleration	GRF(% BW)	Calculated GRF	Diff
1	Trial 1 Jump1	10.27	2.84	1.75	1.09
	Trial 2	9.24	1.63	1.67	0.03
	Trial 3	12.35	2.79	1.93	0.86
	Trial 1 Jump2	7.80	1.68	1.55	0.13
	Trial 2	5.91	1.00	1.39	0.39
	Trial 3	26.55	2.35	3.11	0.76
2	Trial 1 Jump1	6.33	1.83	1.62	0.21
	Trial 2	7.53	1.79	1.91	0.12
	Trial 3	6.58	2.02	1.68	0.33
	Trial 1 Jump2	8.27	1.69	2.09	0.40
	Trial 2	8.43	2.09	2.13	0.04
	Trial 3	8.43	2.24	2.13	0.11
3	Trial 1 Jump1	9.97	3.12	2.13	0.99
	Trial 2	7.66	2.13	1.79	0.34
	Trial 3	10.66	2.38	2.24	0.14
	Trial 4	8.17	2.41	1.86	0.55
	Trial 1 Jump2	10.19	1.87	2.17	0.30
	Trial 2	2.58	1.53	1.02	0.50
	Trial 3	9.76	2.15	2.10	0.04
	Trial 4	10.48	3.59	2.21	1.38
4	Trial 1 Jump1	6.41	1.47	1.25	0.22
	Trial 2	12.20	1.77	2.07	0.30
	Trial 3	7.22	1.64	1.36	0.28
	Trial 1 Jump2	4.97	1.21	1.04	0.17
	Trial 2	8.26	1.35	1.51	0.16
	Trial 3	5.90	1.30	1.17	0.13
5	Trial 1 Jump1	10.57	1.10	1.47	0.37
	Trial 2	9.54	1.85	1.39	0.45
	Trial 3	10.13	1.52	1.44	0.08
	Trial 4	20.21	1.69	2.22	0.52
	Trial 1 Jump2	12.51	1.58	1.62	0.04
	Trial 2	6.43	1.70	1.15	0.54
	Trial 3	12.80	1.87	1.64	0.23
	Trial 4	11.98	1.87	1.58	0.29
6	Trial 1 Jump1	9.78	2.19	2.23	0.04
	Trial 2	11.09	2.28	2.46	0.17
	Trial 3	10.90	2.33	2.42	0.10
	Trial 4	9.35	2.20	2.15	0.05
	Trial 1 Jump2	5.11	1.52	1.42	0.10
	Trial 2	3.13	1.44	1.08	0.36
	Trial 3	4.72	1.49	1.35	0.13
	Trial 4	3.21	1.30	1.09	0.21
7	Trial 1 Jump1	10.28	2.26	2.35	0.09
	Trial 2	11.56	2.23	2.61	0.38
	Trial 3	8.17	1.92	1.93	0.00
	Trial 4	6.80	1.84	1.65	0.19
	Trial 1 Jump2	10.68	2.55	2.43	0.12
	Trial 2	10.54	2.33	2.40	0.07
	Trial 3	12.80	2.72	2.86	0.14
	Trial 4	8.17	2.56	1.92	0.64
8	Trial 1 Jump1	10.96	2.11	2.12	0.01
	Trial 2	8.25	1.57	1.67	0.09
	Trial 3	7.22	1.66	1.50	0.17
	Trial 4	8.93	1.96	1.78	0.18
	Trial 1 Jump2	10.61	2.63	2.06	0.57
	Trial 2	10.91	2.34	2.11	0.23
	Trial 3	12.30	2.18	2.34	0.16
				Average diff	0.29

Table 26: Estimated GRF for Right leg (Jump trials)

Right					
Subject	Trial	Acceleration	GRF(% BW)	Calculated GRF	Diff
1	Trial 1 Jump1	12.72	3.12	3.29	0.16
	Trial 2	7.75	2.06	1.97	0.09
	Trial 3	10.52	3.54	2.71	0.83
	Trial 1 Jump2	11.51	2.65	2.97	0.31
	Trial 2	4.62	1.06	1.14	0.07
	Trial 3	7.34	1.40	1.86	0.46
2	Trial 1 Jump1	6.50	1.74	2.15	0.41
	Trial 2	7.53	2.44	2.48	0.03
	Trial 3	5.09	1.98	1.69	0.29
	Trial 1 Jump2	6.51	2.03	2.15	0.12
	Trial 2	6.08	2.04	2.01	0.02
	Trial 3	6.88	2.58	2.27	0.31
3	Trial 1 Jump1	10.51	2.89	2.32	0.57
	Trial 2	8.44	2.72	1.99	0.73
	Trial 3	9.70	3.64	2.19	1.45
	Trial 4	5.15	1.97	1.46	0.52
	Trial 1 Jump2	10.82	1.97	2.37	0.40
	Trial 2	2.92	1.47	1.10	0.37
	Trial 3	9.63	2.15	2.18	0.03
	Trial 4	10.58	1.77	2.33	0.56
4	Trial 1 Jump1	6.38	1.38	1.18	0.20
	Trial 2	11.13	1.97	2.02	0.04
	Trial 3	9.50	1.97	1.73	0.24
	Trial 1 Jump2	7.61	1.65	1.40	0.26
	Trial 2	7.93	1.24	1.45	0.21
	Trial 3	8.62	1.18	1.57	0.40
5	Trial 1 Jump1	9.93	1.69	1.51	0.18
	Trial 2	4.69	1.68	1.14	0.53
	Trial 3	22.75	2.19	2.40	0.21
	Trial 4	20.55	2.46	2.24	0.22
	Trial 1 Jump2	17.45	1.78	2.03	0.25
	Trial 2	9.52	1.93	1.48	0.45
	Trial 3	10.82	1.79	1.57	0.22
	Trial 4	19.58	1.85	2.18	0.33
6	Trial 1 Jump1	4.69	1.84	1.42	0.42
	Trial 2	7.31	1.83	2.05	0.22
	Trial 3	5.30	1.63	1.57	0.06
	Trial 4	4.94	1.58	1.48	0.09
	Trial 1 Jump2	2.51	1.18	1.90	0.72
	Trial 2	3.85	2.98	1.22	1.76
	Trial 3	4.72	1.16	1.43	0.27
	Trial 4	2.08	1.97	1.80	0.18
7	Trial 1 Jump1	8.31	1.77	1.88	0.11
	Trial 2	6.17	1.91	1.52	0.39
	Trial 3	7.44	1.54	1.73	0.19
	Trial 4	6.39	1.48	1.56	0.08
	Trial 1 Jump2	6.23	1.93	1.53	0.40
	Trial 2	10.36	2.44	2.22	0.23
	Trial 3	13.00	2.15	2.66	0.50
	Trial 4	5.91	1.83	1.48	0.36
8	Trial 1 Jump1	9.08	2.55	2.54	0.01
	Trial 2	10.21	2.38	2.85	0.47
	Trial 3	8.56	2.32	2.40	0.08
	Trial 4	9.12	2.65	2.55	0.10
	Trial 1 Jump2	9.14	3.09	2.56	0.53
	Trial 2	9.91	2.50	2.77	0.27
	Trial 3	9.19	2.67	2.57	0.10
				Average diff	0.33

Table 27: Estimated GRF for Left leg (Run trials)

Left					
Subject	Trial	Acceleration	GRF(% BW)	Calculated GRF	Diff
1	Trial 1	8.45	1.95	2.25	0.31
	Trial 2	5.37	1.75	1.48	0.27
	Trial 3	6.80	2.01	1.84	0.17
2	Trial 1	7.94	1.93	1.85	0.09
	Trial 2	7.79	1.71	1.81	0.11
	Trial 3	8.58	1.85	1.99	0.15
	Trial 4	6.90	1.82	1.61	0.21
3	Trial 1	4.32	1.79	1.79	0.00
	Trial 2	5.03	2.05	2.08	0.03
	Trial 3	4.40	1.96	1.82	0.14
	Trial 4	4.40	1.72	1.82	0.11
4	Trial 1	4.66	1.31	1.41	0.09
	Trial 2	4.64	1.28	1.40	0.12
	Trial 3	3.57	1.37	1.09	0.27
5	Trial 1	11.85	1.48	1.64	0.15
	Trial 2	11.86	1.54	1.64	0.10
	Trial 3	11.26	1.55	1.57	0.01
	Trial 4	6.06	1.47	1.96	0.49
6	Trial 1	3.21	1.96	1.72	0.24
	Trial 2	4.63	2.18	2.44	0.26
	Trial 3	3.65	2.07	1.95	0.13
7	Trial 1	4.54	1.87	1.79	0.08
	Trial 2	4.69	1.88	1.85	0.03
	Trial 3	4.78	1.67	1.88	0.21
	Trial 4	4.16	1.77	1.64	0.12
8	Trial 1	3.90	1.59	1.61	0.02
	Trial 2	3.49	1.42	1.44	0.02
	Trial 3	4.20	1.67	1.73	0.07
	Trial 4	3.61	1.62	1.49	0.12
				Average diff	0.14

Table 28: Estimated GRF for Right leg (Run trials)

Right					
Subject	Trial	Acceleration	GRF(% BW)	Calculated GRF	Diff
1	Trial 1	10.00	1.80	2.22	0.42
	Trial 2	4.73	1.79	1.44	0.35
	Trial 3	3.21	2.01	1.21	0.80
2	Trial 1	10.81	1.63	2.19	0.56
	Trial 2	6.45	1.74	1.49	0.25
	Trial 3	5.55	2.02	1.34	0.67
	Trial 4	8.59	1.91	1.83	0.08
3	Trial 1	3.92	1.96	1.38	0.58
	Trial 2	3.56	1.84	1.30	0.53
	Trial 3	7.71	2.08	2.16	0.08
	Trial 4	7.71	1.71	2.16	0.46
4	Trial 1	4.99	1.32	1.52	0.20
	Trial 2	3.33	1.45	1.05	0.39
	Trial 3	4.35	1.26	1.34	0.08
5	Trial 1	13.61	1.64	2.11	0.47
	Trial 2	9.60	1.82	1.53	0.29
	Trial 3	10.13	1.79	1.61	0.18
	Trial 4	10.88	1.88	1.72	0.17
6	Trial 1	6.85	2.13	3.56	1.43
	Trial 2	5.47	2.04	2.87	0.83
	Trial 3	6.54	1.96	3.41	1.45
7	Trial 1	11.61	1.58	1.74	0.15
	Trial 2	10.81	1.75	1.62	0.12
	Trial 3	12.99	1.73	1.93	0.20
	Trial 4	9.69	1.78	1.46	0.32
8	Trial 1	4.31	2.05	2.06	0.02
	Trial 2	5.57	2.41	2.64	0.22
	Trial 3	4.61	2.21	2.20	0.01
	Trial 4	3.73	2.14	1.80	0.34
				Average diff	0.40

The average difference between the actual ground reaction force and the calculated ground reaction force was also calculated for both jump and run activities for all the eight subjects. The average difference between the actual GRF and the calculated GRF was 0.29 and 0.33 for left and right leg respectively for jumps (Table 29), and the average difference between the actual GRF and calculated GRF was 0.14 and 0.44 for left and right legs for running (Table 29).

Table 29: Average difference of GRF vs estimated GRF

Activity	Left	Right
Jump	0.29	0.33
Run	0.14	0.44

4.2.4 Resultant GRF and Resultant Acceleration

4.2.4.1 Jump trials

The resultant ground reaction force from the force plates and the resultant acceleration from the APDM opal tibial sensor was calculated for eight subjects during jumping and a weak correlation was observed for both the legs when examined all eight subjects (Figure 42 (a) and (b)). The Y-axis represents the resultant acceleration and the X-axis represents the resultant GRF.

Figure 42: (a) Correlation between resultant GRF and acceleration, Left Leg, Jump

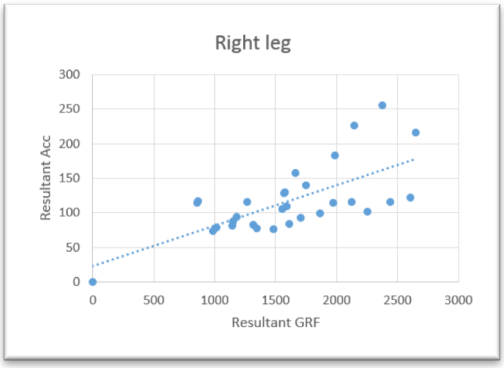

Figure 42: (b) Correlation between resultant GRF and acceleration, Right Leg, Jump

A strong correlation was observed for all the subjects (Table 30) between both left and right legs, apart from one subject (subject 1) when they were examined individually (Figures 43 (a)-(h)). Subject 1 appears to have one data point which may be an outlier.

Table 30: Correlation between resultant GRF vs Acceleration

Subject	Left	Right
1	0.23	0.64
2	0.97	0.99
3	0.89	0.77
4	0.91	0.95
5	0.82	0.93
6	0.99	0.99
7	0.91	0.88
8	0.94	0.97

Figures 42: (a)-(h) show the correlation graphs between resultant GRF and resultant acceleration for left and right legs.

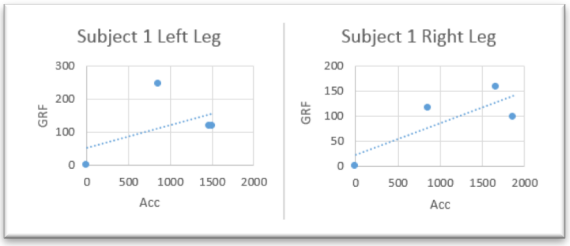

Figure 43: (a)

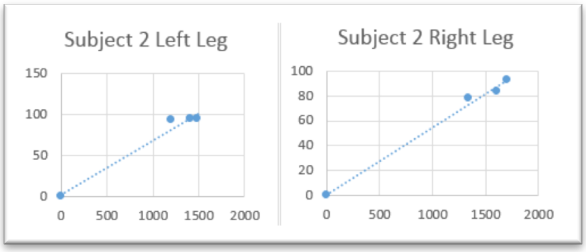

Figure 43: (b)

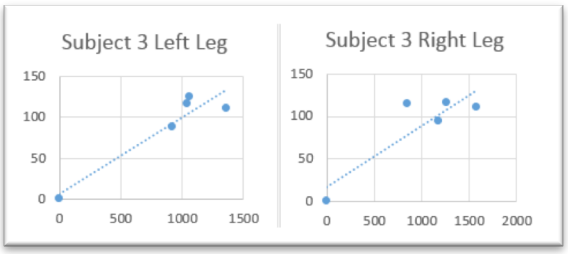

Figure 43: (c)

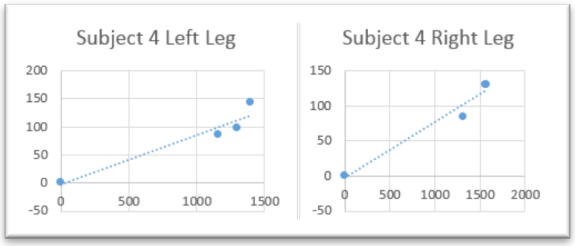

Figure 43: (d)

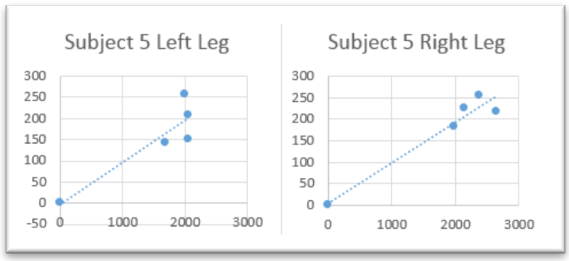

Figure 43: (e)

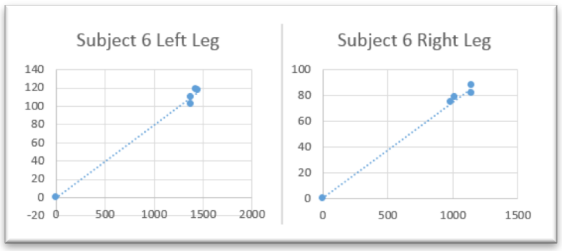

Figure 43: (f)

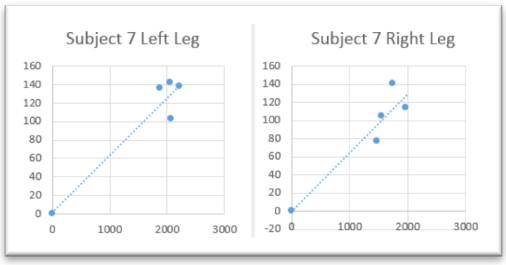

Figure 43: (g)

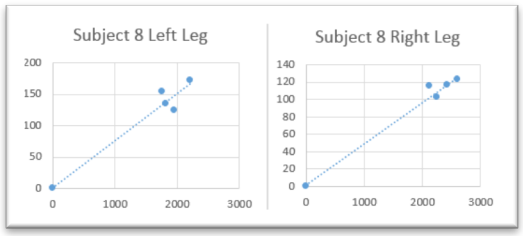

Figure 43: (h)

4.2.4.2 Run trials

The resultant ground reaction force from the force plates and the resultant acceleration from the APDM opal sensors was calculated for eight subjects during running. A weak correlation of 0.48 and 0.30 was observed for both left and right legs when all the eight subjects were examined together. The Y-axis represents the resultant acceleration and the X-axis represents the resultant GRF (Figure 44 (a) and (b)).

Figure 44: (a) Correlation between resultant GRF and acceleration, Left Leg, Run

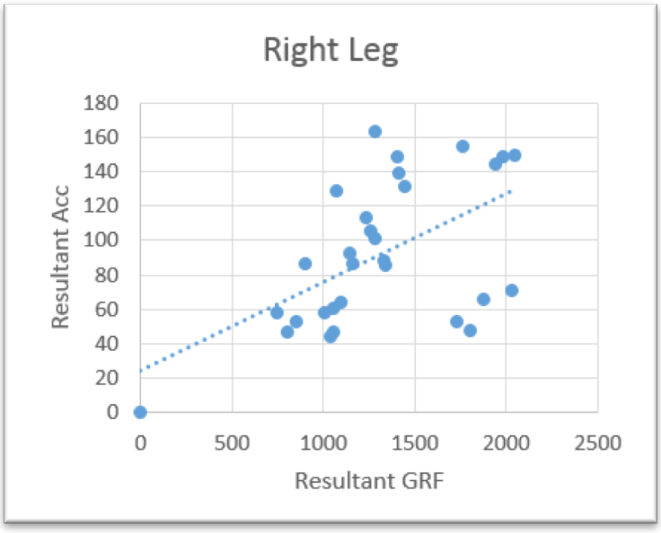

Figure 44: (b) Correlation between resultant GRF and acceleration, Right Leg, Run

A strong correlation was observed for all the subjects (Table 31) between both left and right legs when the eight subjects were examined individually (Figures 45 (a)-(h)).

Table 31: Correlation between resultant GRF vs Acceleration

Subject	Left	Right
1	0.98	0.93
2	0.98	0.78
3	0.99	0.83
4	0.97	0.85
5	0.85	0.97
6	0.95	0.91
7	0.93	0.92
8	0.98	0.94

Figures 45: (a)-(h) show the correlation graphs between resultant GRF and resultant acceleration for left and right legs when examined individually.

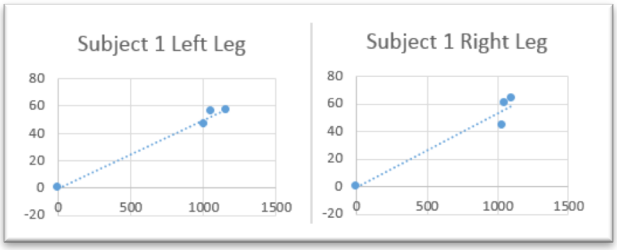

Figure 45: (a)

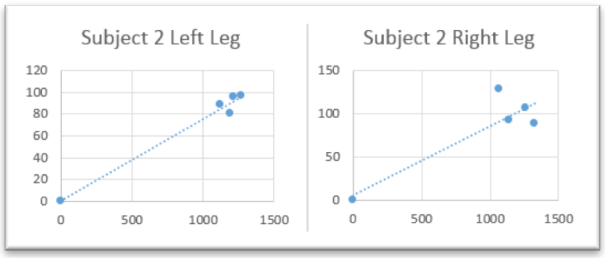

Figure 45: (b)

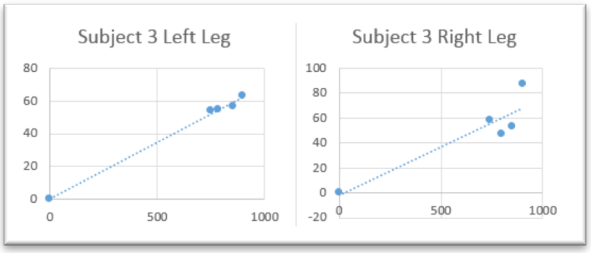

Figure 45: (c)

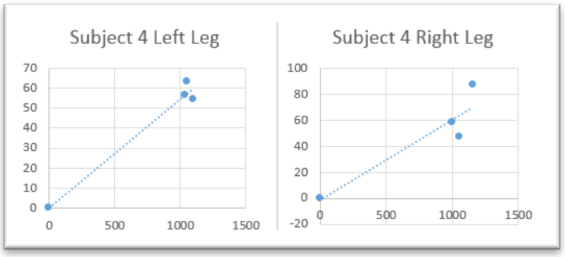

Figure 45: (d)

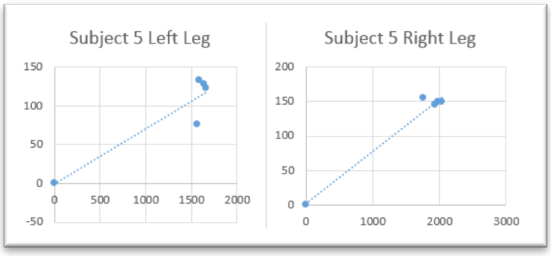

Figure 45: (e)

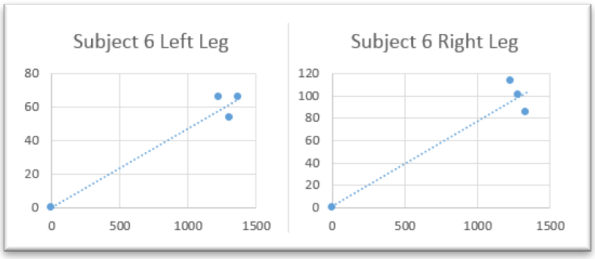

Figure 45: (f)

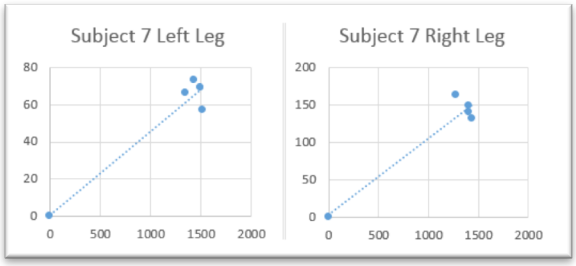

Figure 45: (g)

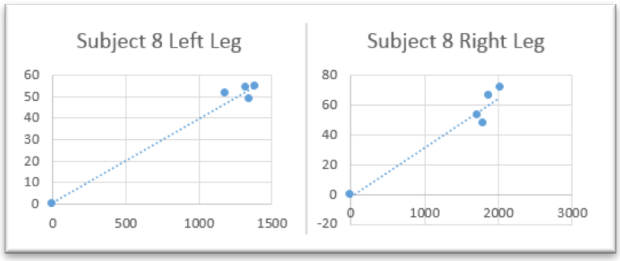

Figure 45: (h)

4.3 Discussion

The results of this study demonstrated the correlation between the Optitrack motion capture system and the APDM system in terms of ground reaction force (as percent body weight) and the peak tibial acceleration. The knee joint angles were also compared for both the Optitrack and APDM systems for both jump and run activities at peak ground reaction force. We compared the knee joint angle values obtained from the motion capture system by processing it using visual 3D and comparing them to the joint angle values obtained from the opal sensors which were processed using MATLAB, but there was a difference observed from the measures of angles from both these systems of around 10°-5°. In this study we used the normalization method to calculate the normalized knee joint angles which also minimized the potential errors produced by misplacement of markers and to maintain uniformity across subjects and data collection sessions.

Previous studies have used video analysis [22] [73] [55] to qualitatively and quantitatively analyze the flexion angles at the time of ACL injuries during various situations. In two of the studies [55] [62], ten video sequences from women's handball and basketball games were analyzed from real time matches in which two activities, cutting and one-legged jump landings were analyzed to monitor lower limb kinematics like the knee flexion angle which was given as 11° to 30° , the knee abduction was -2° to 3° and the rotation angle was -5° to 12° [55]. These studies also reported that there was no direct contact with the knee while an injury situation was observed. In another study [62] which assessed the lower extremity kinematics from real time visual playback (used from actual field game) against a 3D motion analysis system (in a laboratory), it was observed that the flexion angles were rated based on a rater's score and compared to a 3D motion analysis of a drop jump task and running.

The results of this study showed an excellent level of agreement between the video observation and the 3D motion analysis for assessing the lower limb kinematics in slower, speed controlled movements but lower level of agreement was reported for faster movements like running, which might be a reason for the discrepancy observed in run results from our study since the speed was not calculated. A study has demonstrated that in running an increase in knee flexion angle at the point of contact with ground can lead to a decrease in the peak vertical ground reaction force [96].

Using the video analysis [55] [62], it is difficult to quantify exactly when an injury occurs. In general, it has been suggested that video analysis has contributed to the general understanding of several risk factors for the cause of an ACL injury in females showing a low knee flexion. This video data is limited in that, the authors in general fail to examine 'non-injurious; movements to determine whether the same athlete can land in the same way without injuring his/her ACL. While conducting the video analysis the assumption has been that this is an acute injury. However in reality it has never been clear whether it was a single event that caused the ACL injury or whether in some cases, this was caused by a repetitive strain.

Some of the studies have demonstrated that the joint angles at contact and the jump height significantly effect the peak ground reaction force [110], but they have not indicated which of the two effects is more dominant during jump landing. In this study we examined the knee joint angles and the peak GRF measured individually from two systems. In a previous study [14] conducted for sixty healthy college subjects(thirty male and thirty female) to assess the lower extremity biomechanics during the landing of a vertical stop-jump task it was found that the average knee flexion angles at peak ground reaction force were 35.46° and 41.06° for females and males, but the study failed to report any results in the frontal as well as the transverse plane biomechanics i.e. the valgus/varus and internal/external rotation angles as a cause to identify the mechanism of the ACL injury.

The knee flexion angles (Tables 10,11,12 and 13) at peak ground reaction force obtained from our study were like this study [10] for females and males (Table 10 and 11). In another recent study [65] conducted for twelve male and nine female subjects to find the differences in the lower extremity kinematics and kinetics during a vertical drop landing where the task involved stepping off naturally from a 60 cm box onto the force plates. Data was collected at 1200Hz by the Bertec force plates and 120Hz by the three-dimensional motion capture system. They showed a flexion angle of 93°and -98.4° for females and males. While the ground reaction force was expressed in terms of %body weight for both the subject groups. The flexion angles obtained from our results were different from these studies results as the height of the box from which the subject would jump was different (Tables 10, 11, 12 and 13). Another study [83] [107] which examined the valgus knee motion between males and females for a jump landing task. Subjects jumped off a 31 cm box with their feet 35 cm apart and performed two jumps, first directly drop on to the force

plates and immediately to a maximum vertical jump with both their arms in the air imitating a basketball move. Twenty- three reflective markers were placed on the subject's body, and data were sampled at 240 Hz from the motion capture systems and 1200 Hz for the AMTI force plates. The abduction .angles or the knee valgus angles during a vertical jump at peak ground reaction force were averaged out for three trials were found to be between 34.6° for males and 32.1° for female subjects, which indicate that females had higher valgus angle than their counterparts. The results of our study have shown that the knee valgus for both male (9.51°) (Table 10, 11, 12 and 13) and female subjects (9.44°) (Table 10, 11, 12 and 13) were different from this study for a vertical jump landing task. The possible reason for this disagreement of valgus angles might be the 35cm distance between the two legs.

The landing error score system(LESS) is a clinical tool developed for screening the ACL injury risk factors, it identifies the poor jump landing techniques who are at risk for noncontact ACL injury, an investigator after watching the videos records the error on the LESS scoring sheet which scores the individual joint motions in the landing technique. The reliability and validity of the landing error scoring system (LESS) by an expert and novice interrater across thirteen lower limb extremity items were evaluated by Onate [75] to a three-dimensional motion capture system. This particular study was similar to our research in its methodology. Nineteen female soccer athletes free of any knee injuries wore spandex shorts and running shoes while performing the task. The subjects performed three jumps off a 30 cm box and placed at a distance of 30 cm from the force plates.

The subjects were asked to jump and land on the force plates first and immediately jump as high as they could straight up in the air as to imitate a soccer header and land back on the force plates. The initial landing from the first jump was used for analyses and the second landing resulted from the maximum vertical jump was discarded. Eight motion cameras by Vicon Motion Systems Ltd., at a sampling rate of 500Hz and two Bertec 4060-NC force plates with a sampling rate of 500 Hz were used to measure the kinematic data in collaboration with two Sony mini DV handycam to video record the trials at a sampling rate of 30Hz. All the kinematic analyses were done using Visual 3D to obtain the knee joint angles and ground reaction force. The trained observer documented the knee-flexion angle at initial ground contact and the entire range of motion, knee-valgus angle and the foot ground contact symmetry. All the three trials were averaged into a single

score and were analyzed in a SPSS 16.0. A code of 0 or 1 was given to the kinematic data to correspond with the LESS score. A score of 1 was given for a flexion angle less than 30° or 0 for a flexion angle more than 30°. The mean knee flexion angle measured by the three-dimensional motion capture system was within a range of 10° to 37°. For the symmetry of foot contact, the vertical ground reaction force was analyzed by concluding that all the subjects had an asymmetric foot contact. The LESS showed an excellent reliability validation in assessing a drop-jump landing task, which suggests that this LESS could be used a measure of dynamic jump landing motion technique. The joint angles, particularly flexion results for all the four female subjects(1,2,3,4) during jump trials obtained from our study(Table 10,11,12 and 13) were similar to these results, however this study [85] does not shed any light on the joint angles obtained in the other two direction i.e. Y(abduction/adduction) and Z (internal/external rotation) and also it should be kept in mind that all these joint angles were calculated at the initial contact of landing by averaging out the trials and compared the lower extremity results from a three dimensional motion capture system to various other systems but not any wearable inertial measuring units.

Lower limb angles have also been measured using wearable sensors [4] [113] [9] [10] [11]. The angle measurements in our study from the wearable sensors were observed to be slightly different than those obtained from the motion capture system as the knee angle estimation faces notable challenges when measured using IMUs. The knee angle measurements are based on orientation estimates provided by the IMUs, which make them sensitive to sensor-to-body calibration. Another challenge is that the key mechanism for angle estimation is measurement of the 1g gravity vector by the 3-axis accelerometer incorporated inside the IMU, the measurements of the gravity vector (for orientation measurements) are coupled with the acceleration of the actual sensor due to movement. In moments of abrupt movements, the accelerometer can read up to 10g ($98 m/s^2$) as we have measured in Figure 43 and 44 for jump and run lower leg acceleration. This difference in the flexion angle estimation also may be a result of few limitations listed in the next chapter. A study by Bakshi [114] proposed a methodology to measure the motion of knee joint using the IMU sensors in comparison with the joint data from the motion capture system. Two IMU's by SparkFun electronics, Boulder, CO. were placed on the subject's thigh and shank for data collection. An accelerometer was used to find the knee flexion angles. All the data from the sensors were processed using an ATmega328 microcontroller and a custom generated LabVIEW program generated the flexion angles. These calculated flexion angles from the IMU's were compared to

the infrared Vicon motion system. A 26-year-old male subject performed four tasks (swinging the lower leg in a seated position, hip and knee flexion in a standing position, sitting down and standing, gait patterns and squats). The data were collected at a sampling rate of 100Hz and 5Hz for the motion capture and the IMU system respectively. The average errors for knee flexion (0.08°, 3.06°, 1.68° and 2.40°), standard deviation and the correlation coefficient (0.09, 0.97, 0.98 and 0.94) was calculated for the four tasks between both the systems. The average difference for the knee flexion angle calculated from the motion capture system and the wearable sensor devices in our study was higher (14.81°) (Table 14 and 15) than the flexion results of a squat task (similar to a jump task) from this study [114] as the task we performed was a vertical jump. However, a squat is not a dynamic task. It is possible that slower, more controlled movements are less complex and therefore easier to accurately measure using IMUs compared with more dynamic tasks.

We focused on joint angle measurements obtained in all the three directions i.e. the flexion/extension, adduction/abduction and internal/rotation angles for both left and right legs from both the motion capture as well as the APDM opal sensors systems. For some subjects the flexion angles obtained from both the systems closely matched and for some it showed a larger difference. Although there were a number of studies which reported the kinematics of the lower extremity using the three-dimensional motion capture system and the wearable IMU system separately or either by comparing one motion capture system against any other methods(LESS) [65], no study in particular validated both the motion capture and the wearable sensor system for the joint angles in all the three directions (flexion/extension, valgus/varus and internal/external rotation) for running or jumping. In this study we were validating the wearable sensor system by comparing it with the three-dimensional camera system using eight subjects (four male and four female). Previous studies tried to analyze the gender differences in lower extremities as a cause for the ACL injury keeping only either the knee flexion or the valgus angles separately as a major criteria but not comparing the joint angles in all the three directions(X, Y, and Z) at once. The knee joint angles in our study were consistent with those reported in the previous similar studies for jump landing [99] [83] [65] [85]. Overall the right leg joint angle results (Tables 10, 11, 12 and 13) were observed to be more accurate than the left leg for both jumps and runs. This might be because most of the subjects had their dominant leg as the right leg and stepped on the force plates using their right leg first while running so the right leg joint angles were better than the left leg, although this same assumption may not be applicable in case of jumps as the subject would land

on the force plates nearly at the same time. The major assumption of our study was that there is a linear relation between the vertical ground reaction force and tibial acceleration. Of the eight subjects four of the subjects were female and four were male subjects. The correlation between the peak ground reaction force and the tibial acceleration for jump trials was stronger for two female subjects for both left and right legs, while the correlation was weaker for the other two female subjects (Table 22). While the peak ground reaction force and the tibial acceleration was strongly correlated for three of the male subjects for both left and right legs, and was moderately correlated for one male subject (Table 22). Wearable sensors using IMUs have successfully measured a variety of kinematic data. Proposed function of wearable technology includes gait analysis [115] [35] [21] and assistance with rehabilitation [70] [8] [21] [40].

Majority of studies focused on wearable sensing for gait involve either the identification of movement disorders or the assessment of outcomes after surgery [31]. In addition, some studies have focused on athletic performance, particularly, running [113] [36] [46]. One study conducted in the field examined running and the kinematic changes that occur with fatigue [46]. Studies have also been conducted to correlate ground reaction force [7] or vertical loading rates [57] with accelerometers located at the lateral malleolus [57], distal tibia [57] and fibula head [7]. The relationship between the VGRF (%BW) force peaks and tibial acceleration for all the subjects are similar to the results of other studies during running [59] and drop landing [68] [95] [99] [65] [108]. One video analysis study estimated that the peak ground reaction force was 2.7-3.7 times the body weight in injured female athletes [55]. In a study by LaFortune [59] the correlation between the ground reaction force and the tibial acceleration was investigated. Six male recreational athletes without any history of orthopedic injury were consented to participate in the study. Each subject had to perform a jump starting off by standing on the force plates (AMTI Inc.) and touch three markers placed at three different heights to attain a maximal jump height. Wireless accelerometers (Zero-point technology) were attached with the help of support sleeve on each leg to record the acceleration data over the fibular heads. The vertical ground reaction force (VGRF) was collected at a sampling rate of 1000Hz from the force plates. The accelerometer measured acceleration only in one direction i.e. along the tibia with a speed of data acquisition set to 1000Hz to match the frequency of the force plates. Each subject performed 18 jumps, 6 at each specified height. The vertical ground reaction force and the tibial acceleration were measured for both the legs. The force as well as the acceleration data from all the trials for each subject was averaged

and interpolated linearly, the symmetry of landing was not addressed in this study. The jump heights were calculated from the flight time for all the six subjects. The results of this study state that the peak ground reaction force ranged from 4.6-8.2 times the body weight of the subject. They found a strong correlation between the peak GRF and the peak tibial axial acceleration, the jump height and the tibial axial acceleration with correlation values of 0.81 and 0.88 respectively.

The peak vertical ground reaction forces for all the eight subjects in our study for a jump activity was 3.11-3.64 times (Table 25 and 26) the body weight. This result is also in agreement with the earlier studies which reported the relation between body weight and tibial acceleration [4] [55] but are not in agreement with the study by Lafortune [59]. The possible reason for this disagreement might be because of the varied jump height between both the studies and also all the subjects were all males for which a high peak ground reaction force was observed and also use of a single force plate to measure the GRF for both legs which would concentrate all the body's weight on a single force plate. Studies in the past [97] have shown that there is an effect due to the joint angles and the height of the jump on the peak ground reaction force in drop landings. Additional research is required to determine the effect of joint contact angles and jump height on the peak ground reaction force during jumps.

In a controlled laboratory environment, ligamentous structures have been shown to be vulnerable to fatigue failure under cyclic loading conditions [37]. Submaximal repetitive loading is known to cause cumulative micro-damage in other soft tissues, most notably in the elbow [70] [76] [38]. Laboratory research indicates that some non-contact ACL injuries that occur in female athletes may be overuse injuries due to repeated strain on the ACL [50]. In a cadaveric study, application of an impulsive force at 3-4 times body weight, combined with a knee flexion moment and internal tibial torque caused mechanical failure in 13/20 knees (8/10 knees at 4*BW and 5/10 knees at 3*BW) [81] and in vivo laboratory study showed that peak GRF was higher in women than men when performing a jump-cut maneuver [76]. This demonstrates that being able to measure peak GRF and provide feedback to an athlete about their movement patterns could be a method for preventing ACL injury. In our study, we found that we would be able to predict peak GRF within approximately 0.2 BW.

The resultant force or the net force has been calculated from the force plates which is nothing but the vector sum of all the three forces in X, Y and Z directions, since the resultant force is the same

amount of force exerted by the subject as all the individual forces acting together. This resultant force from the force plates has been correlated with the resultant acceleration from the APDM sensor because the sensors might not have been properly aligned relative to the room (i.e global coordinate system as opposed to the body coordinate system). There was a strong correlation value observed for both jump (r^2=0.91) (Table 30) and run (r^2 =0.99) (Table 31) when the resultant force and resultant acceleration were compared from both the systems for all the eight subjects individually. The correlation greatly improved between the GRF and the tibial acceleration when the resultant GRF and resultant tibial acceleration were considered over the vertical GRF and vertical acceleration.

The results obtained from the run trials also showed a linear relation between the peak ground reaction force and the tibial acceleration. The correlation (Table 24) between the ground reaction force and the tibial acceleration was strong for both left and right legs for all the four male subjects during running. While the correlation varied among the female subjects when examining vertical force and vertical acceleration only. Among all the four female subjects only one subject showed a strong correlation for both the legs (Table 24). The running speeds of the subjects were not measured but it was made sure that they hit both the force plates. Although all the subjects tried to imitate a natural run performed in a field due to the limited lab space they could only do at most was a slow jog. Another study discussed the use of a low-power wireless system with a 3D accelerometer to measure the ground reaction force and gave a non-linear relationship between the tibial acceleration and GRF at various speeds [24]. The tibial acceleration measured using the wireless inertial system has been estimated to the ground reaction force measured by the force plates. Three subjects performed a protocol of 42 running trials with six different speeds and sprinting. While running subjects were made sure to hit the force plates with both their legs. A low-power wireless inertial unit (Viperform) was used to record acceleration data and an AMTI OR6 force plate was used to record force data with a sampling rate of 300Hz without any further filtering. Linear and logarithmic approximations were used to correlate the GRF and acceleration. A root mean square error value was calculated to assess the accuracy of the GRF from the force plate and the inertial units. A strong correlation with a value of 0.91 was observed using the logarithmic approach over the linear approach with a correlation value of 0.81. A logarithmic approach was used for further analyzation of the peak activities like heel strike, initial peak acceleration (IPA), peak to peak (Pk2Pk) and maximum peak (MP) from the tibial acceleration to

vertical GRF by defining a logarithmic function. They also investigated the effect of body mass on the logarithmic approximation based on the maximum tibial acceleration peak.

The acceleration for the three subjects was distributed over a range of 2g-10g.The results observed an RMSE average of 151N, 106N and 130N for the three subjects and proved that logarithmic approximation was better than linear approximation between peak GRF and tibial acceleration for running. The acceleration values that were observed in our study were in agreement with the previous study for a run trial and ranged from 2g-14g (Figure 46 and 47) and we also observed that the peak ground reaction force was 2.18-2.41 times (Table 27 and 28) the subject's body weight which agrees with the previous studies as well [4] [55].

In another study by (Zhang, 2016) which compared the correlations between impact loading rates and peak accelerations at two different body sites during a run were found to be very high for an intra subject analysis with a correlation value of 0.95. Eight male and two female subjects performed a nine running trials with four accelerometers (Model 7523A5, Dytran instruments) placed on the distal tibia and by running at different speeds on an instrumented treadmill (AMTI Watertown). The ground reaction force data and the accelerations were sampled at 1000Hz. The average and instantaneous loading rates were calculated for 40 consecutive steps in each trial. There was a high variance observed between the inter-subject coefficients of 8.95 body weights in the vertical average landing rate and 11.36 body weight in vertical impact loading rate, which gives a conclusion that the wireless accelerometers can be used in real time scenario to compare the intra subject vertical loading rates during running but no comparison can be made between inter-subject loading rates [111].

A strong correlation was observed between the resultant ground reaction force and the resultant tibial acceleration during jumping and running between both the legs for the eight subjects. The results of our current study showed that correlation between ground reaction force and tibial acceleration is poor when data from all the subjects were included together. However, the correlation was improved when subjects were examined individually. While the exact reason for this lack of correlation and dissimilarity between the knee joint angles measured from the motion capture system and the opal sensors was not addressed in the study, there are a number of limitations that could have contributed. These are discussed in the next chapter.

CHAPTER 5: LIMITATIONS AND CONCLUSION

5.1 Limitations

We acknowledge that there are several limitations in our present study with the Optitrack Motion capture system as well as the APDM opal sensor system. It is unclear whether the results obtained from the study can be extrapolated and used to a larger population and also because the people who participated were recreational individuals, not actual athletes. We had a small sample size and it is possible that a larger one would give more complete results. However, within our sample, we did have 4 male and 4 female volunteers in order to provide a representative population. One more limitation observed was the reflective markers which were placed on the subject's body might have not stayed at the specified bony locations because of the clothing worn while performing the tasks which might have affected the data recorded by the motion capture system. Also we used a double sided tape to put the reflective markers on the subject's body, due to which the subjects were very cautious while performing so that they would not fall off, but we made sure even if any markers fell off while performing the tasks more trials would be recorded to make sure no data was lost, but it was still not clear if this affected how the subjects performed the tasks. We made every effort to secure the wearable sensors to the subjects. However, it is possible that there was still some movement of the sensor. In addition, the sensors were fixed with Co-Flex and we were not able to see the sensor once it was in place. It is possible that some of the sensors because slightly skewed once they were positioned which also could have affected the results. In future studies, the sensors should first be fixed with an adhesive spray and then secured with Co-flex. Also we did not take into consideration the symmetry of legs landing during jumping.

5.2 Conclusion

This study presents evidence of the validity of the IMU device based measurement technique for measuring the knee angles at peak ground reaction force and also correlating the peak ground reaction force with the tibial acceleration. This IMU device was chosen for its low cost, portability and its ability to be used easily and provides required accelerometer, gyroscopic and magnetometer

data. The validation of the IMU device against the Optitrack motion capture system was performed using two parameters: comparison of knee flexion angles at peak ground reaction force and correlating the vertical ground reaction force or body weight with the tibial acceleration. Eight healthy recreational subjects between 20-39 years of age completed this study by performing two different gait activities. Correlations between the systems were done using the trend lines in Excel. The correlation between the vertical ground reaction force and the tibial acceleration was found to be high for four subjects out of eight for both the left and right legs. An excellent correlation was achieved between the resultant ground reaction force and resultant acceleration. Overall the IMU devices by the APDM Inc. have proven to be potential against the Optitrack motion capture system for the selected parameters. Upon further research and work these devices can be used in the outside environment, possibly on the field to calculate peak GRF and knee angles in the future. Although there is a significant and strong correlation observed between the peak ground reaction force and the tibial acceleration at least for some subjects, it still is unclear whether these results can be applied to larger number of subjects.

Therefore, additional research is needed to determine whether these opal sensors provided by the APDM Inc. can be used on field to measure parameters like knee joint angles and tibial accelerations on real athletes who play actual sports as the subjects participated in the study were not competitive athletes. Also, the motion involved during a real time jump or run activity may be different as in it involves movement in the lateral and forward directions, a tri-axial accelerometer is required to determine if a correlation exists between the horizontal ground reaction force and tibial accelerations.

In spite the lack of a perfect correlation between the ground reaction force and tibial acceleration the results recommend that the systems used in this study can provide a significant in-field biomechanical estimation. The results produced by these small wireless, unobtrusive, portable and lightweight APDM Opal sensors make them ideal wearable devices for field estimations. More research is required to determine the effects of few limitations in this study. However, we believe that this study gives a good beginning for the future estimation of knee joint angles, ground reaction force and accelerations amid different sport activities in the field to decide if these parameters effect the rate or cause of an ACL injury particularly in females.

5.3 Future Scope

In the future an exploratory study to examine whether these wearable sensors can improve knee kinematics in adolescent female athletes during actual practice and game conditions to reduce the potential risk of ACL can be conducted. Also a validation of this device against many other parameters like jump heights, run speeds and angles at landing for different gait activities can be performed. The study can be increased to a larger population and on real time athletes who play sports like soccer, basketball, lacrosse and other games where the rate of ACL injury is more.

References

[1] Adirim, T.A. & Cheng, T.L. Sports Med (2003) 33: 75

[2] Ageberg, E., M. Forssblad, P. Herbertsson and E. M. Roos. Sex differences in patient-reported outcomes after anterior cruciate ligament reconstruction: Data from the swedish knee ligament register. Am J Sports Med 38: 1334-42, 2010.

[3]Agel J, Olson DE, Dick R, et al. Descriptive epidemiology of collegiate women's basketball injuries: National Collegiate Athletic Association Injury Surveillance System, 1988-1989 through 2003-2004. J Athletic Training. 2007; 42:202–10.

[4] Ananthanarayan, S., M. Sheh, A. Chien, H. Profita and K. A. Siek. Designing wearable interfaces for knee rehabilitation. in 8th International Conference on Pervasive Computing Technologies for Healthcare, PervasiveHealth '14,2014.

[5]Anderson AF, Dome DC, Gautam S, Awh MH, Rennirt GW. Correlation of anthropometric measurements, strength, anterior cruciate ligament size, and intercondylar notch characteristics to sex differences in anterior cruciate ligament tear rates. Am J Sports Med 2001;29:58-66

[6] APDM technical guide

[7] Arendt EA, Bershadsky B, Agel J. Periodicity of noncontact anterior cruciate ligament injuries during the menstrual cycle. J Gend Specif Med 2002;5:19-26.

[8] Arendt E, Dick R. Knee injury patterns among men and women in collegiate basketball and soccer. NCAA data and review of literature. Am J Sports Med 1995; 23:694-701.

[9] Arif, M. and A. Kattan. Physical activities monitoring using wearable acceleration sensors attached to the body. PLoS One 10: e0130851, 2015.

[10] Bakshi, S., M. H. Mahoor and B. S. Davidson. Development of a body joint angle measurement system using IMU sensors. 2011 Annual International Conference of the IEEE Engineering in Medicine and Biology Society, Boston, MA, 2011, pp. 6923-6926.

[11] Bamberg, S. J., A. Y. Benbasat, D. M. Scarborough, D. E. Krebs and J. A. Paradiso. Gait analysis using a shoe-integrated wireless sensor system. IEEE Trans Inf Technol Biomed 12: 413-23, 2008.

[12] Barber-Westin SD, Noyes FR, Andrews M. A rigorous comparison between the sexes of results and complications after anterior cruciate ligament reconstruction. Am J Sports Med 1997;25:514- 26.

[13]Barber-Westin SD, Noyes FR, Galloway M. Jump-land characteristics and muscle-strength development in young athletes: a gender comparison of 1140 athletes 9 to 17 years of age. *Am J Sports Med.* 2006; 34(3):375-384.

[14] Barrios, J. A., K. M. Crossley and I. S. Davis. Gait retraining to reduce the knee adduction moment through real-time visual feedback of dynamic knee alignment. J Biomech 43: 2208-13, 2010.

[15] Beynnon, B , Howe, JG , Pope, MH , et al. The measurement of anterior cruciate ligament strain in vivo. Int Orthop. 1992;16:1–12.

[16] Beynnon, BD , Fleming, BC , Johnson, RJ , et al. Anterior cruciate ligament strain behavior during rehabilitation exercises in vivo. Am J Sports Med. 1995;23:24–34.

[17] Beynnon, BD , Johnson, RJ , Fleming, BC , et al. The strain behavior of the anterior cruciate ligament during squatting and active flexion-extension. A comparison of an open and a closed kinetic chain exercise. Am J Sports Med. 1997;25:823–829.

[18] Bien DP. Rationale and implementation of anterior cruciate ligament injury prevention warm-up programs in female athletes. J Strength Cond Res 2011;25:271-85.

[19] Bobbert, M.F., Schamhardt, H.C., & Nigg, B.M. (1991). Calculation of vertical ground reaction force estimates during running from positional data. Journal of Biomechanics, 24*,* 1095-1005

[20] Boden BP, Griffin LY, Garrett WE., Jr Etiology and prevention of noncontact ACL injury. Phys Sportsmed. 2000; 8:53–60.

[21] Boden BP, Torg JS, Knowles SB, Hewett TE. Video analysis of anterior cruciate ligament injury: abnormalities in hip and ankle kinematics. Am J Sports Med. 2009;37(2):252–9. doi: 10.1177/0363546508328107.

[22] Brophy, R. H., J. G. Stepan, H. J. Silvers and B. R. Mandelbaum. Defending puts the anterior cruciate ligament at risk during soccer: A gender-based analysis. Sports Health 7: 244-9, 2015.

[23] Chandrashekar N, Mansouri H, Slauterbeck J, Hashemi J. Sexbased differences in the tensile properties of the human anterior cruciate ligament. J Biomech 2006;39:2943-50

[24] Charry, E & Hu, Vincent & Umer, M & Ronchi, A & Taylor, Simon. (2013). Study on estimation of peak Ground Reaction Forces using tibial accelerations in running. Victoria University-School of Sport and Exercise Science (SES)288-293. 10.1109/ISSNIP.2013.6529804.

[25] Cross, Rod. (1999). Standing, walking, running, and jumping on a force plate. American Journal of Physics - AMER J PHYS. 67. 304-309. 10.1119/1.19253.

[26]D.B. McKeag Epidemiology of athletic injuries Primary care sports medicine, Benchmark Press, Dubuque (IA) (1993), p. 63

[27] Diogo, R., Esteve-Altava, B., Smith, C., Boughner, J. C., & Rasskin-Gutman, D. (2015). Anatomical Network Comparison of Human Upper and Lower, Newborn and Adult, and Normal and Abnormal Limbs, with Notes on Development, Pathology and Limb Serial Homology vs. Homoplasy

[28] Draganich LF, Vahey JW: An in vitro study of anterior cruciate ligament strain induced by quadriceps and hamstrings forces. J Orthop Res 1990;8: 57-63.

[29]D.R. Patel, E.F. Luckstead, D.E. GreydanusSportsInjuriesD.E. Greydanus, D.R. Patel,H.D. P ratt (Eds.), Essential adolescent medicine, McGraw-Hill, New York (2006), pp. 677-692.

[30] Elvin, N., Elvin, A., & Arnoczky, S.P. (2007). Correlation between ground reaction force and tibial acceleration in vertical jumping. Journal of applied biomechanics, 23 3, 180-9.

[31] Fauno P, Wulff Jakobsen B. Mechanism of anterior cruciate ligament injuries in soccer. Int J Sports Med. 2006;27(1):75–9. doi: 10.1055/s-2005- 837485.

[32] Flandry, Fred and Gabriel J. Hommel. "Normal anatomy and biomechanics of the knee." *Sports medicine and arthroscopy review* 19 2 (2011): 82-92.

[33] Ford KR, Myer GD, Hewett TE, Valgus knee motion during landing in high school female and male basketball players. Med.Sci.sports Exerc.,Vol.35,No.10,pp.1745-1750,2003.

[34] Frank CB, Jackson DW: The science of reconstruction of the anterior cruciate ligament. J Bone Joint Surg Am 1997; 79: 1556-1576.

[35] Gilchrist, J., Mandelbaum, B. R., Melancon, H., Ryan, G. W., Silvers, H. J., Griffin, L. Y., Dvorak, J. (2008). A Randomized Controlled Trial to Prevent Noncontact Anterior Cruciate Ligament Injury in Female Collegiate Soccer Players. The American Journal of Sports Medicine, 36(8), 1476–1483.

[36] Gornitzky, A. L., A. Lott, J. L. Yellin, P. D. Fabricant, J. T. Lawrence and T. J. Ganley. Sport-specific yearly risk and incidence of anterior cruciate ligament tears in high school athletes: A systematic review and meta-analysis. Am J Sports Med 2015.

[37] Gregoire L, Veeger HE, Huijing PA, van Ingen Schenau GJ: The role of mono-and biarticular muscles in explosive movements. Int J Sports Med 1984; 5:301-305.

[38] Griffin LY, Albohm MJ, Arendt EA, et al. Understanding and preventing noncontact anterior cruciate ligament injuries: a review of the Hunt Valley II meeting, January 2005. Am J Sports Med 2006;34:1512-32.

[39] Griffin, L. Y., J. Agel, M. J. Albohm, E. A. Arendt, R. W. Dick, W. E. Garrett, J. G. Garrick, T. E. Hewett, L. Huston, M. L. Ireland, R. J. Johnson, W. B. Kibler, S. Lephart, J. L. Lewis, T. N. Lindenfeld, B. R. Mandelbaum, P. Marchak, C. C. Teitz and E. M. Wojtys. Noncontact anterior cruciate ligament injuries: Risk factors and prevention strategies. J Am Acad Orthop Surg 8: 141-50, 2000.

[40] Grood, ES , Suntay, WJ , Noyes, FR , et al. Biomechanics of the knee-extension exercise: effect of cutting the anterior cruciate ligament. J Bone Joint Surg Am. 1984;66:725–734.

[41] Gupton M, Terreberry RR. Anatomy, Bony Pelvis and Lower Limb, Knee. [Updated 2018 Sep 19]. In: StatPearls [Internet]. Treasure Island (FL): StatPearls Publishing; 2018

[42] Habelt S, Hasler CC, Steinbrück K, Majewski M. Sport injuries in adolescents. Orthop Rev (Pavia). 2011;3(2):e18.

[43] Henning, CE , Lynch, MA , Glick, KR . An in vivo strain gage study of elongation of the anterior cruciate ligament. Am J Sports Med. 1985;13:22–26.

[44] Hewett TE, Lindenfeld TN, Riccobene JV, Noyes FR. The effect of neuromuscular training on the incidence of knee injury in female athletes. A prospective study. Am J Sports Med 1999;27:699- 706.

[45] Hewett TE, Myer GD, Ford KR. Anterior cruciate ligament injuries in female athletes: part 1, mechanisms and risk factors. Am J Sports Med 2006;34:299-311.

[46] Hewett TE, Myer GD, Ford KR, et al. Biomechanical measures of neuromuscular control and valgus loading of the knee predict anterior cruciate ligament injury risk in female athletes: a prospective study. Am J Sports Med 2005;33:492-501

[47] Hewett TE, Myer GD, Ford KR. Decrease in neuromuscular control about the knee with maturation in female athletes. J Bone Joint Surg Am 2004;86:1601-8.

[48] Hootman, J. M., R. Dick and J. Agel. Epidemiology of collegiate injuries for 15 sports: Summary and recommendations for injury prevention initiatives. J Athl Train 42: 311-9, 2007.

[49] Hoshino, Y., J. H. Wang, S. Lorenz, F. H. Fu and S. Tashman. Gender difference of the femoral kinematics axis location and its relation to anterior cruciate ligament injury: A 3d-ct study. Knee Surg Sports Traumatol Arthrosc 20: 1282-8, 2012.

[50] Huston LJ, Wojtys EM: Neuromuscular performance characteristics in elite female athletes. Am J Sports Med 1996; 24:427-436.

[51] https://bertec.com/uploads/pdfs/techspecs/plates/FP4060-05-PT.pdf

[52] Ireland ML. The female ACL: why is it more prone to injury? Orthop Clin North Am 2002;33:637-51.

[53] Jeremy J. Baker, Katherine J. Searight, Madeliene Atzeva Stump, et al., “Hip Anatomy and Ontogeny of Lower Limb Musculature in Three Species of Nonhuman Primates,” Anatomy Research International, vol. 2011, Article ID 580864, 13 pages, 2011.

[54] Kobayashi H, Kanamura T, Koshida S, et al. Mechanisms of the Anterior Cruciate Ligament Injury in Sports Activities: A Twenty-Year Clinical Research of 1,700 Athletes. Journal of Sports Science & Medicine. 2010;9(4):669-675

[55]Koga, H., Nakamae, A., Shima, Y., Iwasa, J., Myklebust, G., Engebretsen, L., Krosshaug, T. (2010). Mechanisms for Noncontact Anterior Cruciate Ligament Injuries: Knee Joint Kinematics in 10 Injury Situations from Female Team Handball and Basketball. The American Journal of Sports Medicine, 38(11), 2218–2225

[56] Kunju, N., Kumar, N., Pankaj, D., 2009, "Algorithm for Kinematic Measurements using Active Markers," Advance Computing Conference, 2009. IACC 2009. IEEE International, Anonymous pp. 387-391.

[57]LaBella CR, Huxford MR, Grissom J, et. al. Effect of Neuromuscular Warm-Up on Injuries in Female Soccer and Basketball Athletes in Urban Public High Schools. *Arch Ped & Adolesc Med.* 2011; 165(11):1033-1040.

[58] Ladenhauf, H. N., J. Graziano and R. G. Marx. Anterior cruciate ligament prevention strategies: Are they effective in young athletes - current concepts and review of literature. Curr Opin Pediatr 25: 64-71, 2013.

[59] Lafortune, M.A., Lake, M.J., & Hennig, E. (1995). Transfer function between tibial acceleration and ground reaction force. *Journal of Biomechanics, 28,* 113-117.

[60] Lightfoot, A. J., T. McKinley, M. Doyle and A. Amendola. Acl tears in collegiate wrestlers: Report of six cases in one season. Iowa Orthop J 25: 145-8, 2005.

[61] Liu SH, Al-Shaikh R, Panossian V, et al: Primary immunolocalization of estrogen and progesterone target cells in the human anterior cruciate ligament. J Orthop Res 1996; 14:526-533.

[62] Maclachlan, L., White, S. G. & Reid, D. Observer Rating Versus Three-Dimensional Motion Analysis of Lower Extremity Kinematics during Functional Screening Tests: A Systematic Review. *Int J Sports Phys Ther* 10, 482-492 (2015).

[63] Markolf KL, Burchfield DM, Shapiro MM, Shepard MF, Finerman GAM, Slauterbeck JL: Combined knee loading states that generate high anterior cruciate ligament forces. J Orthop Res 1995; 13:930-935.

[64] McNair PJ, Marshall RN, Matheson JA. Important features associated with acute anterior cruciate ligament injury. N Z Med J. 1990;103(901):537–9.

[65] Michael J Decker, Michael R Torry, Douglas J Wyland, William I Sterett, JRichard Steadman,Gender differences in lower extremity kinematics, kinetics and energy absorption during landing,Clinical Biomechanics,Volume 18, Issue 7,2003.

[66]Miranda, D. L., P. D. Fadale, M. J. Hulstyn, R. M. Shalvoy, J. T. Machan and B. C. Fleming. Knee biomechanics during a jump-cut maneuver: Effects of sex and acl surgery. Med Sci Sports Exerc 45: 942-51, 2013.

[67]Miyazaki, S., 1997, "Long-Term Unrestrained Measurement of Stride Length And Walking Velocity Utilizing a Piezoelectric Gyroscope," Biomedical Engineering, IEEE Transactions on, 44(8) pp. 753-759.

[68]Mizrahi, J., & Susak, Z. (1982). In-vivo elastic and damping response of the human leg to impact forces. Journal of Biomechanical Engineering, 104, 63-66.

[69]Möller Nielsen J, Hammar M. Sports injuries and oral contraceptive use. Is there a relationship? Sports Med 1991; 12:152-60.

[70]Myer, G. D., K. R. Ford and T. E. Hewett. Preventing acl injuries in women. The Journal of Musculoskeletal Medicine 1: 12-38, 2006.

[71]National Institutes of Health Medicine Plus. An Athlete's Nightmare: Tearing the ACL. Accessed August 7, 2013

[72] NaturalPoint, "Motion Capture Systems - OptiTrack Webpage." [Online]. Available: optitrack.com. [Accessed: 09-Jan-2017].

[73]Olsen, O. E., Myklebust G., Engebretsen L. and Bahr. R. Injury mechanisms for anterior cruciate ligament injuries in team handball: A systematic video analysis. Am J Sports Med 32: 1002-12, 2004.

[74]Olsen OE, Myklebust G, Engebretsen L, Holme I, Bahr R. Relationship between floor type and risk of ACL injury in team handball. Scand J Med Sci Sports 2003;13:299-304.

[75] Onate, J., Cortes, N., Welch, C., & Van Lunen, B. L. (2010). Expert versus novice interrater reliability and criterion validity of the landing error scoring system. Journal of sport rehabilitation, 19(1), 41-56.

[76] Putnam CA: Sequential motions of body segments in striking and throwing skills: Descriptions and explanations. J Biomech 1993; 26:125-135.

[77]Renstrom P, Ljungqvist A, Arendt E, et al. Non-contact ACL injuries in female athletes: an International Olympic Committee current concepts statement. Br J Sports Med 2008;42:394-412.
[78] Rozzi SL, Lephart SM, Gear WS, Fu FH: Knee joint laxity and neuromuscular characteristics of male and female soccer and basketball players. Am J Sports Med 1999; 27:312-319.

[79] Salarian, A., Horak, F. B., Zampieri, C., 2010, "ITUG, a Sensitive and Reliable Measure of Mobility," Neural Systems and Rehabilitation Engineering, IEEE Transactions on, 18(3) pp. 303-310.

[80] Salarian, A., Russmann, H., Vingerhoets, F. J. G., 2004, "Gait Assessment in Parkinson's Disease: Toward an Ambulatory System for Long-Term Monitoring," Biomedical Engineering, IEEE Transactions on, 51(8) pp.1434-1443.

[81] Saltzman, B. M., G. L. Cvetanovich, B. U. Nwachukwu, N. A. Mall, C. A. Bush-Joseph and B. R. Bach, Jr. Economic analyses in anterior cruciate ligament reconstruction: A qualitative and systematic review. Am J Sports Med 2015.

[82] Sarma A, Borgohain B, Saikia B. Proximal tibiofibular joint: Rendezvous with a forgotten articulation. Indian J Orthop 2015; 49:489-95.

[83] Sasaki, S., Y. Nagano, S. Kaneko, S. Imamura, T. Koabayshi and T. Fukubayashi. The relationships between the center of mass position and the trunk, hip, and knee kinematics in the sagittal plane: A pilot study on field-based video analysis for female soccer players. J Hum Kinet 45: 71-80, 2015.

[84]Satoshi Kaneko, Shogo Sasaki, Norikazu Hirose, Yasuharu Nagano, Mako Fukano,and Toru Fukubayashi, Mechanism of Anterior Cruciate Ligament Injury in Female Soccer Players.

[85]Senanayake, S. M. N. A., O. A. Malik, M. Iskandar and D. Zaheer. Assessing post-anterior cruciate ligament reconstruction ambulation using wireless wearable integrated sensors. Journal of Medical Engineering and Technology 37: 498-510, 2015.

[86] Scranton PE Jr, Whitesel JP, Powell JW, et al: A review of selected noncontact anterior cruciate ligament injuries in the National Football League. Foot Ankle Int 1997; 18:772-776.

[87]S.G. Rice Risks of injury during sports participation J.A. Sullivan, S.J. Anderson (Eds.), Care of the young athlete, American Academy of Orthopaedic Surgeons and American Academy of Pediatrics, Elk Grove Village (IL) (2000), pp. 9-18

[88] Shambaugh JP, Klein A, Herbert JH. Structural measures as predictors of injury basketball players. Med Sci Sports Exerc 1991;23:522-7

[89] Shelbourne KD, Davis TJ, Klootwyk TE. The relationship between intercondylar notch width of the femur and the incidence of anterior cruciate ligament tears. A prospective study. Am J Sports Med 1998;26:402-8.

[90] Slauterbeck JR, Narayan RS, Clevenger C, et al: Effects of estrogen level on the tensile properties of the rabbit anterior cruciate ligament (ACL). Trans Orthop Res Soc 1997; 22:76.
[91] Stanley CJ, Creighton RA, Gross MT, Garrett WE, Yu B. Effects of a knee extension constraint brace on lower extremity movements after ACL reconstruction. *Clin Orthop* Relat Res. 2010; 469(6):1774-80.

[92]T.A. Adirim, T.L. Cheng Overview of injuries in the young athlete Sports Med, 33 (1) (2003), pp. 75-8.

[93] Tong, K., and Granat, M. H., 1999, "A Practical Gait Analysis System using Gyroscopes," Medical Engineering & Physics, 21(2) pp. 87-94.

[94] Torg JS, Quedenfeld T. Effect of shoe type and cleat length on incidence and severity of knee injuries among high school football players. Res Q 1971;42:203-11.

[95] Toth, A. P. and F. A. Cordasco. Anterior cruciate ligament injuries in the female athlete. J Gend Specif Med 4: 25-34, 2001.

[96] T.R. (2004). The effects of knee contact angle on impact forces and accelerations. Medicine & Science in Sports & Exercise, 36, 832-837.

[97] Uhorchak JM, Scoville CR, Williams GN, Arciero RA, St Pierre P, Taylor DC. Risk factors associated with noncontact injury of the anterior cruciate ligament: a prospective four-year evaluation of 859 West Point cadets. Am J Sports Med 2003;31:831-42[68].

[98] Huston LJ, Greenfield ML, Wojtys EM. Anterior cruciate ligament injuries in the female athlete. Potential risk factors. Clin Orthop Relat Res 2000;(372):50-63.

[99] Van Ingen Schenau GJ, Bobbert MF, Rozendal RH: The unique action of biarticular muscles in complex movements. J Anat 1987:155:1-5.

[100]Van Mechelen W, Hlobil H, Kemper HC. Incidence, severity, aetiology and prevention of sports injuries: a review of concepts. Sports Med. 1992;14:82–99.

[101]Von Porat, A., E. M. Roos and H. Roos. High prevalence of osteoarthritis 14 years after an anterior cruciate ligament tear in male soccer players: A study of radiographic and patient relevant outcomes. Ann Rheum Dis 63: 269-73, 2004.

[102]Walden M, Krosshaug T, Bjorneboe J, Andersen TE, Faul O, Hagglund M. Three distinct mechanisms predominate in non-contact anterior cruciate ligament injuries in male professional football players: a systematic video analysis of 39 cases. Br J Sports Med. 2015;49(22):1452–60. doi: 10.1136/bjsports-2014-094573.

[103] Wearable medical systems for p-Health.Teng XF, Zhang YT, Poon CC, Bonato *P* IEEE Rev Biomed Eng. 2008; 1():62-74.

[104] Wearable sensors and systems. From enabling technology to clinical applications. Bonato P.IEEE Eng Med Biol Mag. 2010 May-Jun; 29(3):25-36.
[105] Yin, L., Sun, D., Mei, Q. C., Gu, Y. D., Baker, J. S., & Feng, N. (2015). The Kinematics and Kinetics Analysis of the Lower Extremity in the Landing Phase of a Stop-jump Task. The open biomedical engineering journal, *9*, 103-7.

[106] Yoo Cho, et al. Gender disparity in anterior cruciate ligament injuries.

[107] Yool Cho*, et al.* Gender disparity in anterior cruciate ligament injuries www.e-aosm.org. 66. ACLinjuries.

[108] Yu**,** Bing et al Lower extremity biomechanics during the landing of a stop-jump task Clinical Biomechanics**,** Volume 21 , Issue 3 , 297 – 305

[109] Yu B, Garrett WE. Mechanisms of non-contact ACL injuries. British Journal of Sports Medicine. 2007; 41(Suppl 1):i47-i51. doi:10.1136/bjsm.2007.037192.

[110] Zhang S.N., Bates, B.T., & Dufek J.S. (2000). Contributions of lower extremity joints to energy dissipation during landings. Medicine & Science in Sports & Exercise, 32, 812-819.

[111]Zhang, Janet H; An, Winko W; Au, Ivan P H; Chen, Tony L; Cheung, Roy T HComparison of the correlations between impact loading rates and peak accelerations measured at two different

body sites: Intra- and inter-subject analysis. Gait & posture, ISSN: 1879-2219, Vol: 46, Page: 53-6 2016

Appendix A: Consent Form

Study ID: HUM00110145 IRB: DearbornDate Approved: 6/3/2016

Consent to Participate in a Research Study

Title of the Project: Development of a Biofeedback Device to Reduce the Incidence of Anterior Cruciate Ligament Injury

Principal Investigator: Amanda Esquivel, Ph.D., University of Michigan Dearborn

Invitation to Participate in a Research Study

I invite you to be part of a research study to determine whether wearable devices can measure knee motion.

Description of Your Involvement

If you agree to be part of the research study, a member of the research team will ask you to put a small sensing device above and below your knee. We will then stick small markers to your hip, knee and ankle. You will be asked to jump down off of a 12 inch box and then jump again. We will also ask you to run a few steps and then quickly turn. These activities are similar to those performed as part of regular athletic activity or when exercising. We will measure what is happening at your knee using these markers, special video cameras that will be set up around the room and software that can track these markers. We will compare data we collect from the camera system to data from the sensing device that is above and below your knee. The video cameras will record your movements and the recordings will include your face. We expect that this will take 30-45 minutes of your time. You can first practice this motion until you are comfortable. We will be recording all of this using camera. In order to participate in the study, you must agree to video recording.

Benefits of Participation

Although you may not directly benefit from being in this study, others may benefit because developing a wearable device to monitor knee motion could help prevent ACL injuries in athletes.

Risks and Discomforts of Participation

There may be some risk or discomfort from your participation in this research. There is a very small risk that you could injure yourself when you jump or run. We will minimize this risk by letting you practice several times slowly until you feel comfortable doing this. Should you become injured, campus security will be called to provide assistance. There is also a very slight risk that data that we collect could be stolen. We will minimize this risk by only storing your data on a password protected computer.

Compensation for Participation

For your participation in this research project, you will not receive compensation.

Confidentiality

I plan to publish the results of this study. I will not include any information that would identify you. I will be recording your movements. Any pictures used for publication will first be altered so that no one can see your face. Your privacy will be protected and your research records will be confidential. It is possible that other people may need to see the information you give us as part of the study, such as organizations responsible for making sure the research is done safely and properly like the University of Michigan.

Storage and Future Use of Data

We will store your data until we are finished collecting and analyzing all data for this study. Your name and any other identifying information will be secured and stored separately from your research data. Only members of the research team will have access to your research files and data. Research data including the measurements that we take when the cameras and wearable device may be shared with other study team members but will never contain any information that could identify you. Digital files will be encrypted to protect the confidentiality of the data.

Voluntary Nature of the Study

Participating in this study is completely voluntary. Even if you decide to participate now, you may change your mind and stop at any time. You do not have to answer a question you do not want to

answer or complete any task that you don't want to do. If you decide to withdraw before this study is completed, we will stop collecting your data and delete it from the files.

Contact Information for the Study Team

If you have questions about this research, including questions about scheduling, you may contact Dr. Esquivel at aoe@umich.edu or call her at 313-593-4320.

Contact Information for Questions about Your Rights as a Research Participant

If you have questions about your rights as a research participant, or wish to obtain information, ask questions or discuss any concerns about this study with someone other than the researcher(s), you may contact the Dearborn IRB Administrator at (734) 763-5084. Written questions should be directed to the Office of Research and Sponsored Programs, 2066 IAVS, University of Michigan-Dearborn, Evergreen Rd., Dearborn MI 48128-2406, (313) 593-5468; the Dearborn IRB Administrator at (734) 763-5084, or email Dearborn-IRB@umich.edu.

Consent

By signing this document, you are agreeing to be in the study. I/we will give you a copy of this document for your records. I/we will keep one copy with the study records. Be sure that I/we have answered any questions you have about the study and that you understand what you are being asked to do. You may contact the researcher if you think of a question later.

I agree to participate in the study.

_____

Printed Name

_____

Signature Date

I agree to allow the research team to publish photos of me from this study.

_____

Printed Name

_____

Signature Date

Appendix B: Pipeline to Build Rigid Body

```
        Remove_Prefix_From_Point_Labels
        ! /INCLUDE_CAL_FILE=TRUE
        ! /OVERWRITE_C3D_FILE=FALSE
        ;
        Apply_Model_Template
        ! /CALIBRATION_FILE=
        ! /MODEL_TEMPLATE=
        ! /SET_PROMPT=Open model file
        ! /VIEW_BUILDMODEL_RESULTS=2
        ;
```

To enter the height of subject

```
        Set_Subject_Height
        ! /CALIBRATION_FILE=
        ! /HEIGHT=
        ! /UNITS=m
        ;
```

To enter the mass of subject

```
        Set_Subject_Mass
        ! /CALIBRATION_FILE=
        ! /WEIGHT=
        ! /UNITS=Kg
        ;
```

Builds a body model based on default landmarks

```
        Build_Model
        ! /CALIBRATION_FILE=
        ! /REBUILD_ALL_MODELS=FALSE
        ! /DISPLAY_RESULTS=TRUE
        ;
```

To Filter the signal

```
        Lowpass_Filter
        /SIGNAL_TYPES=TARGET
        ! /SIGNAL_FOLDER=ORIGINAL
        ! /SIGNAL_NAMES=
        ! /RESULT_FOLDER=PROCESSED
        ! /RESULT_SUFFIX=
        ! /FILTER_CLASS=BUTTERWORTH
        ! /FREQUENCY_CUTOFF=6.0
        ! /NUM_REFLECTED=6
        ! /NUM_EXTRAPOLATED=0
        ! /TOTAL_BUFFER_SIZE=6
        ! /NUM_BIDIRECTIONAL_PASSES=1
```

```
;
```
Computes a signal using model's segment for left knee joint angles
```
Compute_Model_Based_Data
/RESULT_NAME=Left Knee Angle
/FUNCTION=JOINT_ANGLE
/SEGMENT=LSK
/REFERENCE_SEGMENT=LTH
/RESOLUTION_COORDINATE_SYSTEM=
! /USE_CARDAN_SEQUENCE=FALSE
! /NORMALIZATION=FALSE
! /NORMALIZATION_METHOD=
! /NORMALIZATION_METRIC=
! /NEGATEX=FALSE
! /NEGATEY=FALSE
! /NEGATEZ=FALSE
! /AXIS1=X
! /AXIS2=Y
! /AXIS3=Z
! /TREADMILL_DATA=FALSE
/TREADMILL_DIRECTION=UNIT_VECTOR (0, 1, 0)
! /TREADMILL_SPEEED=0.0
;
```
Computes a signal using model's segment for right knee joint angles
```
Compute_Model_Based_Data
/RESULT_NAME=Right Knee Angle
/FUNCTION=JOINT_ANGLE
/SEGMENT=RSK
/REFERENCE_SEGMENT=RTH
/RESOLUTION_COORDINATE_SYSTEM=
! /USE_CARDAN_SEQUENCE=FALSE
! /NORMALIZATION=FALSE
! /NORMALIZATION_METHOD=
! /NORMALIZATION_METRIC=
! /NEGATEX=FALSE
! /NEGATEY=FALSE
! /NEGATEZ=FALSE
! /AXIS1=X
! /AXIS2=Y
! /AXIS3=Z
! /TREADMILL_DATA=FALSE
/TREADMILL_DIRECTION=UNIT_VECTOR (0, 1, 0)
! /TREADMILL_SPEEED=0.0
;
```
To calculate the frame number at which peak force occurs for left leg
```
Event_Global_Maximum
/RESULT_EVENT_NAME=Left Peak Force
/SIGNAL_TYPES=FORCE
! /SIGNAL_FOLDER=ORIGINAL
```

/SIGNAL_NAMES=FP2
/SIGNAL_COMPONENTS=Z
! /FRAME_OFFSET=0
! /TIME_OFFSET=
! /EVENT_SEQUENCE=
! /EXCLUDE_EVENTS=
! /EVENT_SEQUENCE_INSTANCE=0
! /EVENT_SUBSEQUENCE=
! /SUBSEQUENCE_EXCLUDE_EVENTS=
! /EVENT_SUBSEQUENCE_INSTANCE=0
! /EVENT_INSTANCE=0
;

To calculate the frame number at which peak force occurs for right leg

Event_Global_Maximum
/RESULT_EVENT_NAME=Right Peak Force
/SIGNAL_TYPES=FORCE
! /SIGNAL_FOLDER=ORIGINAL
/SIGNAL_NAMES=FP1
/SIGNAL_COMPONENTS=Z
! /FRAME_OFFSET=0
! /TIME_OFFSET=
! /EVENT_SEQUENCE=
! /EXCLUDE_EVENTS=
! /EVENT_SEQUENCE_INSTANCE=0
! /EVENT_SUBSEQUENCE=
! /SUBSEQUENCE_EXCLUDE_EVENTS=
! /EVENT_SUBSEQUENCE_INSTANCE=0
! /EVENT_INSTANCE=0
;

Appendix C: Pipeline to Compute Various Events

To compute the frame number at landing of left leg

```
Event_Threshold
/RESULT_EVENT_NAME=Left Landing
/SIGNAL_TYPES=FORCE
! /SIGNAL_FOLDER=ORIGINAL
/SIGNAL_NAMES=FP2
/SIGNAL_COMPONENTS=Z
! /FRAME_OFFSET=0
! /TIME_OFFSET=
! /EVENT_SEQUENCE=
! /EXCLUDE_EVENTS=
! /EVENT_SEQUENCE_INSTANCE=0
! /EVENT_SUBSEQUENCE=
! /SUBSEQUENCE_EXCLUDE_EVENTS=
! /EVENT_SUBSEQUENCE_INSTANCE=0
/EVENT_INSTANCE=1
/THRESHOLD=0.05
/ON_ASCENT=TRUE
/ON_DESCENT=FALSE
/FRAME_WINDOW=25
! /ENSURE_FRAMES_BEFORE=FALSE
! /ENSURE_FRAMES_AFTER=FALSE
;
```

To compute the frame number at landing of right leg

```
Event_Threshold
/RESULT_EVENT_NAME=Right Landing
/SIGNAL_TYPES=FORCE
! /SIGNAL_FOLDER=ORIGINAL
/SIGNAL_NAMES=FP1
/SIGNAL_COMPONENTS=Z
! /FRAME_OFFSET=0
! /TIME_OFFSET=
! /EVENT_SEQUENCE=
! /EXCLUDE_EVENTS=
! /EVENT_SEQUENCE_INSTANCE=0
! /EVENT_SUBSEQUENCE=
! /SUBSEQUENCE_EXCLUDE_EVENTS=
! /EVENT_SUBSEQUENCE_INSTANCE=0
/EVENT_INSTANCE=1
/THRESHOLD=0.05
/ON_ASCENT=TRUE
```

/ON_DESCENT=FALSE
/FRAME_WINDOW=25
! /ENSURE_FRAMES_BEFORE=FALSE
! /ENSURE_FRAMES_AFTER=FALSE
;

To compute the frame number at flexion for left leg

Event_Global_Minimum
/RESULT_EVENT_NAME=Left Flexion
/SIGNAL_TYPES=LINK_MODEL_BASED
! /SIGNAL_FOLDER=ORIGINAL
/SIGNAL_NAMES=Left Knee Angle
/SIGNAL_COMPONENTS=X
! /FRAME_OFFSET=0
! /TIME_OFFSET=
! /EVENT_SEQUENCE=
! /EXCLUDE_EVENTS=
! /EVENT_SEQUENCE_INSTANCE=0
! /EVENT_SUBSEQUENCE=
! /SUBSEQUENCE_EXCLUDE_EVENTS=
! /EVENT_SUBSEQUENCE_INSTANCE=0
! /EVENT_INSTANCE=0
;

To compute the frame number at flexion for right leg

Event_Global_Minimum
/RESULT_EVENT_NAME=Right Flexion
/SIGNAL_TYPES=LINK_MODEL_BASED
! /SIGNAL_FOLDER=ORIGINAL
/SIGNAL_NAMES=Right Knee Angle
/SIGNAL_COMPONENTS=X
! /FRAME_OFFSET=0
! /TIME_OFFSET=
! /EVENT_SEQUENCE=
! /EXCLUDE_EVENTS=
! /EVENT_SEQUENCE_INSTANCE=0
! /EVENT_SUBSEQUENCE=
! /SUBSEQUENCE_EXCLUDE_EVENTS=
! /EVENT_SUBSEQUENCE_INSTANCE=0
! /EVENT_INSTANCE=0
;

To compute the frame number at abduction for left leg

Event_Global_Maximum
/RESULT_EVENT_NAME=Left Abduction
/SIGNAL_TYPES=LINK_MODEL_BASED
! /SIGNAL_FOLDER=ORIGINAL
/SIGNAL_NAMES=Left Knee Angle
/SIGNAL_COMPONENTS=Y
! /FRAME_OFFSET=0
! /TIME_OFFSET=

```
! /EVENT_SEQUENCE=
! /EXCLUDE_EVENTS=
! /EVENT_SEQUENCE_INSTANCE=0
! /EVENT_SUBSEQUENCE=
! /SUBSEQUENCE_EXCLUDE_EVENTS=
! /EVENT_SUBSEQUENCE_INSTANCE=0
! /EVENT_INSTANCE=0
;
```

To compute the frame number at abduction for right leg

```
Event_Global_Minimum
/RESULT_EVENT_NAME=Right Abduction
/SIGNAL_TYPES=LINK_MODEL_BASED
! /SIGNAL_FOLDER=ORIGINAL
/SIGNAL_NAMES=Right Knee Angle
/SIGNAL_COMPONENTS=Y
! /FRAME_OFFSET=0
! /TIME_OFFSET=
! /EVENT_SEQUENCE=
! /EXCLUDE_EVENTS=
! /EVENT_SEQUENCE_INSTANCE=0
! /EVENT_SUBSEQUENCE=
! /SUBSEQUENCE_EXCLUDE_EVENTS=
! /EVENT_SUBSEQUENCE_INSTANCE=0
! /EVENT_INSTANCE=0
;
```

To compute the frame number at internal rotation for left leg

```
Event_Global_Minimum
/RESULT_EVENT_NAME=Left Internal Rotation
/SIGNAL_TYPES=LINK_MODEL_BASED
! /SIGNAL_FOLDER=ORIGINAL
/SIGNAL_NAMES=Left Knee Angle
/SIGNAL_COMPONENTS=Z
! /FRAME_OFFSET=0
! /TIME_OFFSET=
! /EVENT_SEQUENCE=
! /EXCLUDE_EVENTS=
! /EVENT_SEQUENCE_INSTANCE=0
! /EVENT_SUBSEQUENCE=
! /SUBSEQUENCE_EXCLUDE_EVENTS=
! /EVENT_SUBSEQUENCE_INSTANCE=0
! /EVENT_INSTANCE=0
;
```

To compute the frame number at internal rotation for right leg

```
Event_Global_Maximum
/RESULT_EVENT_NAME=Right Internal rotation
/SIGNAL_TYPES=LINK_MODEL_BASED
! /SIGNAL_FOLDER=ORIGINAL
/SIGNAL_NAMES=Right Knee Angle
```

```
/SIGNAL_COMPONENTS=Z
! /FRAME_OFFSET=0
! /TIME_OFFSET=
! /EVENT_SEQUENCE=
! /EXCLUDE_EVENTS=
! /EVENT_SEQUENCE_INSTANCE=0
! /EVENT_SUBSEQUENCE=
! /SUBSEQUENCE_EXCLUDE_EVENTS=
! /EVENT_SUBSEQUENCE_INSTANCE=0
! /EVENT_INSTANCE=0
;
```

Appendix D: MATLAB Script to Calculate Tibial Acceleration And Joint Angles From Opal Sensors

```
%%% Script to calculate when peak force occurs for the Moveo sensors

% Step 1. Rename .h5 files to correct name
% Step 2. Run the code
% Step 3. Compare the generated figure to the n instances
    % Look for negative peak in the blue X line

%%%%%%%%%%%%%%%%%%%%%%%%%%%%%%%%%%%%%%%%%%%%%%%%%%%%%%%%%%%%%%%%%%%%%%%%%%%%%%%

clear % clears the current workspace

%%%%%%%%%%%%%%%%%%%%%%%%%%%%%%%%%%%%%%%%%%%%%%%%%%%%%%%%%%%%%%%%%%%%%%%%%%%%%%%

%%% Extract Joint Angles (degrees) from processed data

nsamples = h5readatt('j2.h5','/Processed/Joint Angles','nSamples');
i=1;

for i=1:1:nsamples %%% Loop to store number of samples in matrix t
    t(i,:) = i;
end

%%% Left Knee
leftkneex=h5read('j2.h5','/Processed/Joint Angles/Knee/Left/X');
l_knee_y=transpose(leftkneex); % X in Moveo is valgus-varus (Y in V3D)
leftkneey=h5read('j2.h5','/Processed/Joint Angles/Knee/Left/Y');
l_knee_z=transpose(leftkneey); % Y in Moveo is rotation (Z in V3D)
leftkneez=h5read('j2.h5','/Processed/Joint Angles/Knee/Left/Z');
l_knee_x=transpose(leftkneez); % Z in Moveo is flexion-extension (X in V3D)

left_knee_angles = [l_knee_x l_knee_y l_knee_z]; % Summary matrix [XYZ]

%%% Right Knee
rightkneex=h5read('j2.h5','/Processed/Joint Angles/Knee/Right/X');
r_knee_y=transpose(rightkneex);
rightkneey=h5read('j2.h5','/Processed/Joint Angles/Knee/Right/Y');
r_knee_z=transpose(rightkneey);
rightkneez=h5read('j2.h5','/Processed/Joint Angles/Knee/Right/Z');
r_knee_x=transpose(rightkneez);

right_knee_angles = [r_knee_x r_knee_y r_knee_z]; % Summary matrix [XYZ]

%%%%%%%%%%%%%%%%%%%%%%%%%%%%%%%%%%%%%%%%%%%%%%%%%%%%%%%%%%%%%%%%%%%%%%%%%%%%%%%

%%% Extract Acceleration (m/s^2) from raw data

a_1917=h5read('j2raw.h5','/Sensors/1917/Accelerometer');
```

```
l_lowerleg_acc=transpose(a_1917);

a_1939=h5read('j2raw.h5','/Sensors/1939/Accelerometer');
l_upperleg_acc=transpose(a_1939);

a_1901=h5read('j2raw.h5','/Sensors/1901/Accelerometer');
r_lowerleg_acc=transpose(a_1901);

a_1929=h5read('j2raw.h5','/Sensors/1929/Accelerometer');
r_upperleg_acc=transpose(a_1929);

a_1943=h5read('j2raw.h5','/Sensors/1943/Accelerometer');
lumbar_acc=transpose(a_1943);

%%%%%%%%%%%%%%%%%%%%%%%%%%%%%%%%%%%%%%%%%%%%%%%%%%%%%%%%%%%%%%%%%%%%%%%%%%%%

%%% Peak Force: Identify max force as peak negative acceleration (F=ma)
%%% Note: this is based on the lower leg acceleration

[left_min,left_min_frame]=min(l_lowerleg_acc(:));
[right_min,right_min_frame]=min(r_lowerleg_acc(:));

left_min_frame  % Display where left min acceleration occurs
left_peakforce_angle=left_knee_angles(left_min_frame,:)
right_min_frame % Display where right min acceleration occurs
right_peakforce_angle=right_knee_angles(right_min_frame,:)

%%% Plot lower leg acceleration to verify minimum was in x-direction
figure(1)
subplot(211),plot(t,l_lowerleg_acc);
title('Left Lower Leg Acceleration');
ylabel('Acceleration (m/s^2)');
legend('X','Y','Z');
grid on;
subplot(212),plot(t,r_lowerleg_acc);
title('Right Lower Leg Acceleration');
ylabel('Acceleration (m/s^2)');
legend('X','Y','Z');
grid on

%%%%%%%%%%%%%%%%%%%%%%%%%%%%%%%%%%%%%%%%%%%%%%%%%%%%%%%%%%%%%%%%%%%%%%%%%%%%
```